Monitoring bird collisions - meso and micro avoidance at offshore wind farm Eneco Luchterduinen

Final Report

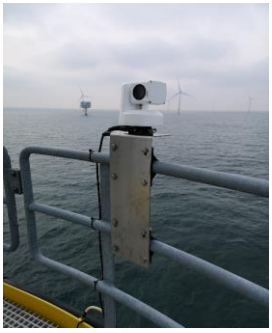

December 2022

This proposal has been prepared under the DHI Business Management System certified by Bureau Veritas to comply with ISO 9001 (Quality Management)

Monitoring bird collisions - meso and micro avoidance at offshore wind farm Eneco Luchterduinen

Final Report

Prepared for	Eneco
Represented by	Marin van Regteren

Authors	Henrik Skov, Rune Skjold Tjørnløv

Project number	11821366
Approval date	2nd December 2022
Revision	2
Classification	Confidential

Video screening: Mick Kirkegaard, Sven Suneson, Circle Consult

Video analyses: Lars Schmidt, Troels E. Ortvad, Henrik V. Christensen, Jens Tomas Larsen, Marine Observers

Software integration: Brian Hansen, Cim Industrial Systems A/S

Photos: Thomas W. Johansen

CONTENTS

FIGURES

TABLES

0 Executive summary

The ENECO Luchterduinen (LUD) MEP project aims for accurate measurements of species-specific meso and micro avoidance behaviour, and collisions of Lesser black-backed gull, Herring gull, Great black-backed gull, and Northern Gannet. This information can be used for improved input into bird collision models. More specifically, the following quantitative aims have been identified:

Quantify meso and micro avoidance behaviour at the species level for large gulls during daylight in all kinds of weather conditions (including adverse weather)

Quantify total bird fluxes inside the wind farm (unspecified radar track densities)

Quantify total number of collisions of large gulls at the species level

Provide micro and meso avoidance rates for use in bird collision models.

Provide information on species-specific flight height for the tracks recorded by both radar and camera

The LUD MEP project has used the MUSE system developed and tested during the ORJIP BCA Project. In the LUD MEP project the MUSE system has been based on integrated monitoring by one radar (Furuno FAR-3000 S-band) installed on the Offshore High Voltage Station (OHVS) platform and four daylight cameras (RVision) installed on WTGs. Compared to the version of MUSE applied in the ORJIP project the technical improvements of the monitoring equipment and especially the radar employed in LUD made it possible to track large gulls inside the array and measure fluxes and meso-avoidance more confidently. Due to the full integration of radar and video tracks and the high temporal resolution of the track data (2.5 secs) the fluxes (track length density) and meso-avoidance behaviour could be assessed in unprecedented spatial detail. Further, the radar in the LUD MEP project has been configured to reduce false positives by applying strong dynamic clutter filters which remove noise from waves. The application of these filters dampens not only reflections by waves during strong weather, but it also inhibits detection of all birds. However, as seabird flight behaviour is assessed using proportional statistics the dynamic noise filters has not compromised the assessment of avoidance behaviour as flight behaviour in the different parts of the LUD array is assessed in comparable weather conditions.

The target sample size for species-specific meso-avoidance of 250 was not reached for any of the target species. This can both be explained by the relatively low density of these species in the LUD wind farm (Heinänen & Skov 2018, Leemans et al. 2022), but also by the technical standard of the optics of the applied RVision camera (not HD) and the standard video tracking technology applied (not AI-based). The estimates of meso avoidance in large gulls were limited to wind speeds below 10 m/sec where the cameras were operating in dual mode with the radar and provided species id to the selected radar tracks. Maximum meso-avoidance levels recorded were at least 0.5 for all three large gull species. These avoidance rates are lower than the rates estimated in the ORJIP BCA study which were between 0.842 and 0.961, yet the distances of birds to rotor-swept zones in the ORJIP project was determined based on the video documentation, and track lengths were estimated based on mean track speeds. Accordingly, the meso avoidance rates from the LUD MEP project are likely to be more reliable and are in line with meso avoidance rates for large gulls recorded with the same monitoring equipment in the Aberdeen EOWFD study (Tjørnløv et al. 2021). The sample size of coupled radar and camera tracks was insufficient for estimation of meso avoidance rate for individual species of large gulls.

The results strongly indicates that the meso avoidance response of large gulls towards turbines mainly takes place within 120 m distance from rotors and that the response intensifies as the gulls approach the rotor blades. Overall, only 2.1 % of large gull videos showed birds inside the rotor-swept zones, and only three videos showed occurrence of Northern Gannet inside the zones. In proximity to the rotors, the recorded meso-avoidance response behaviour for all three target

species was manifested as a complex 3-dimensional pattern in which the gulls increased altitude and reduced flight speed while approaching the rotors and finally deflected the blades mostly by flying along the rotor plane.

Using machine learning it was possible to investigate these flight behaviours in more detail and gain insight into the influence of wind conditions. The increase in flight height of large gulls closer to the rotor as seen in the mean profiles seemed only evident in high tail and cross wind speeds, and black-backed gulls only seemed to increase flight height on approach to the rotor during low wind speeds. Whereas large gulls were predicted to reduce flight speed when approaching the rotor during all weather scenarios, black-backed gulls were predicted to do so only during calm wind scenarios. Regarding the tendency to reduce the relative difference in direction when approaching the rotor the model resolved that the flight direction of large gulls as well as black-backed gulls was most pronounced during calm wind conditions. The change in orientation translated into flights close to but along the rotor being the dominant type of micro avoidance of large gulls. The recorded micro-avoidance rates were high (0.800 for all black-backed gulls and 0.861 for all larger gulls), yet markedly lower than reported by similar methods in the ORJIP BCA study and in the Aberdeen EOWDC study.

Given the recorded high levels of meso and micro avoidance it is now evident that the large gulls will be exposed to low risks of collision in this wind farm. The low risk of collision for large gulls in the LUD wind farm (LUD) was also substantiated by the fact that only two collisions were recorded during the two and half years of monitoring. Scaling up from this recorded number of collisions the total annual number of collisions of seabirds in LUD can be estimated at 2.6. The results for meso avoidance and micro avoidance of large gulls in the LUD MEP project will be combined with the results of the RWS radar project which uses a Robin Radar system in LUD executed by Bureau Waardenburg. In order to achieve an overall avoidance rate for large gulls in LUD it is recommended to combine macro avoidance rates obtained in the Rijkswaterstaat (RWS) radar project with a meso avoidance rate of 0.5 and micro avoidance rates of 0.800 for Lesser and Great black-backed gulls and 0.861 for Herring gull.

As the target sample size for estimation of species-specific micro avoidance rates of 100 could not be achieved for any of the three target species it is recommended to undertake further monitoring of micro avoidance of large gulls in offshore wind farms using the best available camera technology. Increasing the sample size of large gulls recordings in the rotor-swept area will also likely increase the micro avoidance rate to the levels recorded in the ORJIP BCA and the Aberdeen EOWDC studies.

Introduction

Wind farm Eneco LUD needs to comply with a number of requirements for monitoring and evaluation in order to obtain the necessary operating permits. Eneco licenses parts 7 and 8 include flux measurements of seabirds and colony breeders and measurements of avoidance and/or collisions of seabirds and colony breeders. At an earlier stage (2013) it was agreed by Rijkswaterstaat (RWS) to join the Offshore Renewables Joint Industry Programme (ORJIP) Bird Collision Avoidance (BCA) project 2014-2017 as a first step. After finalization of that project, the second phase, including monitoring in the field, is now being implemented.

In 2016, RWS has started the Wind Offshore Ecological Program (WOZEP). This program focuses on the ecological effects of OWF's on protected species as birds, bats and marine mammals. One of the research interests is the effect of collision risk on seabirds and migratory birds. Therefore, Wozep contracted Bureau Waardenburg (BuWa) for a project to get more knowledge on bird fluxes, behaviour and collisions in Luchterduinen (LUD, Figure 1). This is one of the locations where Rijkswaterstaat has installed a bird radar. This system measures bird fluxes outside the wind farm area (macro-avoidance) and also gives information about bird fluxes within the wind farm (although there will be blind spots because of the turbines and the OHVS). The radar is combined with a camera and visual observations in the windfarm. As part of the LUD project, Rijkswaterstaat has asked BuWa to integrate the findings of the WOZEP project and this project to obtain estimates of the overall avoidance and collision rates in the wind farm.

At the start of this project, i, the predicted cumulative impact of OWF's on a few gull species (Great black-backed gull *Larus marinus*, Lesser black-backed gull *Larus fuscus* and Herring gull *Larus argentatus*) seemed to be just within maximum allowable limits using the best available knowledge and applying a precautionary approach. To assess if further developments of OWF's will not harm the mentioned gull populations, information about the real behaviour in the wind farms and number of collisions is urgently needed. Information about avoidance at all levels (macro/meso/micro) is needed as well as actual collision rates.

This project aims for accurate measurements of species-specific meso and micro avoidance behaviour and collisions of (at least) Lesser black-backed gull, Herring gull and Great black-backed gull. This information can be used for improved input into bird collision models.

More specifically, the following quantitative aims have been identified:
Quantify meso and micro avoidance behaviour at the species level for large gulls during daylight in all kinds of weather conditions (including adverse weather);
Quantify total bird fluxes inside the wind farm (unspecified)
Quantify total number of collisions of large gulls at the species level
Provide micro and meso avoidance rates and total fluxes for use in bird collision models.
Provide information on species-specific flight height for the tracks recorded by both radar and camera

The Eneco monitoring project at LUD has used the MUSE system which is based on integrated monitoring by radar and cameras developed and tested during the ORJIP BCA Project. The monitoring plan was discussed with RWS and further discussed with the LUD MEP Expert Panel[1], and was scheduled to run for a period of 24 months.

The Final Report provides the results for the LUD-MEP monitoring project within the LUD wind farm area based on the data collected during the period September 2019 to March 2022.

[1] An international Expert Panel consisting of scientists involved in research on seabird interactions with offshore wind farms has provided advise to the LUD MEP project throughout the 2.5 years monitoring period

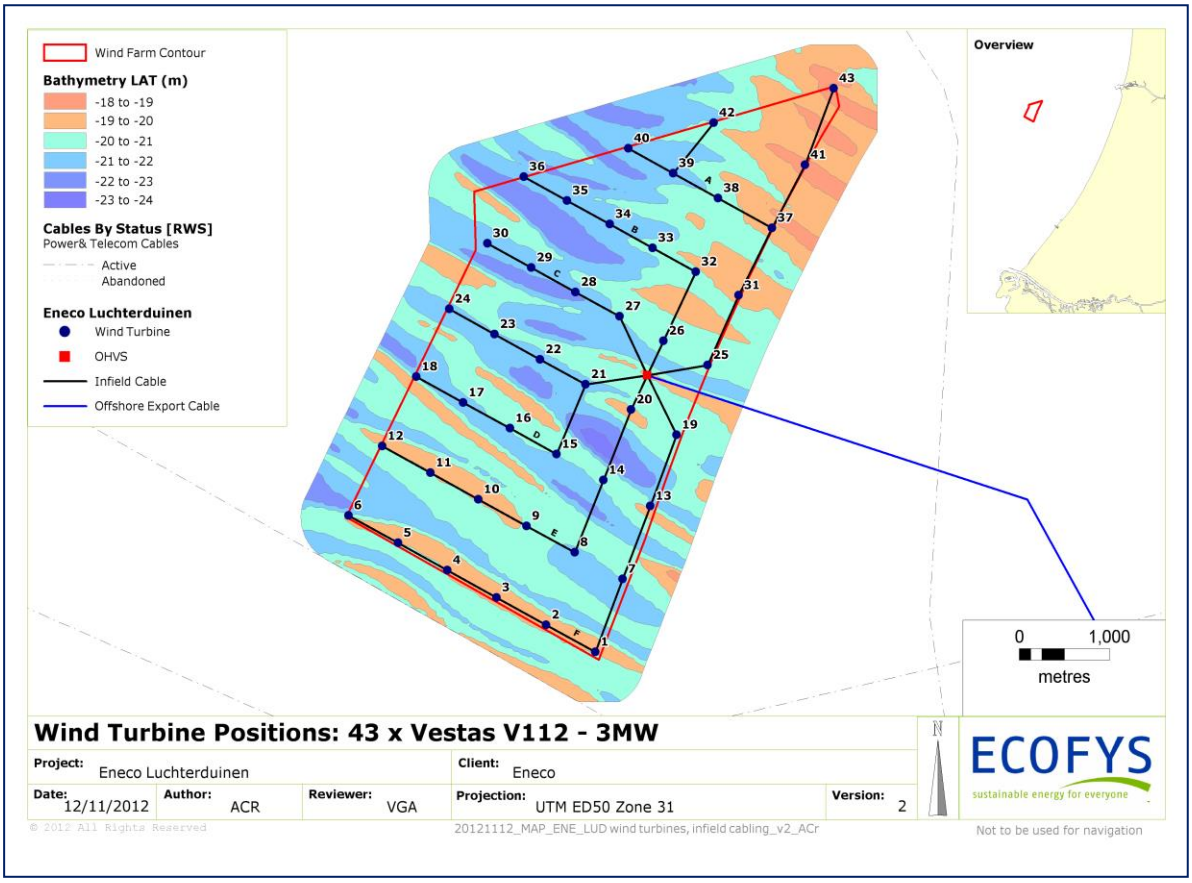

Figure 1 Overview of LUD footprint and turbine array

Definitions

We use the same definitions as used in the ORJIP BCA study:

MACRO AVOIDANCE: Bird behavioural responses to the presence of the wind farm occurring beyond its perimeter, resulting in a redistribution of birds inside and outside the wind farm.

MESO AVOIDANCE: Bird behavioural response within the wind farm footprint to individual turbines (considering a 10 m buffer around the rotor swept zone (RSZ)) and resulting in a redistribution of the birds within the wind farm footprint.

MICRO AVOIDANCE: Bird behavioural response to single blade(s) within 10 m of the RSZ, considered as the bird's 'last-second action' taken to avoid collision with the blades identified as a dynamic ellipse oriented perpendicularly to the wind direction.

MUSE system

The MUSE solution used for the LUD bird collision and micro and meso avoidance study is a unit which combines a horizontal radar and four digital cameras (figure 2). The communication

between the camera and radar is facilitated by a multi-sensor, high-speed processing software (DHI MUSE); this software allows birds discovered by the radar to be automatically targeted by the cameras and followed, using motion detection and video. The horizontal radar is a FAR-3000 solid state S-band radar with pulse compression and enhanced sea and rain clutter suppression. The digital cameras are RVision SeeHP pan-tilt daylight cameras which have been tested by DHI at the DHI test site in Ebeltoft Harbour, Denmark and at the FINO 2 research platform in the Baltic Sea.

A maximum range of 3 km is set for the horizontal radar which has enabled automated scanning of bird movements over a major part of the wind farm, while the cameras have operated within a range of approximately 1 km allowing for recording of avoidance behaviour around and within the RSZ of a total of 15 turbines. Tracking information from the radar is continuously recorded to a geo-database by the system. Samples of radar tracks that have triggered video recordings are combined with images from the camera, which are flagged with the same track identification code. Information about the height of the bird is also recorded during the period it is viewed by the camera; the target's height is calculated using the MUSE software by triangulation of the combined distance measurements from the radar and the measurements of inclination angle by the camera. A summary of monitoring equipment, data output and location within the LUD array is included within Table 1.

Table 1 Monitoring equipment data output expected, and location (see images below).

EQUIPMENT TYPE	EQUIPMENT NUMBER AND OCATION	DATA OUTPUT
FAR-3000 Radar	1 x FAR-3000 Radar placed on OHVS platform within the turbine array	Localised avian movement patterns within 3 km range, selected tracks coupled to digital cameras
MUSE Camera	4 x Rvision SEE HP cameras including tracker unit have been placed on turbines 11, 15, 27, 38 within the turbine array	Videos of selected bird movements within 1000 m distance in the defined scanning range (180°)

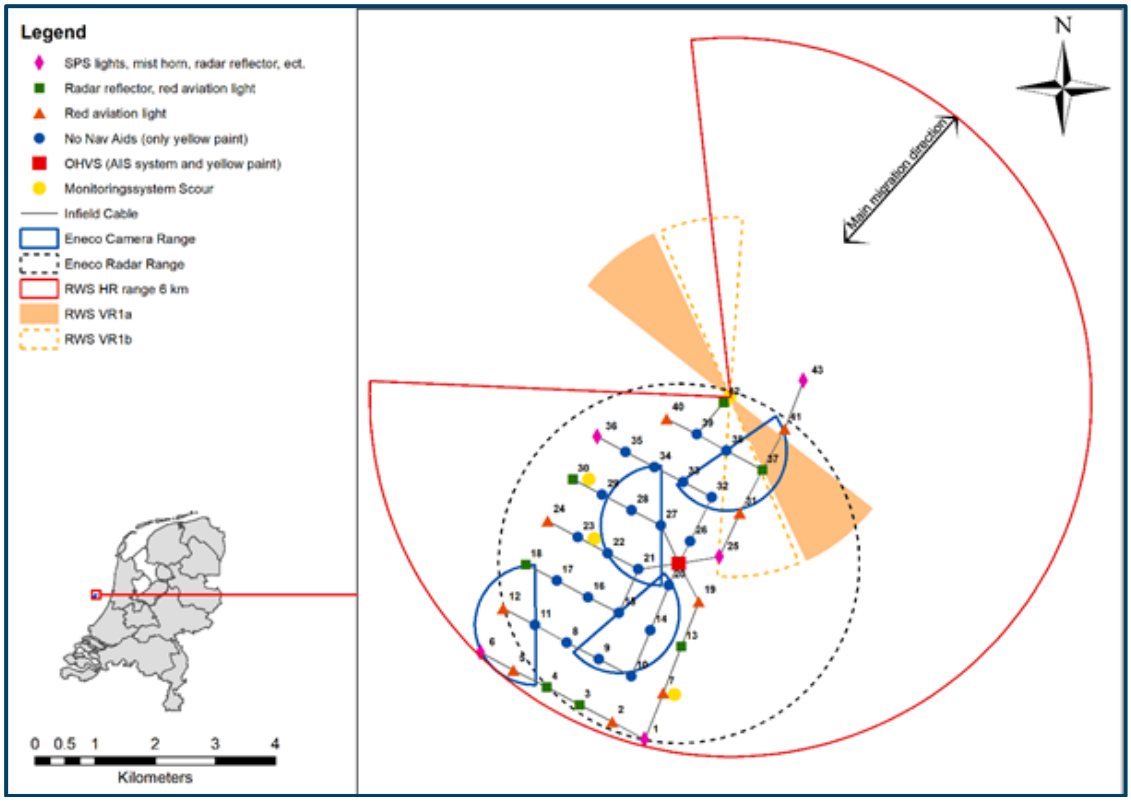
Legend
SPS lights, mist horn, radar reflector, ect.
Radar reflector, red aviation light
Red aviation light
No Nav Aids (only yellow paint)
OHVS (AIS system and yellow paint)
Monitoringssystem Scour
Infield Cable
Eneco Camera Range
Eneco Radar Range
RWS HR range 6 km
RWS VR1a
RWS VR1b
0 0.5 1 2 3 4
Kilometers
N
Main migration direction

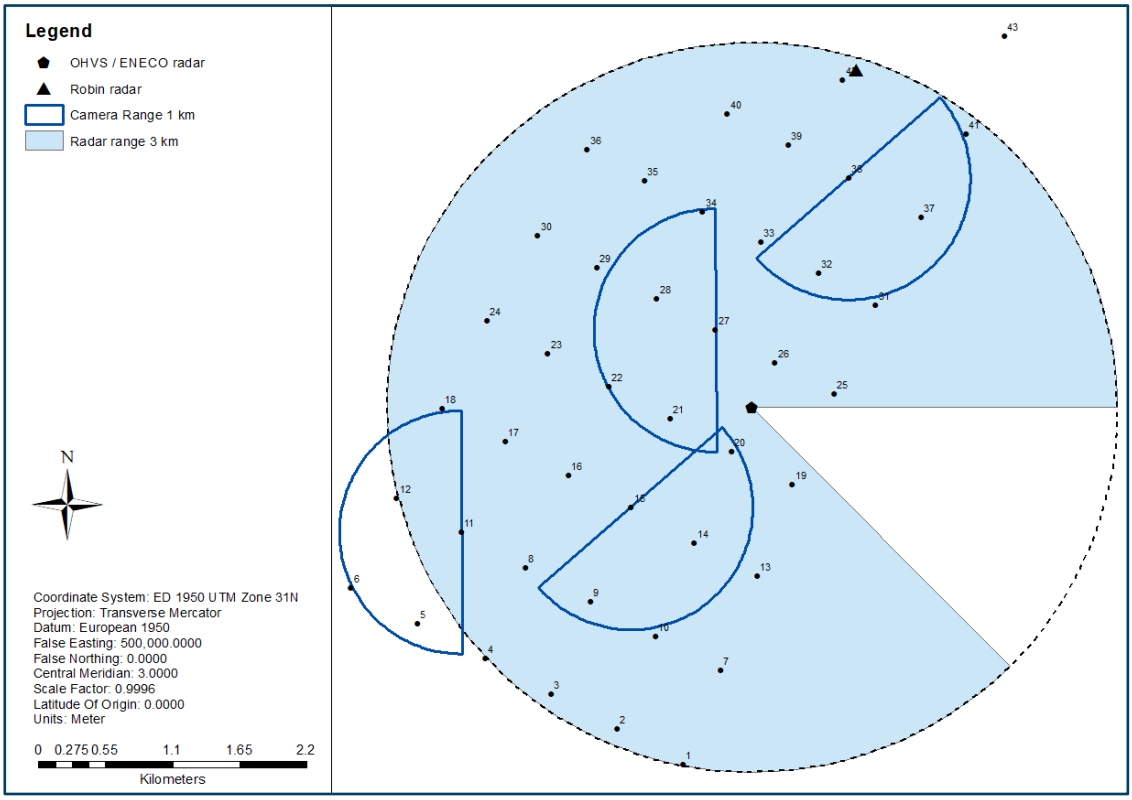

Figure 2 Set-up and tracking ranges of ENECO radar and cameras as well as RWS radars

Prior to installation, field tests were undertaken at a coastal test location in Ebeltoft, Denmark. Checks and calibration of all radar signal processing in the MUSE software were carried out in a laboratory. The database storage was tested with track data from the field; the MUSE system saves all bird tracks as geo-referenced tracks with unique ID which includes a timestamp. Parameters included and checked in the database include UTM coordinates for each node in the tracks, order of track nodes, flight direction, variation of flight direction and flight speed. The alignment of the camera with the initial target position was tested by including annotations of the angle, elevation, and zoom level in the video output from the camera.

Following calibration of the radar, the cameras were calibrated remotely to optimise focus and zoom levels, motion detection controls and division of the scanned area between cameras.

Radar specification, including tracking of seabirds

The FAR-3000 S-band solid state radar is used for horizontal scanning of bird movements within the wind farm. The FAR-3000 S was selected due to its good clutter suppression and bird tracking capacity in conditions with prominent sea and rain clutter. Simulations of the vertical coverage and detection probability of different sizes of birds (radar cross sections) have been made using Carpet software (*https://www.tno.nl/en/focus-areas/defence-safety-security/roadmaps/information-sensor-systems/carpet-computer-aided-radar-performance-evaluation-tool/*). The results show good detection of passerines at distances up to 3 km, of gulls up to 4 km, of gannets up to 5 km and of large flocks of birds up to 6 km during sea state 0. During high sea states (sea state 4+) the detection of passerines and gulls close to the radar drops. Within the distances of good detection, the vertical coverage is at least 400 m for all types of birds. In conclusion, the radar provides good detection of the target species (large gulls) within the entire 3 km range applied in the EOWDC. During higher sea states the detection of gulls close to the radar is reduced.

The MUSE software samples at 100 MHz and performs real time filtering of standardized echo sizes based on calibrated dB-values from the radar. Both static and dynamic noise is filtered by the software before initiating tracking. Each track consists of nodes with a temporal resolution of 2.5 seconds equivalent to one antenna rotation. Additional to the generation of bird tracks the MUSE system automatically stored radar screen images every 2 seconds. These data constituted a backup facility and supplementary data. On account of the vertical angle (12.5°) of the radar beam and the height of the radar on AWF10, low-flying (< 10 m) seabirds could not be detected closer than 30 m from the radar.

Camera specifications, including tracking of seabirds

The RVision See HP camera is a rugged daylight camera, which consists of a pan-tilt housing with a Sony x30 daylight camera block (figure 2, Appendix 2). The rugged camera system is designed for long-term deployment in offshore conditions. During the 2.5-year monitoring period some deterioration of the quality of the videos was observed, which may have been mitigated by regular cleaning of the lenses. The pan-tilt camera's environmental housing is fully capable of sustaining the harsh environment of the salty sea conditions offshore. Additionally, the camera is sufficiently durable to withstand continuous operation in an offshore environment.

The range at which movements of seabirds can be tracked by motion detection is approximately 1,000 m, and the minimum distance is approximately 50 m. The video format applied in MUSE is PAL and was used during the field tests.

The camera turn response speed on the radar signal for the initial bird detection has been tested. The speed of the RVision is 20 degrees per second. Each camera scanned areas of maximum 250˚ in LUD. Accordingly, the maximum delay related to the turn speed is 12.5 seconds (RVision). As the cameras are zoomed out initially, this delay is not likely to limit the detection of the bird by the cameras to any large degree. To further reduce the delay, a decision rule was introduced in the MUSE software which in cases of multiple targets makes the camera select the target which is closest to its current position.

Radar-camera integration and operating modes

The dynamic and fully integrated coupling between the horizontal radar and the pan-tilt cameras in MUSE allows the cameras to operate in two dimensions and detect and follow birds across a large area of the wind farm. Triggered by the radar, the digital camera will detect the bird target and will zoom and focus on the bird and track and record its movements. The radar-based control of the cameras has been thoroughly tested prior to commissioning in this and other projects. Recordings of flight height and tracking of 3-D movements of birds were obtained by triangulation of measurements of distance from FAR-3000 and inclination angle measured by the cameras (figure 2 and 3). The integrated track database included flags for horizontal tracks with associated height data, and height measurements were added for each node in the horizontal track.

The triangulation was made using the radar measurement of its distance and the angle observed with the camera, which was obtained from the fraction of the total field of view (FOV). The % accuracy was given by the sum of the % accuracy in the angle and the distance. Test using drones of the accuracy of the height estimates are ongoing in Denmark.

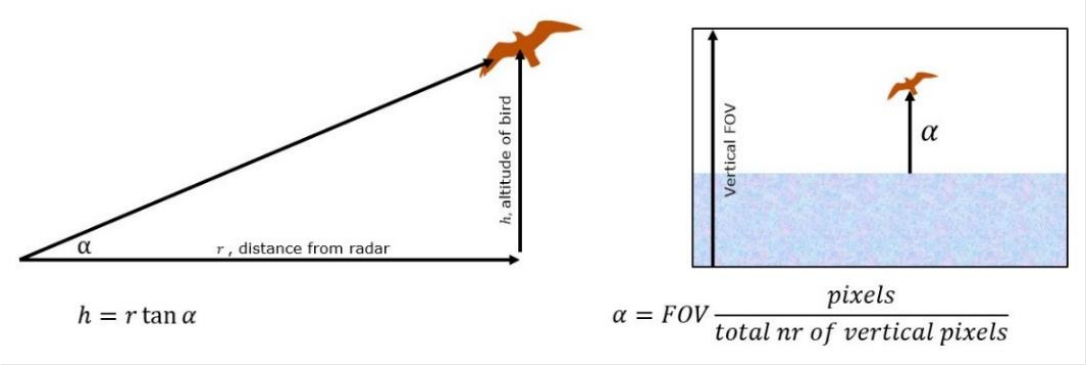

Figure 3 Sketch of the estimation of flight height by triangulation of radar and camera measurements

Potential sources of bias

The analytical framework for this project has been based on proportional statistics on behavioural data without assuming detection of all birds in the ranges of radar and cameras. Still, potential biases may have been introduced. The monitoring design assumes that the observed behavioural responses are representative of any weather and visibility conditions. Tests of false negatives and false positive detections by the FAR-3000 radar have documented that although false positives are controlled efficiently by the clutter filter of the MUSE system, false negatives will appear as sea states increase above sea state 4. As track densities are only compared for the same weather scenarios the tendency for false negatives may not necessarily introduce a bias. However, during severe weather with sea states above 5 it is likely that the level of false negatives will be significant leading to small sample sizes and less robust patterns of track distributions. The tendency for false negatives during adverse weather conditions will be the same irrespective of the flight height of the birds. Hence, a bias against low-flying birds should not be expected.

Obviously, during the course of the project oceanographic and habitat variability in time and space has been taking place as water masses and currents at the wind farm has been continuously changing in response to tidal, estuarine and weather dynamics. Although the effect of the variability in the weather conditions on seabird flight behaviour has been quantified, the oceanographic variability has not been accounted for within this study. The same holds true for variability induced by commercial fishing activities near the wind farm. The oceanographic variability has most likely affected the dynamics of abundance of seabirds within LUD but is unlikely to have biased recordings of avoidance behaviour.

A few seabirds appeared not to change their flight path by flying below/above the RSZ. Accordingly, these have not been included in the account of vertical meso-avoidance. Thus, vertical meso avoidance measurements are judged as un-biased.

Tracking effort at all distances from the turbines is considered similar, as only radar and camera data from zones of high detection probability for seabirds have been included. The radar has been operating with an S2 pulse, which has an even detection probability for seabirds within the entire 3 km range of the radar, and hence no detection bias is likely to have been introduced.

Collected data

Following installation during 24-26 April 2019 the radar was optimally configured in relation to the priority species (large gulls) and the local conditions doing observations during radar tracking from the OHVS platform. After this, the calibration of the cameras took until late August before the motion detection and video tracking worked satisfactorily. Collection of monitoring data ran continuously between 1. September 2019 and 31 March 2022. The monitoring period was extended after September 2021 to allow reaching the target level of operational time of 95% during the monitoring period of 24 months. The six months extension resulted in an overall uptime of radar and cameras at or just above 100% as compared the original period of 24 months. Overviews of the performance and sample sizes of collected data are provided in figure 4 and table 3 and in chapter 5 (Analysed data).

A total of 45,311 daylight videos with bird information have been screened automatically from the period between 1 September 2019 and 31 March 2022. As seen in figure 4 the number of recorded bird radar tracks was frequently between 10,000 and 20,000, while more than 10,000 videos were mainly recorded during the first year of monitoring. During the last year of monitoring, a large number of videos was only recorded during February 2022. This reduction in the number of videos took place following the decision in mid 2021 to operate the cameras in solo mode during periods with wind speeds exceeding 10 m/sec. Also based on the experience from analysing the videos it seems that the video quality from the RVision cameras deteriorated over time which may have reduced the number of good quality videos further during the last part of the monitoring period.

Weather conditions

Based on wind data collected in the LUD offshore wind farm at intervals of 10 minutes examples of the prevailing wind conditions during the period July 2020 to June 2021 are shown in figure 5. Unsurprisingly, the site is dominated by southwesterlies, and often accompanied by rather strong wind speeds due to the exposure to winds from the west. However, winds from the east are frequent, and dominated the months of April and June 2021. Calm conditions with wind speeds below 6 m/sec occur relatively infrequently. With the exception of June 2021 calm conditions occurred in less than 5% of the time during the depicted period.

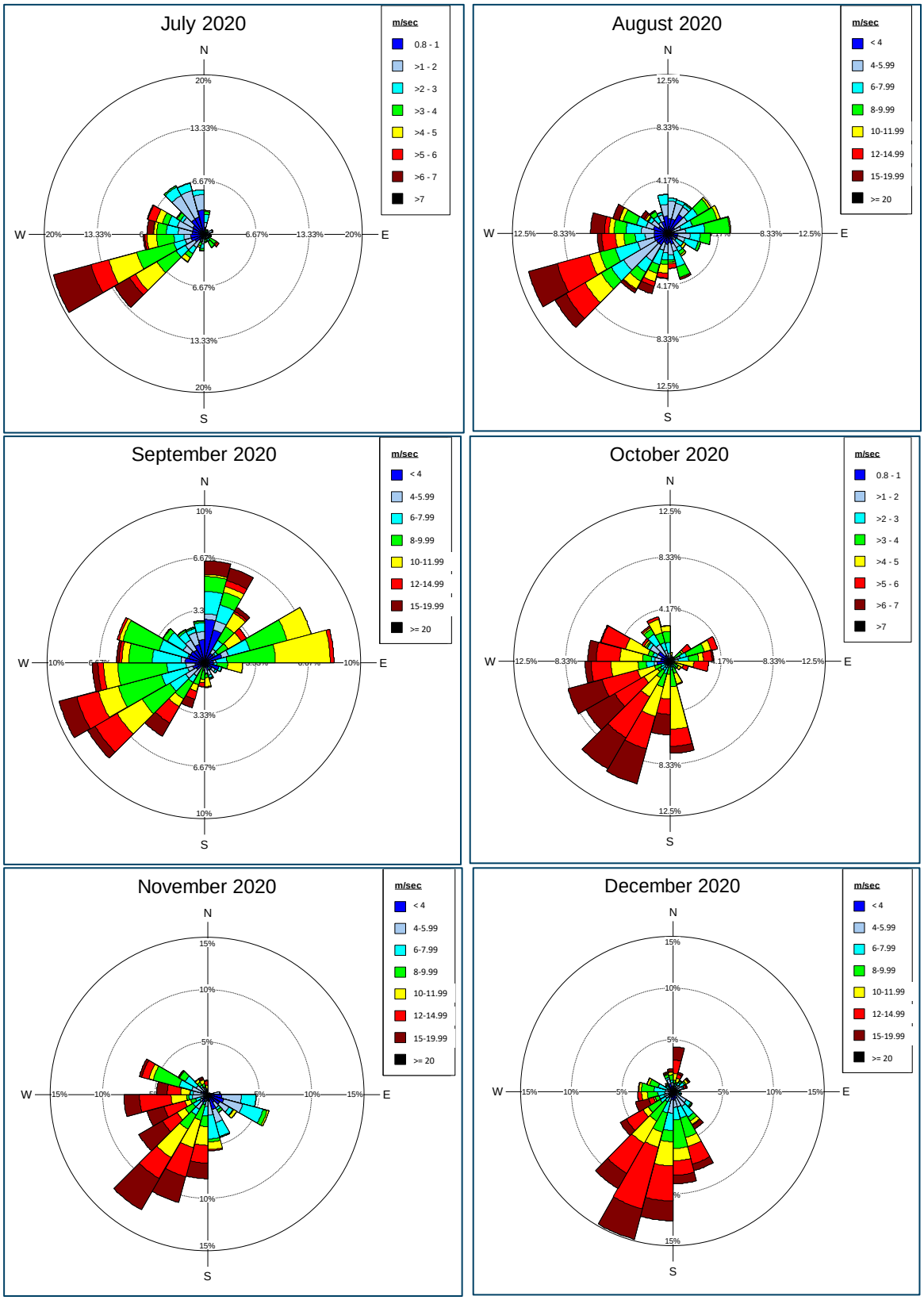
July 2020
m/sec
0.8 - 1
>1 - 2
>2 - 3
>3 - 4
>4 - 5
>5 - 6
>6 - 7
>7
N
W
E
S
August 2020
m/sec
< 4
4-5.99
6-7.99
8-9.99
10-11.99
12-14.99
15-19.99
>= 20
September 2020
October 2020
November 2020
December 2020

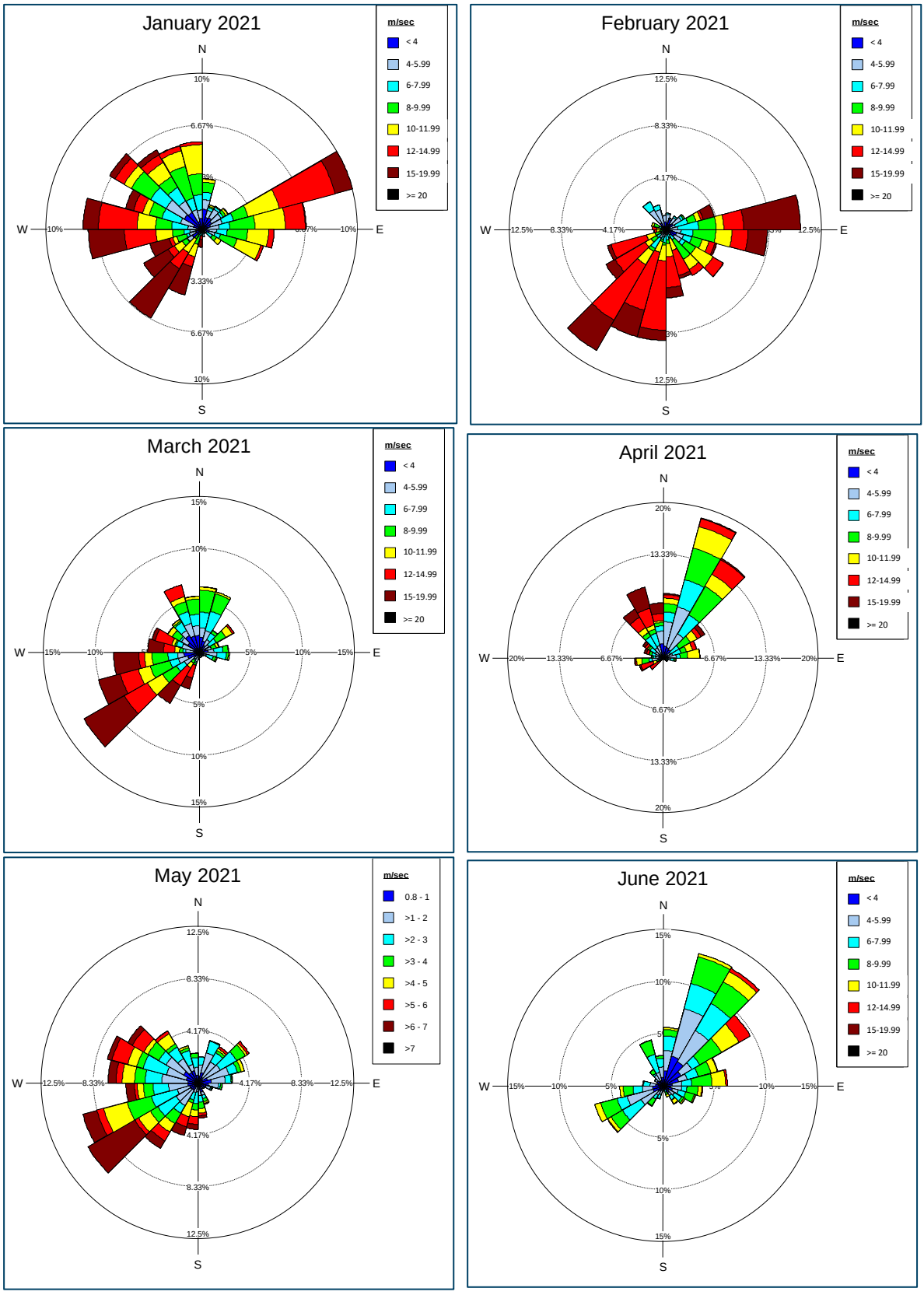

Figure 5 Wind conditions (wind speed and direction) in LUD shown as monthly wind roses for the period July 2020 to June 2021

1 Analyses

1.1 Analysed data

A total of 45,311 daylight videos with bird information have been screened automatically from the period between 1 September 2019 and 31 March 2022. The screening process was undertaken using a machine learning algorithm which has been trained on historic bird videos to detect flying birds from other moving objects recorded on video. The screening of these videos recognised 9,702 videos or 21.4% with bird information, based on bird presence in >1% of frames. By manual screening, this number was reduced to 5,250 videos or 11.6%.

The vast majority or 97.2% of the videos recorded birds had a meso avoidance behaviour, i.e. flying within the windfarm footprint area, but outside the rotor swept zone (Table 3). A much smaller proportion of the videos or 2.8% showed birds flying in the micro zone. Two of the videos contained recordings of bird collisions. Based on the video data it was possible to identify 13 different bird species as well as several species groups or pairs, but a small subset contained videos of birds that could not be identified or classified at any level. The species tracked and identified from the videos included both low-flying species like cormorants and higher-flying species like gulls. There was a noticeable difference in both the number of videos and the number of bird species recorded between the four cameras.

A total of 256 radar tracks had associated video data with information on large gulls (Table 4). The majority of coupled radar tracks and videos were collected after 1 June 2020 when the settings in the digital communication between radar and cameras were changed. Before 1 June 2020, cameras could block information from the radar if they were engaged in tracking in solo mode. After 1 June, camera tracking in solo mode is only allowed during adverse weather conditions (wind speed > 10 m/sec) to allow for the generation of as large a sample of linked radar and camera data as possible. The change between dual and solo mode was controlled automatically by real-time wind measurements from LUD.

Table 3 Overview of analysed video d

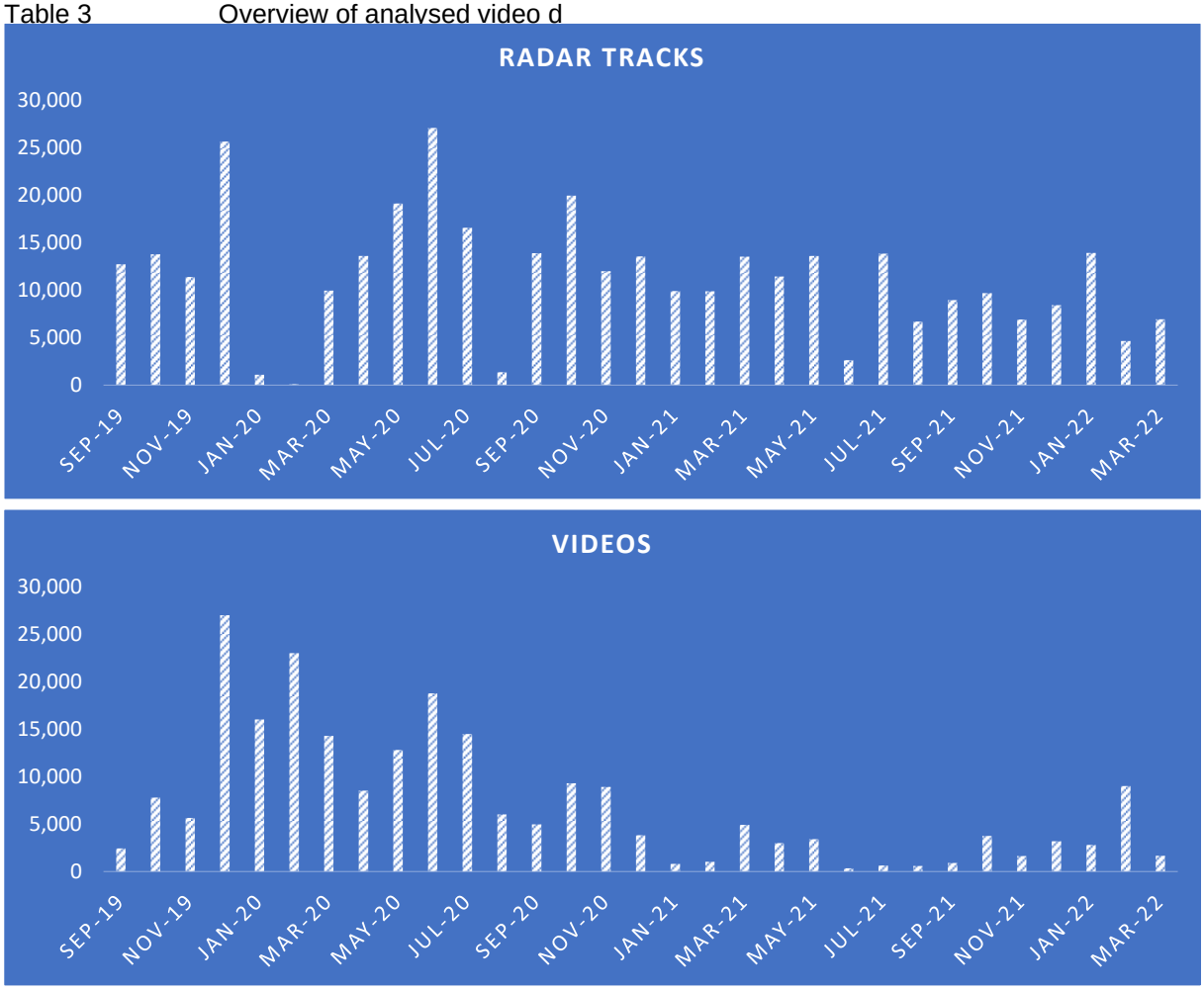

Figure 4 Number of recorded radar tracks and bird videos per month of monitoring

Table 2 Performance indicators and sample sizes collected by the monitoring equipment (daylight and night-time).

Performance indicators:

Month	Radar track data	Camera T 11	Camera T 15	Camera T 27	Camera T 38	Radar screen images
September 2019 Coverage %	90%	99%	73%	99%	99%	99%
September 2019 Downtime dates	Tracker down 5-6 Sep Outage 23 Sep	Outage 23 Sep	Outage 23 Sep and subsequent power failure until 30 Sep	Outage 23 Sep	Outage 23 Sep	Outage 23 Sep
October 2019 Coverage %	95%	87%	36%	87%	87%	95%
October 2019 Downtime dates	Maintenance OHVR 7 Oct Outages 7-10 Oct	Outages 7-10 Oct	No connection from power failure 30 Sep until 20 Oct	Outages 7-10 Oct	Outages 7-10 Oct	Maintenance OHVR 7 Oct Outages 7-10 Oct
November 2019 Coverage %	98%	63%	57%	77%	73%	98%
November 2019 Downtime dates	Outages 20-21 Nov	Outages 20-21 Nov No contact to T11 after 26 Nov	Outages 20-21 Nov	Outages 20-21 Nov	Outages 20-21 Nov	Outages 20-21 Nov
December 2019 Coverage %	99%	0%	100%	100%	100%	45%
December 2019 Downtime dates		No contact to T11 all month				Framegrabber stopped between 3 and 19 December
January 2020 Coverage %	100%	No contact to T11 all month	100%	100%	100%	100%
January 2020 Downtime dates						
February 2020 Coverage %	72.4%	79.3%	100%	100%	100%	72.4%
February 2020 Downtime dates	NAS server breakdown 14-21 Feb	Contact re-established				NAS server breakdown 14-21 Feb

Month	Radar track data	Camera T 11	Camera T 15	Camera T 27	Camera T 38	Radar screen images
March 2020 Coverage %	38.7%	74.2%	74.2%	74.2%	74.2%	93.5%
March 2020 Downtime dates	Outages 16 and 31 Mar Malfunctioning MUSE communication after 16 March	Outages 16 and 31 Mar Malfunctioning MUSE communication after 16 March	Outages 16 and 31 Mar Malfunctioning MUSE communication after 16 March	Outages 16 and 31 Mar Malfunctioning MUSE communication after 16 March	Outages 16 and 31 Mar Malfunctioning MUSE communication after 16 March	Outages 16 and 31 Mar
April 2020 Coverage %	64%	86.7%	100.0%	100.0%	100.0%	100.0%
April 2020 Downtime dates	Malfunctioning MUSE database manager before 11 April	Videos not saved 18-21 April				
May 2020 Coverage %	100.0%	100.0%	100.0%	100.0%	100.0%	100.0%
May 2020 Downtime dates						
June 2020 Coverage %	100.0%	100.0%	100.0%	100.0%	100.0%	100.0%
June 2020 Downtime dates						
July 2020 Coverage %	91.3%	96.8%	93.5%	96.8%	96.8%	96.8%
July 2020 Downtime dates	Radar tracks not saved 14-16'th of July	Communication with camera malfunctioning 16'th of July	Communication with camera malfunctioning 16' and 31'st of July	Communication with camera malfunctioning 16'th of July	Communication with camera malfunctioning 16'th of July	Data stream off 31st of July
August 2020 Coverage %	13%	100%	100%	100%	100%	13%
August 2020 Downtime dates	Malfunctioning On/Off switch on the OHVS In addition, maintenance on 8/8, 24/8, 25/8 and 31/8					Malfunctioning On/Off switch on the OHVS In addition, maintenance on 8/8, 24/8, 25/8 and 31/8

Month	Radar track data	Camera T 11	Camera T 15	Camera T 27	Camera T 38	Radar screen images
September 2020 Coverage %	45%	78%	78%	78%	78%	95%
September 2020 Downtime dates	Malfunctioning On/Off switch on the OHVS	Malfunctioning On/Off switch on the OHVS	Malfunctioning On/Off switch on the OHVS	Malfunctioning On/Off switch on the OHVS	Malfunctioning On/Off switch on the OHVS	Malfunctioning On/Off switch on the OHVS
October 2020 Coverage %	100%	100%	100%	100%	100%	100%
October 2020 Downtime dates						
November 2020 Coverage %	100%	100%	100%	100%	100%	100%
November 2020 Downtime dates						
December 2020 Coverage %	100%	100%	100%	100%	100%	100%
December 2020 Downtime dates						
January 2021 Coverage %	100%	100%	100%	100%	100%	100%
January 2021 Downtime dates		10 days with no videos				
February 2021 Coverage %	89.3%	78.6%	78.6%	78.6%	78.6%	92.9%
February 2021 Downtime dates	7-8/2 MUSE communication stalled	7-8/2 MUSE communication stalled	7-8/2 MUSE communication stalled	7-8/2 MUSE communication stalled	7-8/2 MUSE communication stalled	27/2 – 28/2
March 2021 Coverage %	90%	100%	100%	100%	100%	90%
March 2021 Downtime dates	Full server disk 1/3 – 3/3					Full server disk 1/3 – 3/3

Month	Radar track data	Camera T 11	Camera T 15	Camera T 27	Camera T 38	Radar screen images
April 2021 Coverage %	87%	87%	87%	87%	87%	87%
April 2021 Downtime dates	Radar stand-by following service visit to platform 15-19 April	Radar stand-by following service visit to platform 15-19 April	Radar stand-by following service visit to platform 15-19 April	Radar stand-by following service visit to platform 15-19 April	Radar stand-by following service visit to platform 15-19 April	Radar stand-by following service visit to platform 15-19 April
May 2021 Coverage %	68%	90%	90%	90%	90%	100%
May 2021 Downtime dates	1-5/5, 13/5, 20-23/5	1-2/5, 13/5	1-2/5, 13/5	1-2/5, 13/5	1-2/5, 13/5	
June 2021 Coverage %	40%	50%	0%	50%	50%	100%
June 2021 Downtime dates	Large maintenance activities 1/6, 5-7/6, 9-16/6, 18-20/6, 22-23/6, 30/6	Large maintenance activities 1/6, 5-7/6, 10-16/6, 18-20/6, 30/6	Network string failure 1-30/6	Large maintenance activities 1/6, 5-7/6, 10-16/6, 18-20/6, 30/6	Large maintenance activities 1/6, 5-7/6, 10-16/6, 18-20/6, 30/6	
July 2021 Coverage %	55%	77%	0%	77%	77%	100%
July 2021 Downtime dates	Maintenance activities 1-7/7, 14-16/7, 28-31/7	Maintenance activities 1-6/7, 31/7	Network string failure 1-31/7	Maintenance activities 1-6/7, 31/7	Maintenance activities 1-6/7, 31/7	
August 2021 Coverage %	90%	35%	0%	81%	90%	100%
August 2021 Downtime dates	Radar stand-by following service visit to platform 2/8, 5/8, 13/8	5-6/8, 10-15/8, 19-27/8, 29-31/8	Network string failure 1-31/8	4-5/8, 11/8, 16-17/8, 19/8	5-6/8, 19/8	

Month	Radar track data	Camera T 11	Camera T 15	Camera T 27	Camera T 38	Radar screen images
September 2021 Coverage %	47%	40%	27%	60%	60%	100%
September 2021 Downtime dates	Maintenance activities 4-5/9, 11-12/9, 14/9, Strong weather and stalled radar tracker 16-24/9, strong weather 27-30/9	No connection to camera 1-2/9, 4-5/9,11-13/9, 15-24/9, 28/9	Network string failure 1-22/9	No connection to camera 1/9, 4-5/9,11-12/9, 16-22/9	No connection to camera 4-5/9,11-12/9, 16-22/9, 24/9	
October 2021 Coverage %	100%	100%	100%	100%	100%	100%
October 2021 Downtime dates						
November 2021 Coverage %	80%	90%	90%	90%	90%	100%
November 2021 Downtime dates	Radar stand-by following service visit to platform 4-8/11, 25/11 Strong weather 17-22/11, 30/11	Camera off following service visit to platform 4-8/11, 25/11	Camera off following service visit to platform 4-8/11, 25/11	Camera off following service visit to platform 4-8/11, 25/11	Camera off following service visit to platform 4-8/11, 25/11	
December 2021 Coverage %	100%	100%	100%	100%	100%	100%
December 2021 Downtime dates	Radar stand-by following service visit to platform 17-19/12	Radar stand-by following service visit to platform 17-19/12	Radar stand-by following service visit to platform 17-19/12	Radar stand-by following service visit to platform 17-19/12	Radar stand-by following service visit to platform 17-19/12	

Month	Radar track data	Camera T 11	Camera T 15	Camera T 27	Camera T 38	Radar screen images
January 2022 Coverage %	84%	100%	100%	100%	100%	100%
January 2022 Downtime dates	Strong weather 27-31/1					
February 2022 Coverage %	89%	100%	100%	100%	100%	100%
February 2022 Downtime dates	19-21/2, strong weather					
March 2022 Coverage %	45%	77%	81%	94%	94%	48%
March 2022 Downtime dates	1-2/3, 15-17/3, Radar stand-by following service visit to platform 19-31/3 NAS-drive full	1-2/3 Radar stand-by following service visit to platform	1-2/3 Radar stand-by following service visit to platform	1-2/3 Radar stand-by following service visit to platform	1-2/3 Radar stand-by following service visit to platform	15-31/3 NAS-drive full

Sample sizes (video level reflects the number of camera movements which is indicative of length and quality of video in terms of showing bird behaviour):

Month	Number of radar bird tracks	Number of videos Level 0	Number of videos Level 1-2	Number of videos Level 3-5	Number of videos >= Level 6
September 2019	12,738	7,782	1,450	564	442
October 2019	13,800	2,445	1,628	3,240	2,925
November 2019	11,406	5,870	2,643	1,266	1,759
December 2019	25,676	7,174	12,990	5,650	8,366
January 2020	1,098	1,131	7,961	3,734	4,330
February 2020	102	1,588	10,788	8,385	3,848
March 2020	9,966	721	7,360	4,693	2,249
April 2020	13,616	838	5,670	2,130	733
May 2020	19,155	900	7,532	3,492	1,782
June 2020	27,099	1,152	10,043	5,794	2,956
July 2020	16,600	1,624	6,199	5,141	3,155
August 2020	1,382	239	2,292	1,932	1,790
September 2020	13,925	2,688	1,529	1,758	1,694
October 2020	19,987	309	3,024	3,818	2,468
November 2020	12,002	296	2,874	3,678	2,374
December 2020	13,582	1,431	1,378	1,488	974
January 2021	9,919	1,463	386	245	181
February 2021	9,900	1,777	639	316	76
March 2021	13,547	2,046	1,080	2,191	1,669
April 2021	11,453	1,230	1,081	1,195	720
May 2021	13,629	2,106	1,237	1,268	917
June 2021	2,648	821	173	142	41
July 2021	13,876	1,714	371	184	82
August 2021	6,712	459	226	210	156
September 2021	8,961	1,217	395	304	202
October 2021	9,701	1,341	1,029	1,508	1,218
November 2021	6,923	1,069	580	628	438
December 2021	8,434	789	522	1,405	1,285
January 2022	13,937	2,468	1,081	1,121	612
February 2022	4,664	1,144	2,376	3,944	2,691
March 2022	6,960	5,170	697	628	330

*Video level reflects the number of camera movements which is indicative of length and quality of video in terms of showing bird behaviour

2 Weather conditions

Based on wind data collected in the LUD offshore wind farm at intervals of 10 minutes examples of the prevailing wind conditions during the period July 2020 to June 2021 are shown in figure 5. Unsurprisingly, the site is dominated by southwesterlies, and often accompanied by rather strong wind speeds due to the exposure to winds from the west. However, winds from the east are frequent, and dominated the months of April and June 2021. Calm conditions with wind speeds below 6 m/sec occur relatively infrequently. With the exception of June 2021 calm conditions occurred in less than 5% of the time during the depicted period.

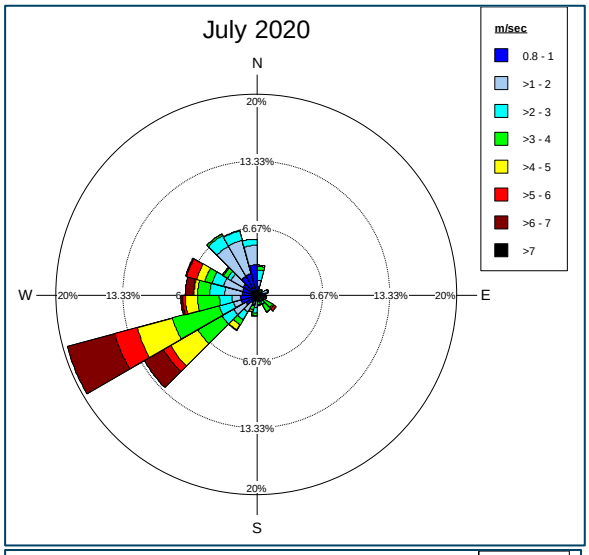
July 2020
m/sec
0.8 - 1
>1 - 2
>2 - 3
>3 - 4
>4 - 5
>5 - 6
>6 - 7
>7
N
S
W
E
20%
13.33%
6.67%

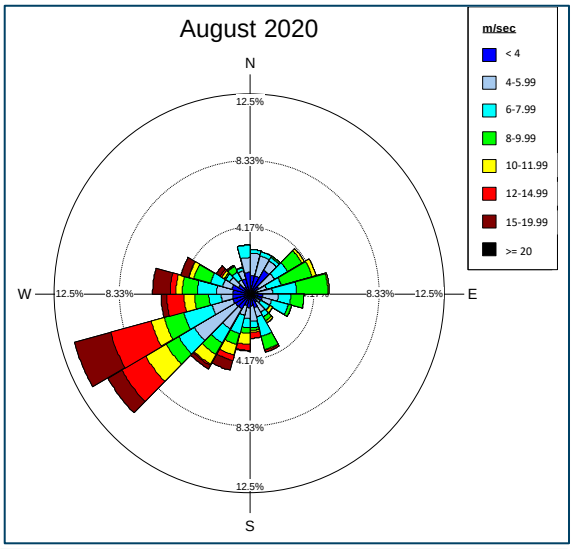
August 2020
m/sec
< 4
4-5.99
6-7.99
8-9.99
10-11.99
12-14.99
15-19.99
>= 20
N
S
W
E
12.5%
8.33%
4.17%

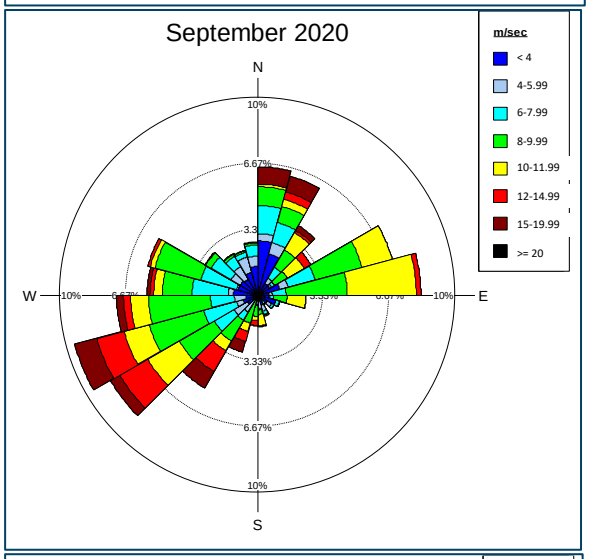
September 2020
m/sec
< 4
4-5.99
6-7.99
8-9.99
10-11.99
12-14.99
15-19.99
>= 20
N
S
W
E
10%
6.67%
3.33%

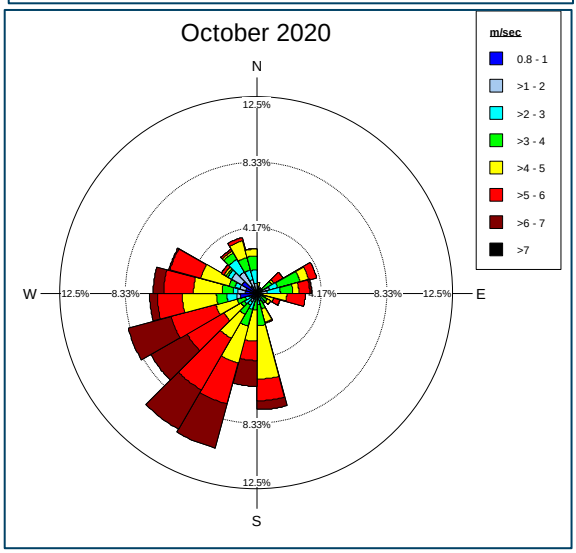
October 2020
m/sec
0.8 - 1
>1 - 2
>2 - 3
>3 - 4
>4 - 5
>5 - 6
>6 - 7
>7
N
S
W
E
12.5%
8.33%
4.17%

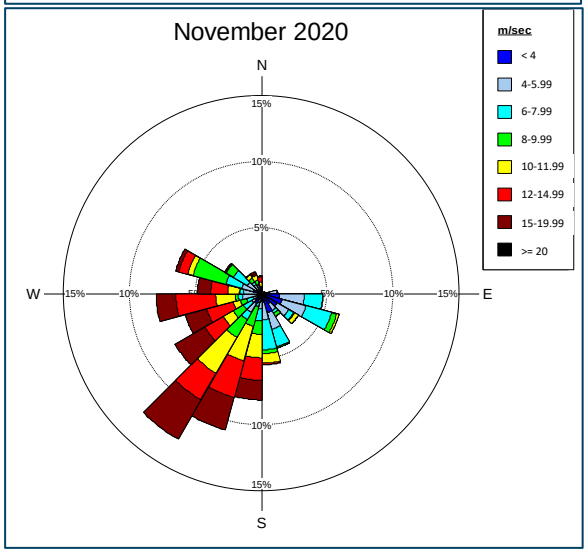
November 2020
m/sec
< 4
4-5.99
6-7.99
8-9.99
10-11.99
12-14.99
15-19.99
>= 20
N
S
W
E
15%
10%
5%

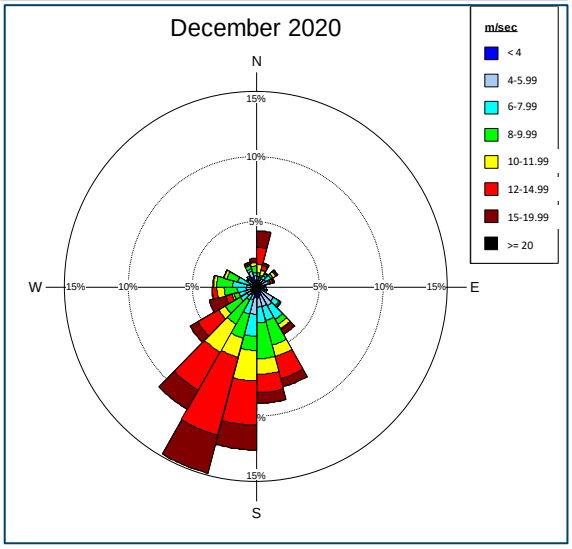
December 2020
m/sec
< 4
4-5.99
6-7.99
8-9.99
10-11.99
12-14.99
15-19.99
>= 20
N
S
W
E
15%
10%
5%

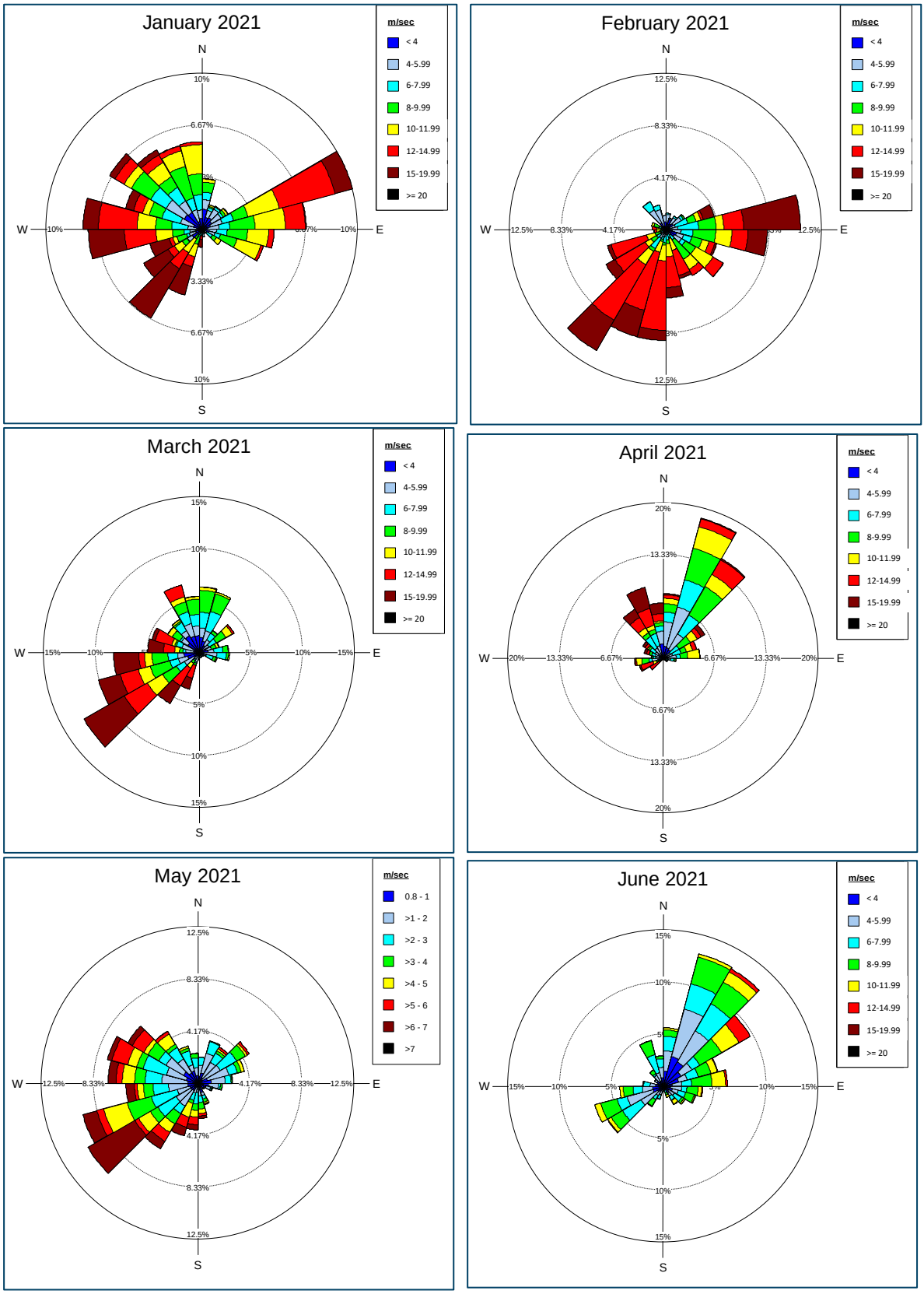

Figure 5 Wind conditions (wind speed and direction) in LUD shown as monthly wind roses for the period July 2020 to June 2021

3 Analyses

3.1 Analysed data

A total of 45,311 daylight videos with bird information have been screened automatically from the period between 1 September 2019 and 31 March 2022. The screening process was undertaken using a machine learning algorithm which has been trained on historic bird videos to detect flying birds from other moving objects recorded on video. The screening of these videos recognised 9,702 videos or 21.4% with bird information, based on bird presence in >1% of frames. By manual screening, this number was reduced to 5,250 videos or 11.6%.

The vast majority or 97.2% of the videos recorded birds had a meso avoidance behaviour, i.e. flying within the windfarm footprint area, but outside the rotor swept zone (Table 3). A much smaller proportion of the videos or 2.8% showed birds flying in the micro zone. Two of the videos contained recordings of bird collisions. Based on the video data it was possible to identify 13 different bird species as well as several species groups or pairs, but a small subset contained videos of birds that could not be identified or classified at any level. The species tracked and identified from the videos included both low-flying species like cormorants and higher-flying species like gulls. There was a noticeable difference in both the number of videos and the number of bird species recorded between the four cameras.

A total of 256 radar tracks had associated video data with information on large gulls (Table 4). The majority of coupled radar tracks and videos were collected after 1 June 2020 when the settings in the digital communication between radar and cameras were changed. Before 1 June 2020, cameras could block information from the radar if they were engaged in tracking in solo mode. After 1 June, camera tracking in solo mode is only allowed during adverse weather conditions (wind speed > 10 m/sec) to allow for the generation of as large a sample of linked radar and camera data as possible. The change between dual and solo mode was controlled automatically by real-time wind measurements from LUD.

Table 3 Overview of analysed video data

TURBINE	SPECIES	VIDEOS IN MESO ZONE	VIDEOS IN MICRO ZONE	COLLISION
T11	Unidentified large gull	423	6	
	Unidentified gull	157	4	
	Lesser black-backed gull	118	7	
	Great/Lesser black-backed gull	84	8	
	Unidentified bird	69		
	Great black-backed gull	84	3	
	Herring gull	79	1	
	Herring/Lesser black-backed gull	35	4	
	Great cormorant	10		
	Northern gannet	7		
	Unidentified goose	1		
	Unidentified raptor	1		
	Black-legged kittiwake	1	1	
	Unidentified seabird	2		
	Sum of records	**1,071**	**34**	**0**
T15	Herring gull	318		1
	Unidentified large gull	302	8	1
	Unidentified gull	119		
	Unidentified bird	57		
	Common gull	55		
	Northern gannet	57		
	Great black-backed gull	98	1	
	Great cormorant	50	1	
	Unidentified small gull	19	1	
	Lesser black-backed gull	25		
	Black-legged kittiwake	8		
	Unidentified duck	8		
	Great/Lesser black-backed gull	5	2	
	Common scoter	3		
	Grey heron	1		
	Northern fulmar	1		
	Unidentified seabird	5		
	Common eider	1		
	Sandwich tern	1		
	Unidentified small wader		1	
	Sum of records	**1,133**	**14**	**2**
T27	Unidentified large gull	636	21	
	Great/Lesser black-backed gull	107	10	
	Great black-backed gull	109	5	
	Lesser black-backed gull	94	5	
	Great cormorant	59	7	
	Herring gull	55	8	
	Unidentified gull	137	5	
	Northern gannet	36	3	

TURBINE	SPECIES	VIDEOS IN MESO ZONE	VIDEOS IN MICRO ZONE	COLLISION
T27 cont.	Common eider	1		
	Unidentified seabird	1		
	Unidentified bird	44		
	Herring/Lesser black-backed gull	21	3	
	Unidentified small gull	13	1	
	Common gull	11	2	
	Black-headed gull	5		
	Unidentified passerine	2		
	Unidentified duck	1		
	Sum of records	**1,334**	**70**	**0**
T38	Great Cormorant	19		
	Northern Gannet	28		
	Great/Lesser black-backed gull	6		
	Great black-backed gull	46		
	Lesser black-backed gull	27	2	
	Herring gull	47	5	
	Black-headed gull	1		
	Great Skua	2		
	Unidentified large gull	719	6	
	Unidentified small gull	2		
	Unidentified gull	201		
	Unidentified duck	1		
	Unidentified seabird	11		
	Unidentified skua	1		
	Unidentified bird	12		
	Sum of records	**1,123**	**13**	**0**

Table 4 Overview of radar tracks coupled to video data

SPECIES	Coupled radar and video tracks
Lesser black-backed gull	17
Great black-backed gull	16
Herring gull	14
Lesser/Great black-backed gull	17
Herring gull/Lesser black-backed gull	4
Unidentified large gull	196
Unidentified gull	57
Black-legged kittiwake	3
Northern gannet	1
Great cormorant	16
Unidentified bird	3
TOTAL	**344**

3.2 Analytical framework

This study focuses on estimating the meso and micro avoidance rates for large gulls recorded in the LUD wind farm. Both tracks from the radar and video footage from the four cameras have been used to assess densities and bird movements in the wind farm. The calculated avoidance rates (macro, meso and micro) will be used by the Bureau Waardenburg RWS project 'Bird Radar LUD' to estimate the overall avoidance rate. For a complete overview of the analytical framework see figure 6.

The detection sensors in LUD both operate in dual model with integrated radar and camera tracking and in solo mode with camera tracking without receiving trigger detections from the radar. Sensor dual mode with integrated radar and camera tracking was initially the priority mode of operation. In this mode the radar will always trigger the camera to record the bird movement by motion detection, and unless the camera is engaged in tracking it is available to receive information on bird targets from the radar. The camera records the bird movement for as long as the bird can be detected by the camera's motion detection. If the camera loses the target, information on the location of the bird is transferred from the radar to the camera, in which case it can continue following the bird. No target amount of sampling time in dual mode has been determined.

The performance of the radar is affected during strong weather conditions in which high waves cause the dynamic clutter filter in the MUSE software to generate a high level of false negative bird detections (failure to record birds), which affects the system when operating in dual mode. In spring 2021, it was therefore decided that the system should switch to operating in solo mode during windy condition. In solo mode the view of the camera is fixed, i.e. looking out over a specified area and awaits a target to follow by motion detection. In solo mode, a bird's movement is followed and recorded if a bird is detected in the camera frame; however, no associated radar track of its position is generated. The wind speed threshold for solo mode was set to 10 m/sec, and the camera mode was changed automatically by the system by reading wind speeds recorded by the wind farm. The use of solo mode was implemented to increase the sample size of videos of birds' movements during adverse conditions, yet resulted in a lower than expected sample of coupled radar and camera tracks.

Weather data measured in real time in LUD has been used to control the shift between dual and solo sensor mode. Wind speed measurements were integrated with the MUSE software in real-time, and when the wind speed exceeded 10 m/s the mode changed to solo mode.

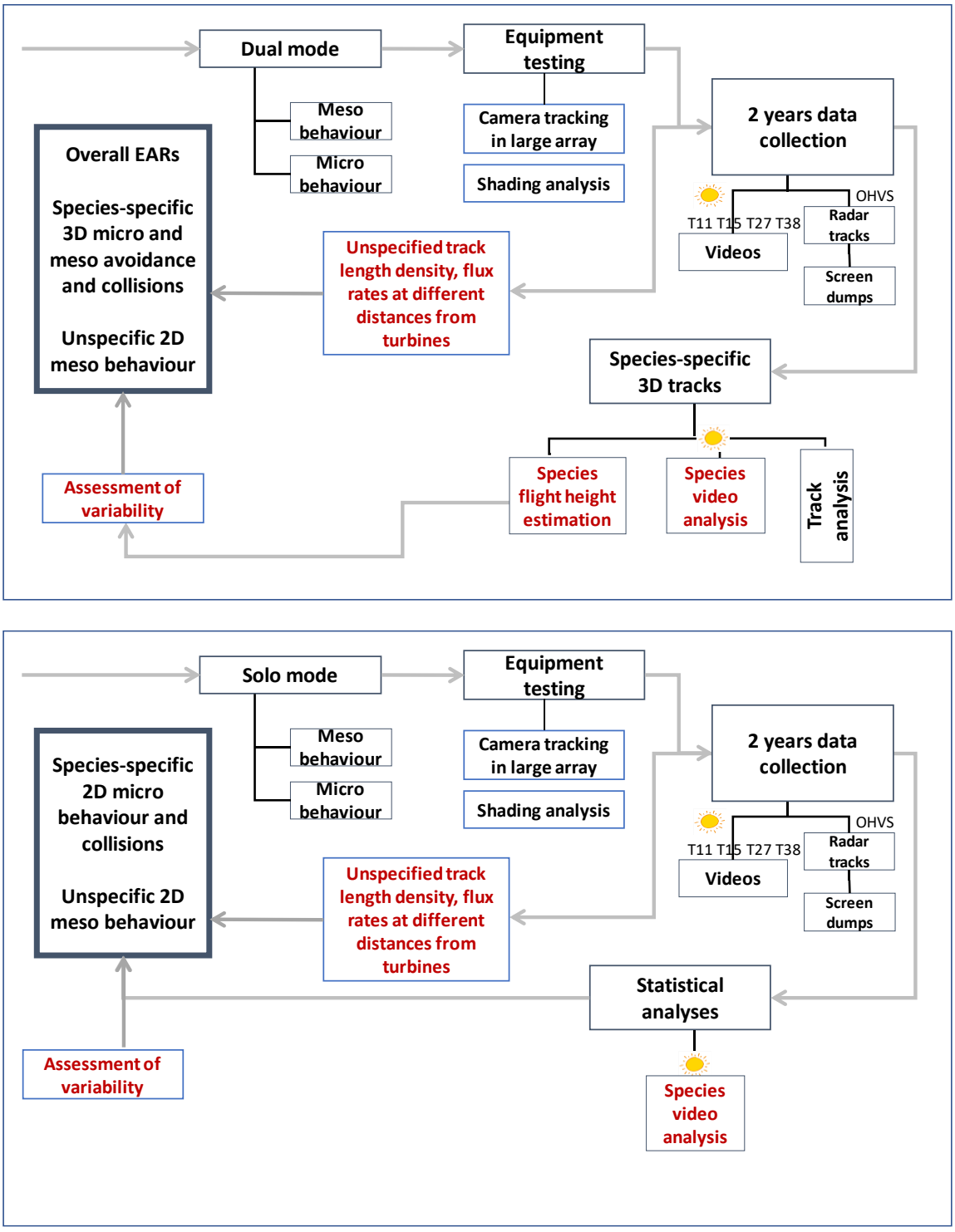

Figure 6 Overview of the analytical framework of the MEP-LUD project

3.3 Protocols applied by video analysts

Recording of tracking information by radar and cameras

- Track-id to facilitate coupling of radar tracks and videos
- Date and time
- Spatial assessment by radar (Yes/No). Judged by visual inspection of the associated radar track

Recording of weather conditions

- Judgement of sea state from the video recording according to the Beaufort wind force scale.

Recording of seabirds and flight behaviour

- Identification of target species to the level of species or species group
- Aging of bird targets if possible
- Recording of feeding/commuting behaviour, feeding including searching for prey
- Classification of seabird flight behaviour using standardized European Seabirds at Sea (ESAS) codes
- Behavioural confidence rating (high, medium, low)

Recording of the position of bird targets in space relative to turbines and rotors

- Categorization of the position of bird targets in macro-zone (outside wind farm array), meso-zone (inside wind farm array) and micro-zone (within +10m from rotors incl. orientation towards rotor plane)
- Orientation of the seabird towards the rotor
- Meso and micro-avoidance/non-avoidance behaviour of bird targets
- Collision

3.4 QA procedures for video analyses

For validation, the data generated by the video analyses were subject to quality assurance. Because of the large sample sizes of analysed videos, it was not feasible to conduct a complete quality assurance of all analysed videos. quality assurance was performed partially by jack-knifing every 10th video analysis, and in addition focusing on specific parts of the video analysis that was considered particularly important:

- All recordings of micro-avoidance and collisions, including potential collisions
- All recordings of vertical meso-avoidance

3.5 Meso-avoidance behaviour

Meso-avoidance behaviour was assessed for the target species: lesser black-backed gull, herring gull and great black-backed gull using both the radar track and video data. Species and species groups were identified using video data, and vertical meso-avoidance was also assessed with the video data. Although only a minor proportion of all radar tracks were associated with videos, the composition of bird species analysed from the videos were considered representative. This assumption is indeed valid as cameras were operating in dual mode for most of the time, during which their initial targets were triggered by the radar.

Spatial gradients in avoidance and attraction of target species within the array were quantified based on the coupled radar track and video data calculated as $1 - \frac{N_{in}}{N_{ref}}$, where N_{in} is the mean track length per unit area within the RSZ + 10 m wide buffer zones and N_{ref} is the mean track length per unit area throughout the sub-area of the wind farm covered by the cameras. The meso-avoidance rates have been calculated at 10 m intervals from the tip of the rotor blades to approximately half distance between turbines.

The meso-avoidance behaviour was further analysed 3-dimensionally by assessing spatial gradients inside the turbine array in the following derived flight parameters which combined radar tracks and coupled dual-mode videos:

- Mean flight height
- Mean flight speed
- Mean change in flight direction relative to the orientation of the rotor

The flight statistics of the above parameters were calculated separately for feeding and commuting individuals as judged from the videos.

3.6 Micro-avoidance behaviour

Assessment of micro-avoidance behaviour was primarily based on the qualitative judgements of the video analysts and quantified by calculating the proportion of birds adjusting/not adjusting their flight in the space of the rotors. The video data was screened to ensure quality data for the micro-avoidance analysis using the same process as applied in the ORJIP BCA project (Skov et al. 2018). The screening process consisted of three subsequent steps which included removing irrelevant material of movements other than birds, low quality video material and re-assessing previously coded behaviour.

The micro-avoidance analysis considered the behavioural reaction of the bird(s) to the orientation of the rotor and the presence of blades when entering the rotor swept zone (RSZ) and a 10 m buffer around it, unlike the meso-avoidance analysis, where only the position of the collected data was considered. The micro-avoidance behaviours were coded into one of the following five categories:

- Adjusting by returning before crossing the spinning rotor
- Adjusting by stopping before crossing the spinning rotor
- Adjusting flight path relative to rotor orientation when crossing the RSZ, sub-divided into different types of paths, i.e. perpendicular, oblique, along, etc
- Non-adjusting flight path and crossing the RSZ
- Collision

Figure 7 below illustrates the assessment scheme for micro-avoidance behaviour within the RSZ (blue circle) and 10 m buffer (red circle). Black arrows represent bird movement in relation to the rotor (dark blue ellipse + 10 m). The light blue arrow represents the wind direction.

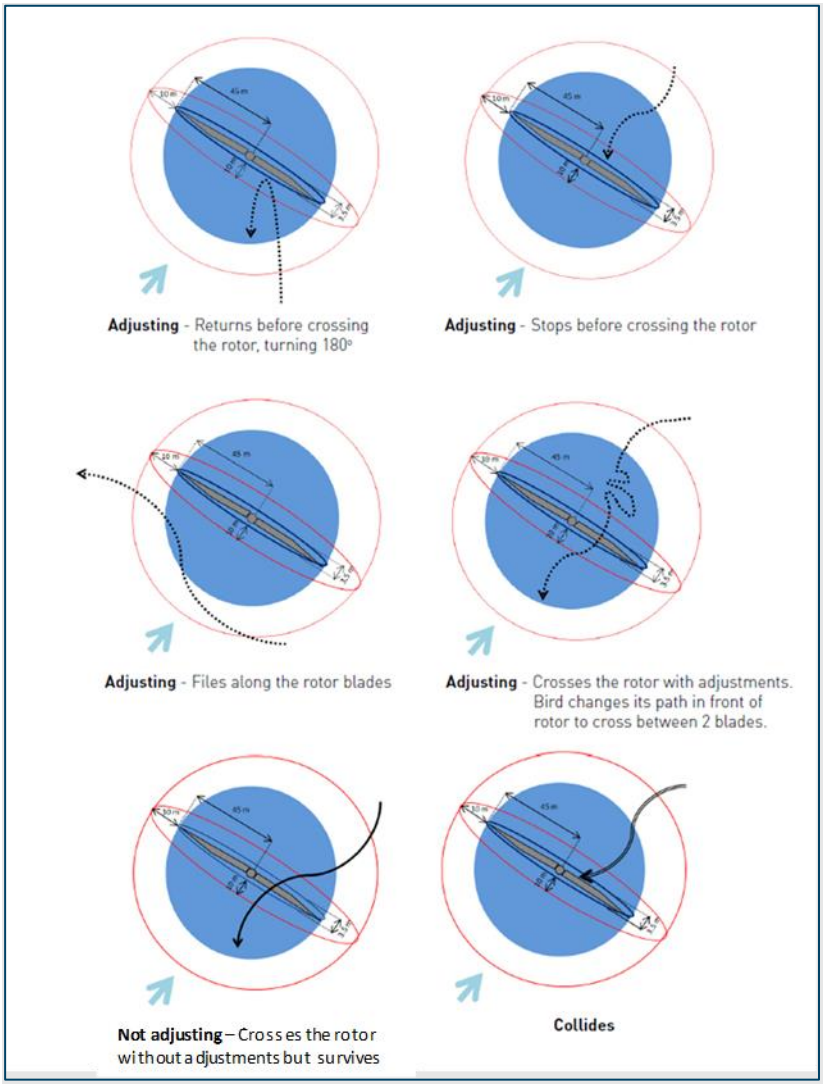

Figure 7 Assessment scheme for micro-avoidance behaviour - altered from the ORJIP BCA study (Skov et al. 2018)

Mean micro-avoidance rates for species or species groups with sufficient sample size were calculated as:

$$\frac{N_{birds\ adjusting\ flight}}{(N_{birds\ adjusting}+N_{birds\ not\ adjusting}+N_{birds\ colliding}}.$$

3.7 Collisions

Videos showing collisions between birds and rotor blades as well as videos showing potential collisions were scrutinised by at least two analysts and quality assured to reach a final judgement of collision/no collision. The details of each collision were described in terms of turbine number, bird species, bird flight behaviour on approach to the blades, collision position on the blades, and evidence of collision.

The number of recorded collisions were scaled up to the entire LUD wind farm by taking account of the coverage of turbines and the number of hours of camera operation. It was assumed that the four cameras covered 15 turbines for 26.4 months.

3.8 Flight altitude, flight speed and flight direction

Flight height was estimated by triangulating the radar and video recordings of the same individual in close to real time for selected species. The estimated flight height was added to the video track data based on the track-id. The resolution of the 3-D tracks was similar to the 2-D tracks (approximately 30 m between track nodes) which was sufficient to generate detailed statistics on flight heights in relation to distance from rotors.

Seabird flight speeds in the wind farm were estimated from the radar tracks as the mean speed per segment of a track (every 2.5 sec) rather than the mean speed measured over the whole track.

Flight directions were assessed from the radar tracks by calculating the direction of a bird relative to the orientation of the rotors at that time. The orientation of the rotor was taken as perpendicular to the wind direction measured in the wind farm by Eneco at 10-minute intervals.

3.9 Classification of feeding/commuting birds

The analysis of bird behaviour assessed from the video recordings was undertaken by a team of trained specialists, highly skilled in species identification and good knowledge of flight behaviour. The video analysts were specifically instructed to distinguish between feeding and commuting behaviour of the identified species. The video analysts first recorded if the behaviour of a bird could be assigned to either feeding or commuting based on the flight path (tortuosity or unidirectional flight) or flight behaviour (flight speed or changes herein) as well as apparent interest (or lack thereof) in local conditions. Upon the primary classification, the type of flight behaviour was further classified using standardized codes (ESAS) for seabird flight behaviour (Camphuysen & Garthe 2004). Behaviour that could not be clearly assigned to either feeding or commuting, were assigned as ‘not determined’ and thus not included in the analysis regarding differences in flight behaviour of feeding and commuting birds. A track of a bird involved in feeding during part of or during the whole video was only classified as ‘feeding’.

3.1 Flight behaviour model

Flight altitude, speed, and relative orientation in relation to wind turbine rotor were used as key parameters describing the 3-D flight and avoidance behaviour of birds in the near field of the wind turbine rotor. These three behaviours were coupled to the local wind and turbulence conditions to assess the seabird avoidance behaviour within the wind farm. The behaviours were investigated using a machine learning (ML) random forest (RF) classifier. Recently, machine learning algorithms such as RF have been shown to outperform the traditional regression-based classifiers in studies of complex interactions between species behaviour/distribution and environmental

variables (Breiman 2001). The traditional regression modelling approaches are strictly assumption based (e.g., normality, data independency, and additivity) and the predictor variables need to be pre specified. These model assumptions are seldom true in an ecological context. In case of a large number of explanatory variables, the traditional regression-based approaches have a tendency of overfitting the data unless some information criteria such as Akaike Information Criterion (AIC) are employed to reduce the number of parameters.

Here the avoidance-related flight behaviours of target species were coupled to the wind conditions at the time of observation with a precision of 1 hour. Predictor variables were wind speed (m/s), and wind class (headwind, tailwind, sidewind). Distance to the tip of rotor blades of the nearest turbine was also included as a predictor as evidence from the avoidance study in the Aberdeen Offshore Wind Farm indicates that seabirds change their meso-avoidance behaviour as a function of distance to the turbines (Tjørnløv et al. 2021).

The relationship between flight patterns and wind conditions are likely to be non-linear, as avoidance is erratic by nature. Additionally, the bird movements inferred from the radar track nodes were spatially autocorrelated, as the position of a bird in a specific time is highly dependent on the previous position of the bird. Thus, the RF classifier was selected as appropriate. Furthermore, RF allows for fitting of non-linear relationships, while also being less sensitive to temporal and spatial auto-correlation than other non-linear methods like generalized additive models (Skov & Heinänen 2013).

3.1.1 Weather data

Data on wind speed (m/s) and wind direction was derived from weather data collected at one turbine within the wind farm. The temporal resolution of the collected weather data was averaged over one hour. Local measurements of wind speed and wind direction were then temporally assigned to the radar bird tracks based on their time stamps.

3.1.1 Fitting of seabird flight model

The avoidance behaviour model was fitted as a multivariate RF classifier, using the r-package RandomForestSRC. Rather than fitting each behavioural response in a univariate model, the multivariate setup allows for using the other models as covariates, when modelling each behaviour (Segal & Xiao 2011).

An individual model was fitted for each species group, based on a subset of data, only using observations of the target species group. Subsequently, all three behaviours were fitted as dependent variables and climatic variables as independent using the training data set. The number of trees grown and number of variables tested per split were optimized for each species using the tune function (package RandomForestSRC).

Model residuals from each behaviour were calculated and residual autocorrelation was estimated. Additionally, model coefficients and variable importance were extracted. Model precision was estimated OOB (out-of-bag) error rate, along with a prediction on the training data and a subsequent comparison between observed and predicted values from the training data set, using Spearman's and Pearson's correlation coefficients.

3.1.2 Predicting flight behaviour around rotors

The flight behaviour around the turbine rotors was predicted using static deployment data, where only one predictor would vary, keeping all other predictors steady. As the key interest was to see how birds changed their behaviour when closing in on rotors, distance to rotor was selected as the varying predictor. Next, two climatic scenarios were created, with high/low wind speeds. Based on recorded wind speeds in LUD, high wind speeds were defined as 11m/s wind, and low wind speeds was defined as 1 m/s. Each scenario was predicted with a relative wind direction of head wind, tail wind and side wind, resulting in a total of 6 predictions per species group.

The results of the flight models are presented in the chapters covering each of the flight parameters. The validation of the models can be found in Appendix 5.

4 Dynamics of seabirds in LUD

4.1 Northern gannet

Northern gannet was only recorded irregularly in LUD during the monitoring period (figure 8). Even during the main period of post-breeding dispersal few birds were observed by the cameras. Surprisingly, an influx was recorded during January 2020. The background for this influx is not known.

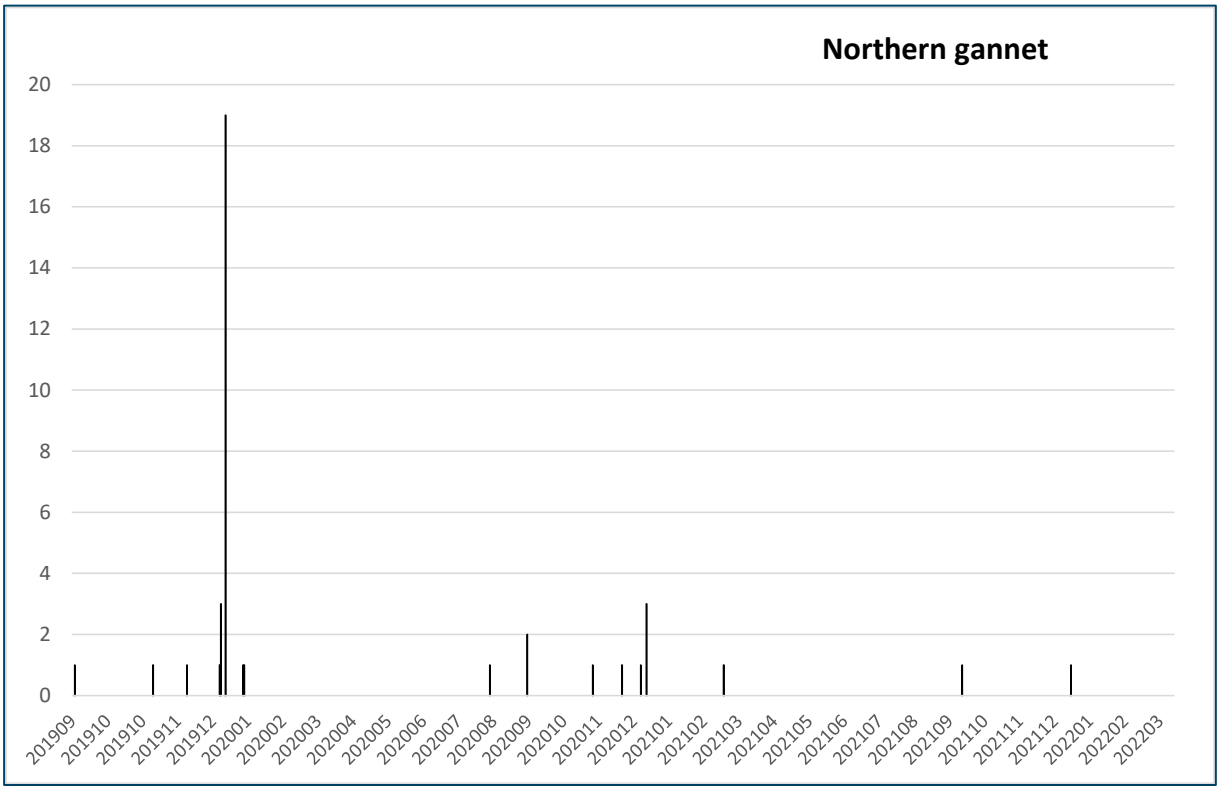

Figure 8 Temporal distribution of Northern gannets in videos between September 2019 and March 2022. Graph shows total number of videos per day

4.2 Large gulls

There was a considerable variation over time in the number of individuals of different species of large gulls recorded by the four cameras. While Great black-backed gulls occurred in small numbers but regularly during most of the year, the majority of Lesser black-backed gulls and Herring gulls were recorded during a much more narrow time window in June and July 2020. In general, the number of large gull species recorded in the videos varied substantially between the four turbines. Great black-backed gulls were recorded almost equally frequently by cameras at all four turbines, hence both close to the wind farm perimeter and closer to the wind farm centre. In contrast, Herring gulls were more frequently recorded at turbine 15, than at the other three turbines, whereas Lesser-blacked gulls were most frequently recorded at turbine 11 and 27, with

very few records at turbines 15 and 38. These spatial patterns may reflect species-specific flight routes through the windfarm area or may simply be a result of differences in distance to the different cameras or turbines because identification declines with distance.

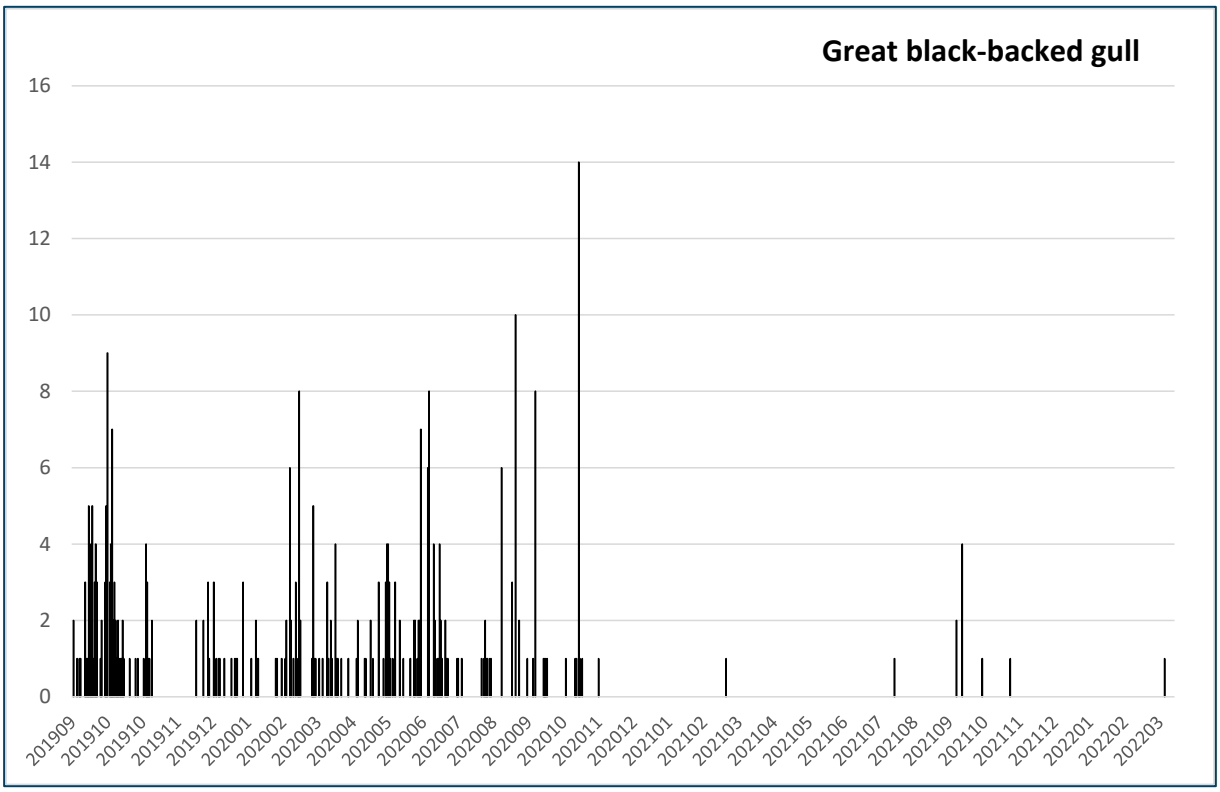

Figure 9 Temporal distribution of Great black-backed gulls in videos between September 2019 and March 2022. Graph shows total number of videos per day

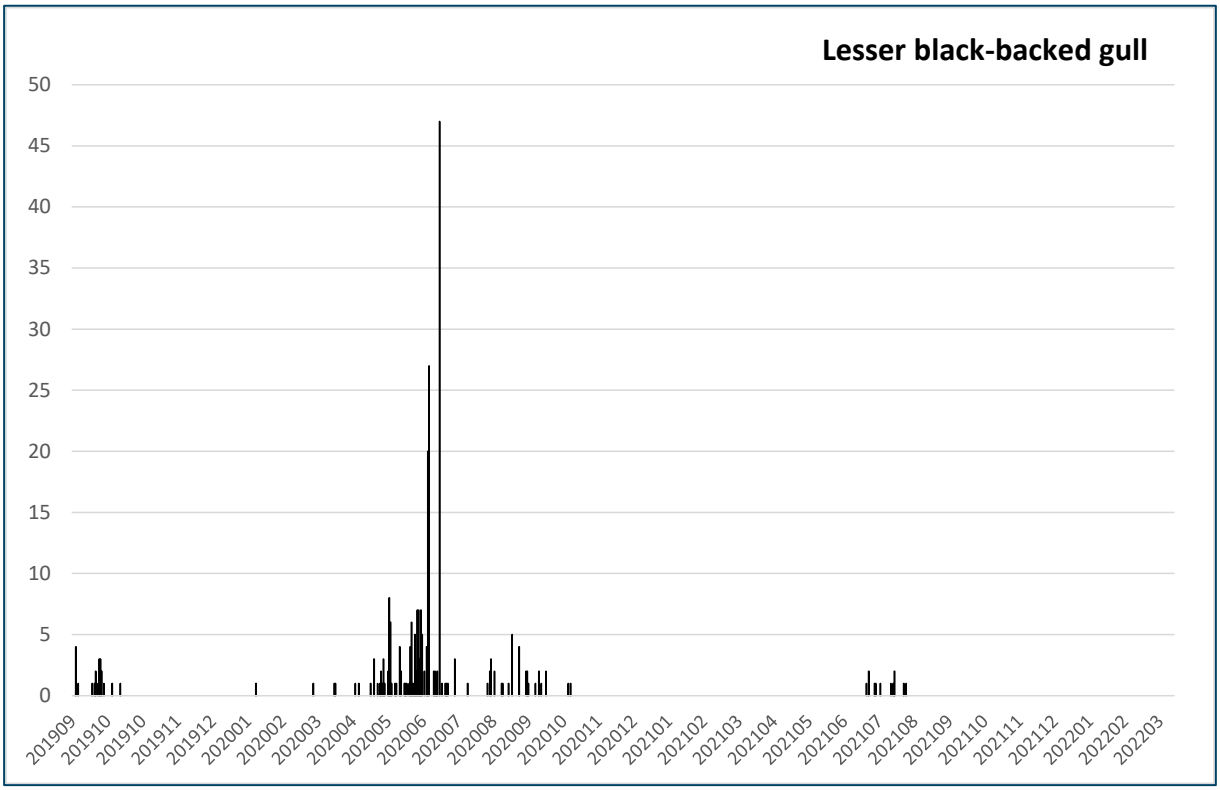

Figure 10 Temporal distribution of Lesser black-backed gulls in videos between September 2019 and March 2022. Graph shows total number of videos per day

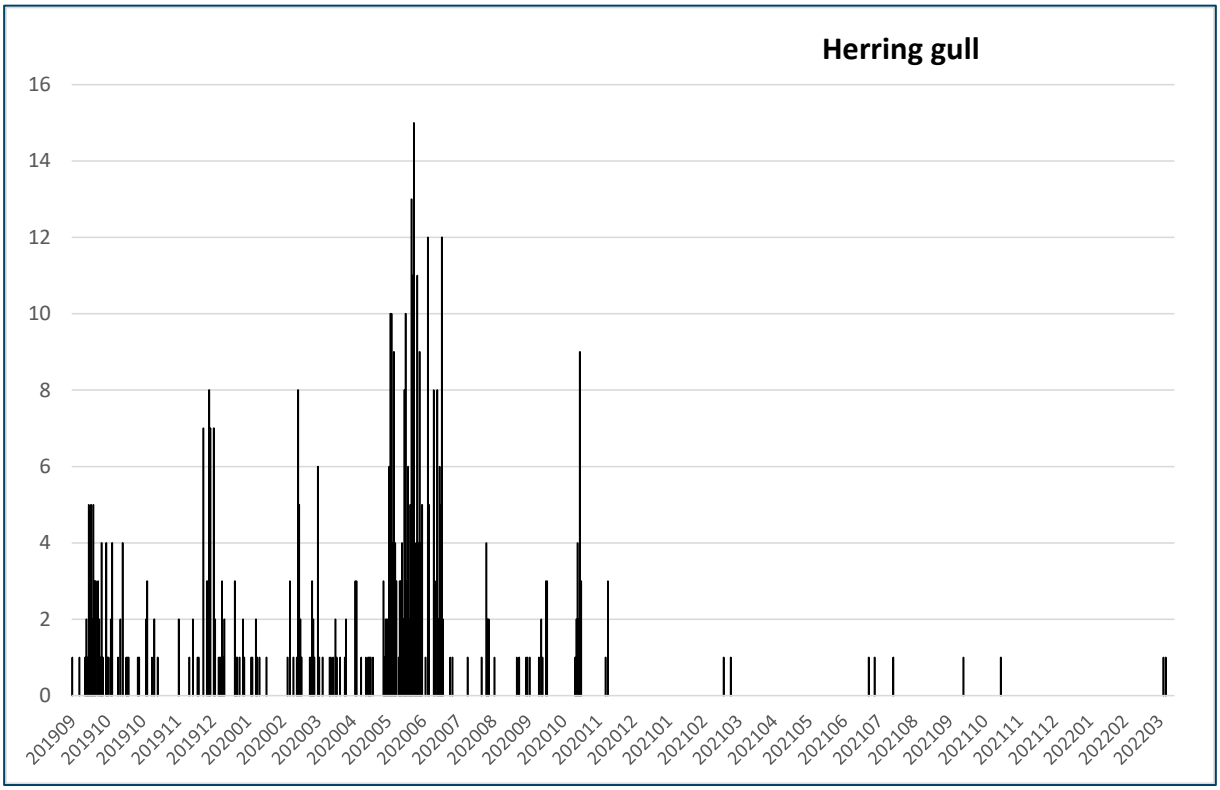

Figure 11 Temporal distribution of Herring gulls in videos between September 2019 and March 2022. Graph shows total number of videos per day

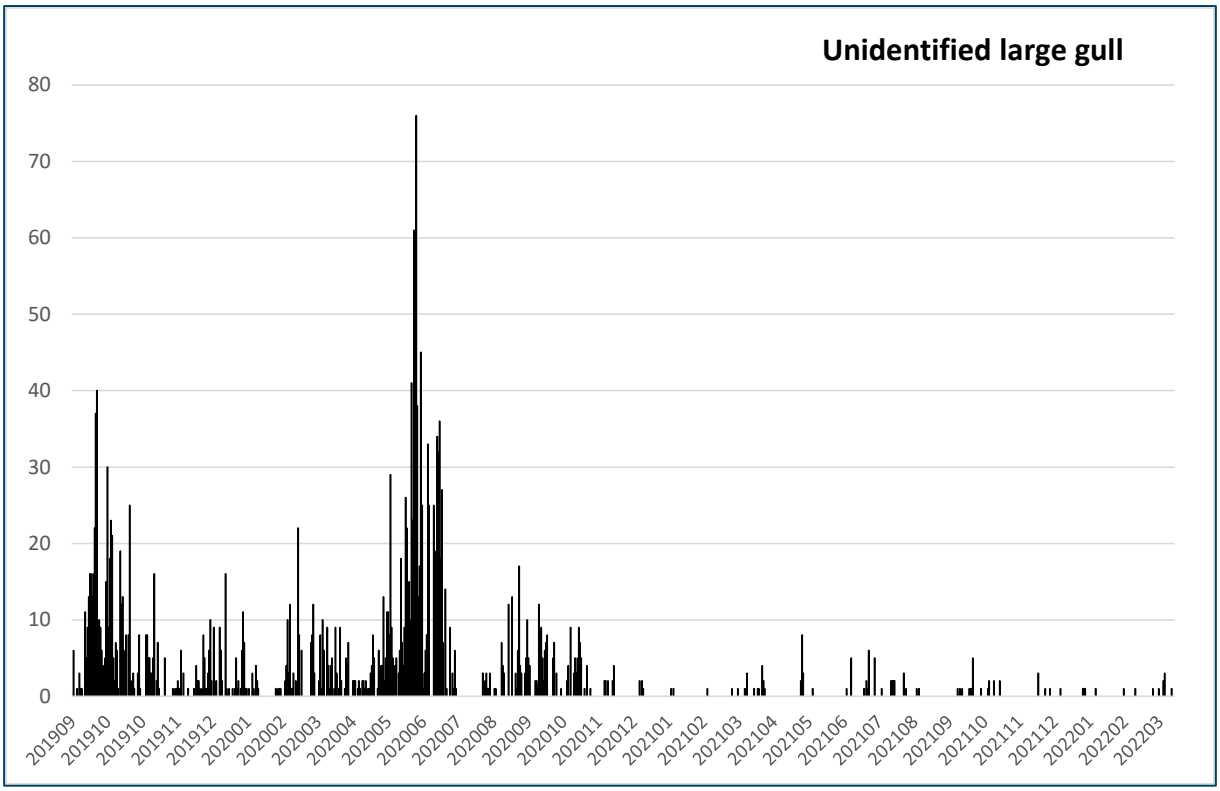

Figure 12 Temporal distribution of unidentified large gulls between September 2019 and March 2022. Graph shows total number of videos per day

4.3 Feeding

Feeding behaviour of large gulls has been determined based on video recordings of feeding individuals or individuals searching for prey. More than 10% feeding birds were observed in the videos showing Great black-backed gulls, Herring gulls, Northern Gannet and unidentified large gulls (Table 5).

Table 5 Number of video recordings of feeding large species of gulls. Only videos in which feeding, or no feeding could be determined have been included

	N	Feeding	% feeding
Lesser/Great black-backed gull	17	1	5.88
Lesser black-backed gull	43	3	6.98
Lesser black-backed / Herring gull	1	0	0.00
Unidentified large gull	450	160	35.56
Great black-backed gull	102	18	17.65
Herring gull	101	14	13.86
Northern Gannet	58	32	55.17

4.4 Resting on turbine foundations

The video documentation included several recordings of large gulls sitting on or flying to/from the turbine foundation of the camera turbine (Table 6). These resting gulls were almost exclusively Herring gulls and Great black-backed gulls, whereas almost no Lesser black-backed gulls used the infrastructures for resting. Great cormorants were also frequently recorded sitting on the turbine foundations.

Table 6 Number of videos of target species either 'sitting on' or 'flying to/from' the wtg platform.

SPECIES	SITTING ON WTG	FLYING TO/FROM WTG
Unidentified large gulls	11	8
Herring gull	112	3
Great black-backed gull	83	1
Lesser black-backed gull	1	0
Great/Lesser black-backed gull	1	0

5 Radar track densities

Mean track lengths (unspecified) have been extracted from the radar data to obtain spatio-temporal overviews of recorded mean densities of flying birds, at day and night through the period September 2019 to March 2022. Monthly overviews of tracks length densities during day/night hours are shown in Appendix 1 and 2, and below examples are shown for the month of September. The spatial distribution of birds highlights meso avoidance patterns throughout the array, and due to the detection distances involved most recorded movements are likely medium-sized/large species of birds. Lower densities of flying medium-sized/large species of birds were recorded during night than during day hours.

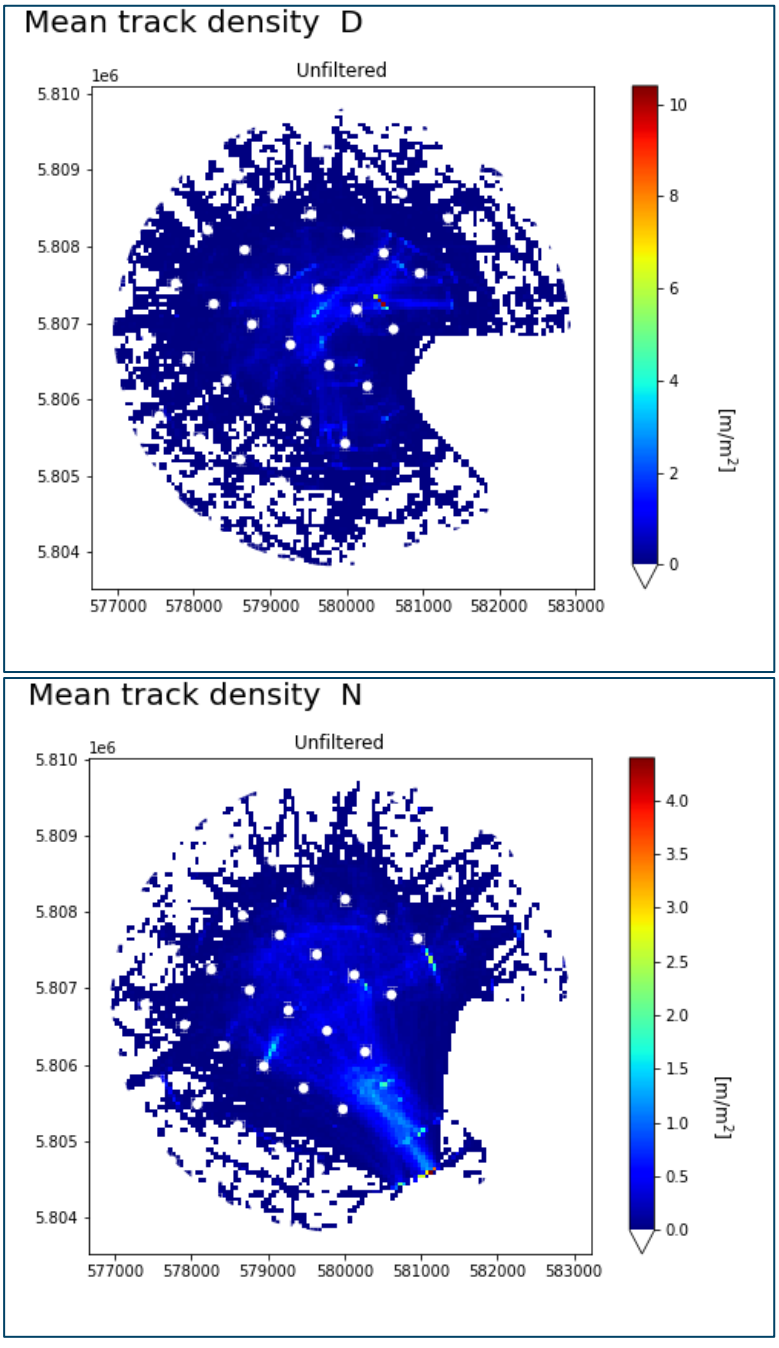

Figure 13 Mean track length density (m/m^2) for the month of September across 2019, 2020 and 2021. The plot has been split into daytime (D) and night-time (N).

6 Species-specific behavioural patterns extracted from radar and video data

6.1 Meso avoidance of large gulls

Northern gannets were exclusively recorded on video displaying horizontal meso avoidance (Table 7). Large gulls were recorded in 3461 or 66% of the bird videos and were thus the far most frequently recorded group of birds within the wind farm array. In 30% of the large gull videos birds could be identified as either Great black-backed gull, Lesser black-backed gull, or Herring gull. Analysis of the videos showed that in 92% of the recordings large gulls avoided by flying in between the turbines, although 19 Herring gulls and 50 Great black-backed gulls equivalent of 3.93% and 17.61% respectively were recorded flying below the rotor (Table 7). The latter seems to reflect the interactions of Great black-backed gulls and Herring gulls with the turbine's platforms.

Table 7 Meso avoidance behaviour of Northern gannet and large gulls recorded by cameras between autumn 2019 and spring 2022

SPECIES	VIDEOS IN MESO ZONE	BELOW ROTOR	ABOVE ROTOR
Northern gannet	60	0	0
Unidentified large gulls	2184	24	25
Herring gull	483	19	1
Great black-backed gull	284	50	4
Lesser black-backed gull	263	2	1
Great/Lesser black-backed gull	194	6	3
Herring/Lesser black-backed gull	53	1	2

Mean meso avoidance patterns are shown in figure 14, displaying mean meso avoidance rates at different distance from rotors for all Black-backed and all unidentified large gulls from the coupled radar track and video data. Even though the samples for the identified species tracks were too small for estimation of the avoidance rates the results indicate that large gulls display the strongest meso response (at or just above 0.5) at close distance (less than 25 m distance from the tip of the rotors) and start to display avoidance between 75 and 100 m distance. This avoidance pattern is countered by attraction to the areas at more than 150 m distance.

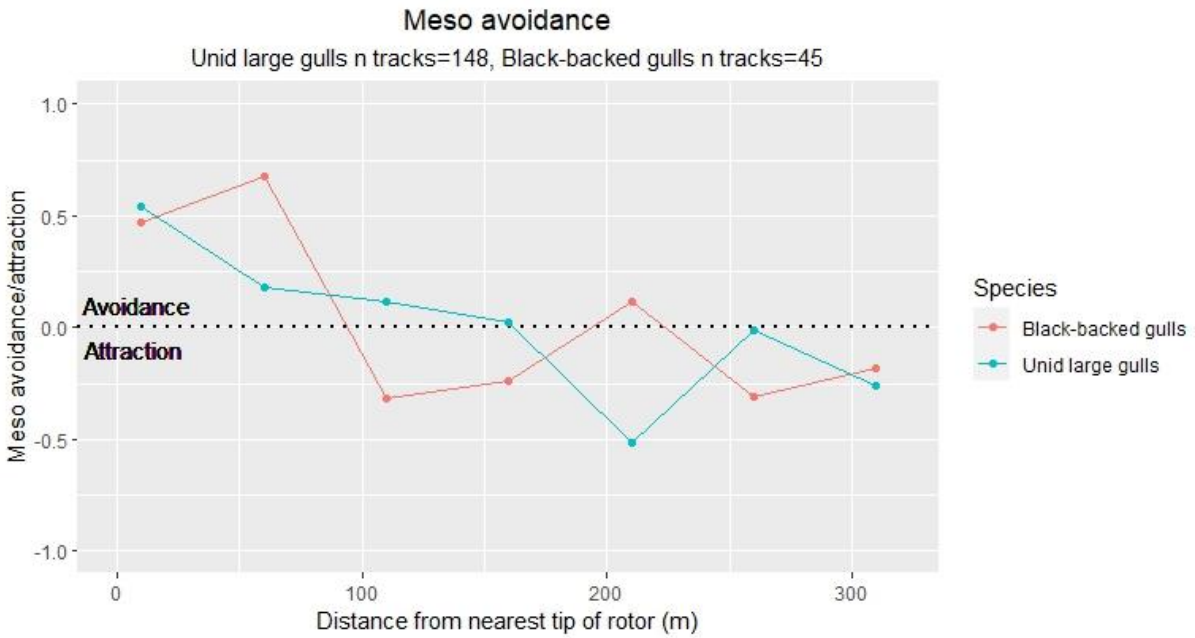

Figure 14 Mean meso avoidance rate of all black-backed large gulls and all unidentified large gulls

(calculated from the combined radar and video tracks at 50 m intervals in relation to distance from nearest rotor during daytime hours. Sample sizes are number of tracks)

6.2 Micro avoidance of northern Gannet and large gulls

Three Northern gannets were recorded within the rotor-swept zone (Table 3) defined as a circular area with a radius equivalent to the length of the rotor blades (55 m) plus 10 m buffer (Table 8). In general, large gulls also tended to avoid flying into the rotor-swept zone but were infrequently recorded here. Hence, only 108 large gull videos or 2.1% showed birds flying in the micro zone. In 86% of these videos large gulls adjusted their flight in order to avoid the spinning blades. In the remaining 15 videos or 14%, large gulls showed non-avoidance behaviour either by crossing the rotor swept area without making adjustments in flight behaviour or altitude or by colliding with the spinning blades (Table 9). These results give micro avoidance rates of 0.950 for all unidentified large gulls, 0.800 for all black-backed gulls and 0.861 for all large gulls (Table 10).

In 44% of the videos with birds flying in the micro zone, large gulls avoided the spinning blades by flying along the rotor. In 15% of the videos large gulls avoided the blades by stopping before crossing the rotor swept zone. In 20% of the videos in the micro zone showed large gulls crossing the rotor swept area while making adjustments in flight behaviour. In 6% of the cases in the micro zone large gulls returned rather than crossing the rotor swept zone.

Two videos of large gulls showed a collision with a spinning blade – both at turbine 15. This fate was recorded for one unidentified large gull and one Herring gull.

Table 8 Species-specific micro avoidance behaviour of Northern gannet and large gulls based on video data collected between September 2019 and March 2022.

SPECIES	VIDEOS IN MICRO ZONE	RETURNS	STOPS BEFORE CROSSING	ALONG ROTOR	CROSSING WITH ADJUSTMENS
Northern gannet	3			3	
Unidentified large gulls	40	2	9	17	10
Great/Lesser black-backed gull	21	1	3	5	6
Lesser black-backed gull	15	2	0	8	3
Great black-backed gull	9	1	2	5	0
Herring gull	15	1	1	10	2
Herring/Lesser black-backed gull	8	0	1	3	1

Table 9 Species-specific micro non-avoidance behaviour of large gulls based on video data collected between September 2019 and March 2022

SPECIES	VIDEOS IN MICRO ZONE	CROSSING WITHOUT ADJUSTMENTS	COLLISIONS
Northern gannet	3		
Unidentified large gulls	40	1	1
Great/Lesser black-backed gull	21	6	
Lesser black-backed gull	15	2	
Great black-backed gull	9	1	
Herring gull	15		1
Herring/Lesser black-backed gull	8	3	

Table 10 Species-specific micro avoidance rate of large gulls based on video data collected between September 2019 and March 2022

SPECIES	MEAN MICRO AVOIDANCE RATE	SAMPLE SIZE
Unidentified large gulls	0.950	40
Black-backed gulls	0.800	45
All large gulls	0.861	108

6.3 Recorded flight heights, speeds, and directions of large gulls

The use of the combined radar track and video data for estimation of changes in flight height, speed and direction in the LUD array was assessed by extracting the mean recorded flight height, speed and direction of all large gulls in relation to distance from the rotors (figures 15, 16 and 17).

All the large gulls were predominantly recorded flying at rotor height, but with a clear tendency to increase flight height from the central parts of the areas between the turbine rows. Unlike for black-backed gulls all large gulls displayed a slight drop in flight altitude within the nearest 90 m from the tip of the rotor. Examples of 3D track trajectories are visualised in figure 18. For all large gulls recorded flight speeds changed markedly with distance from the tip of the rotors and showed a strong decline from 6-10 m/s at distance beyond 250 m to less than 5 m/s closer than 120 m from the rotor. In other words, the changes in flight height and speed mirrored the recorded patterns of meso avoidance.

Combined radar track and video data also allowed for estimation of changes in the flight direction of the target species in relation to distance from the rotors. Estimated changes in flight direction relative to the orientation of the rotor indicated that large gulls deflected around 50 m distance from the rotors or inside the rotor-swept zone (figure 15**Error! Reference source not found.**). Hence, the change in flight direction could be seen as reflecting the main type of micro avoidance recorded in terms of gulls flying along the plane of the spinning rotor.

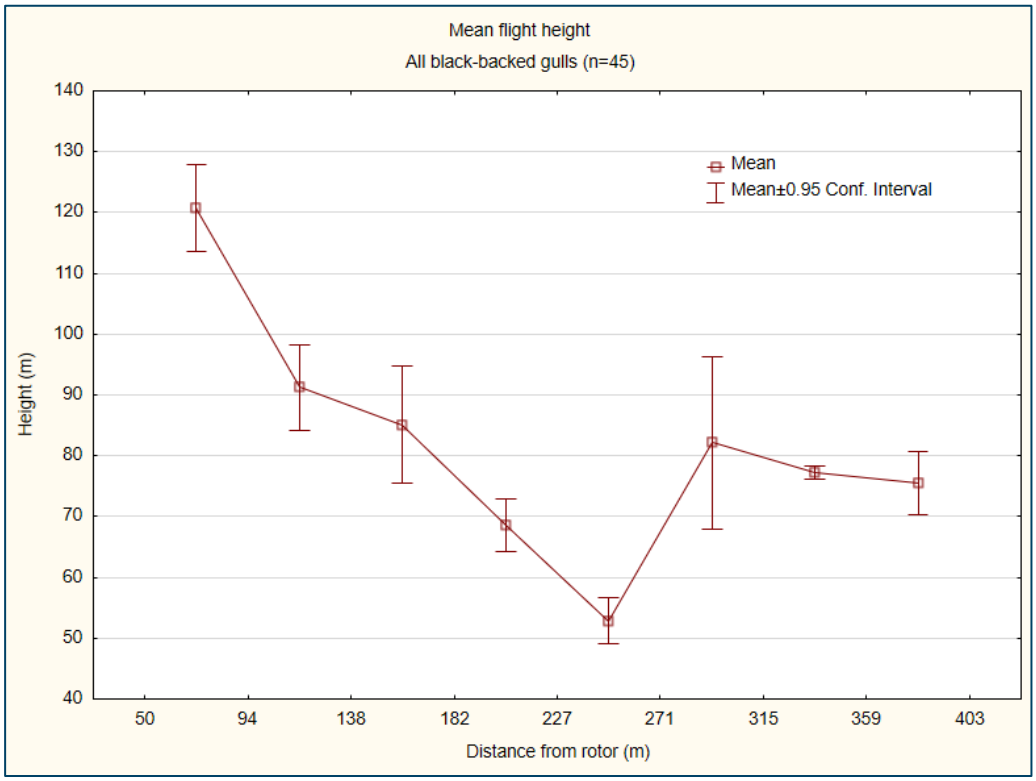

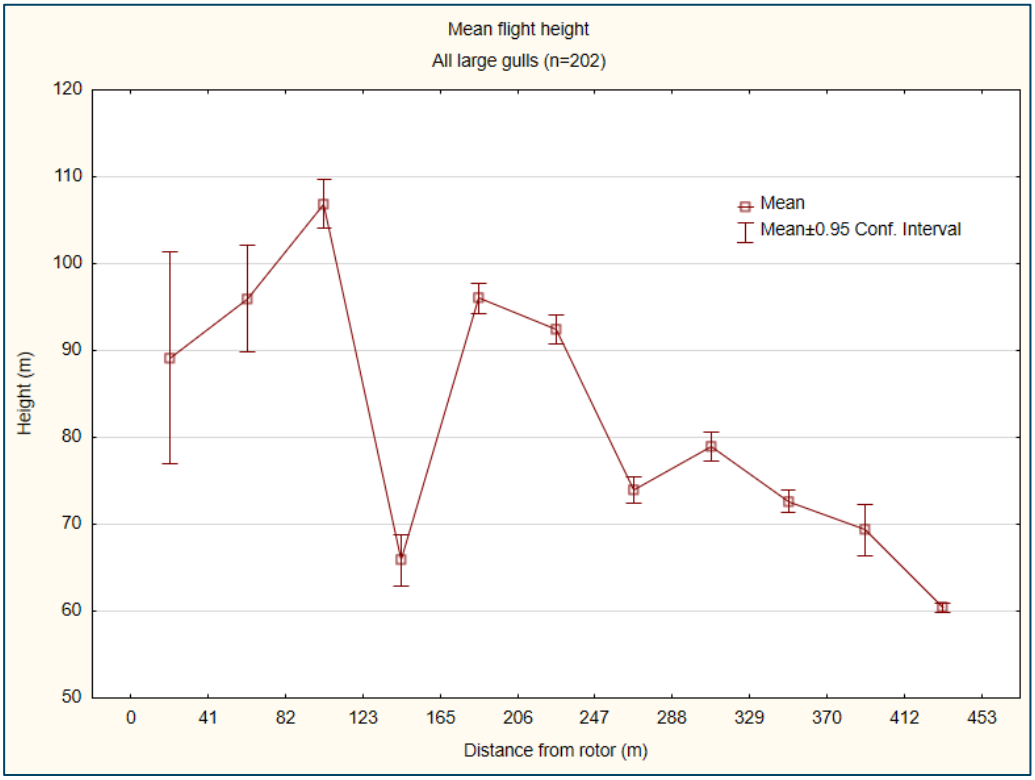

Figure 15 Mean estimated flight heights of all black-backed gulls and all large gulls

(using triangulation and shown in relation to distance from nearest turbine during daytime hours. Sample sizes indicate number of tracks involved)

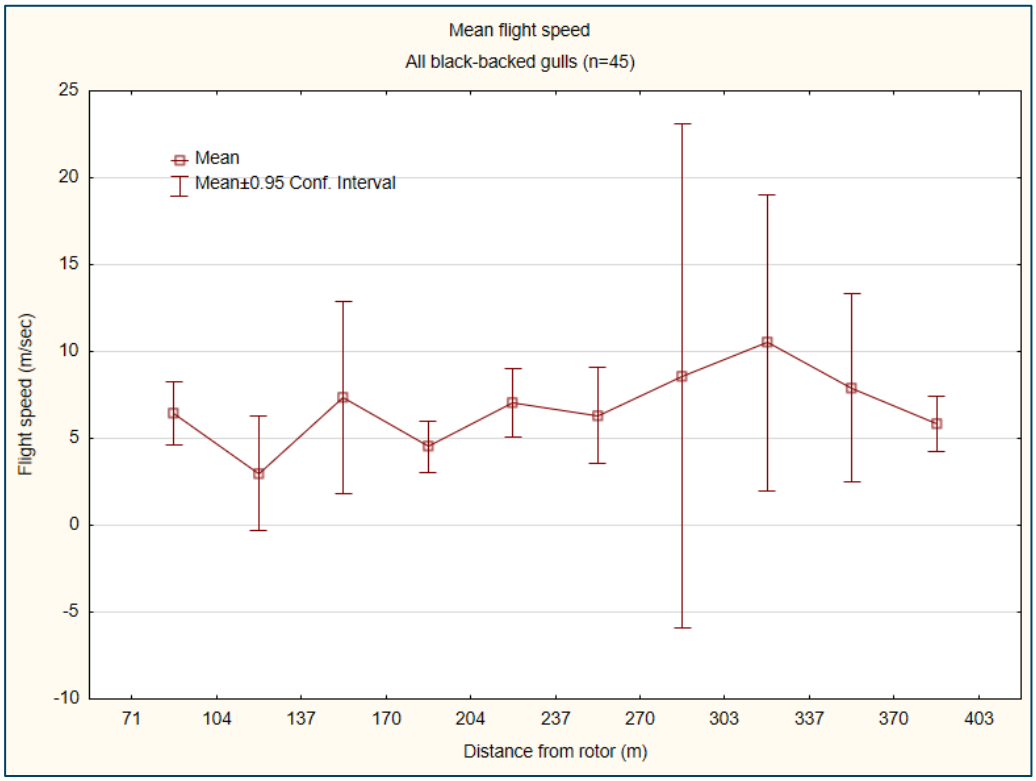

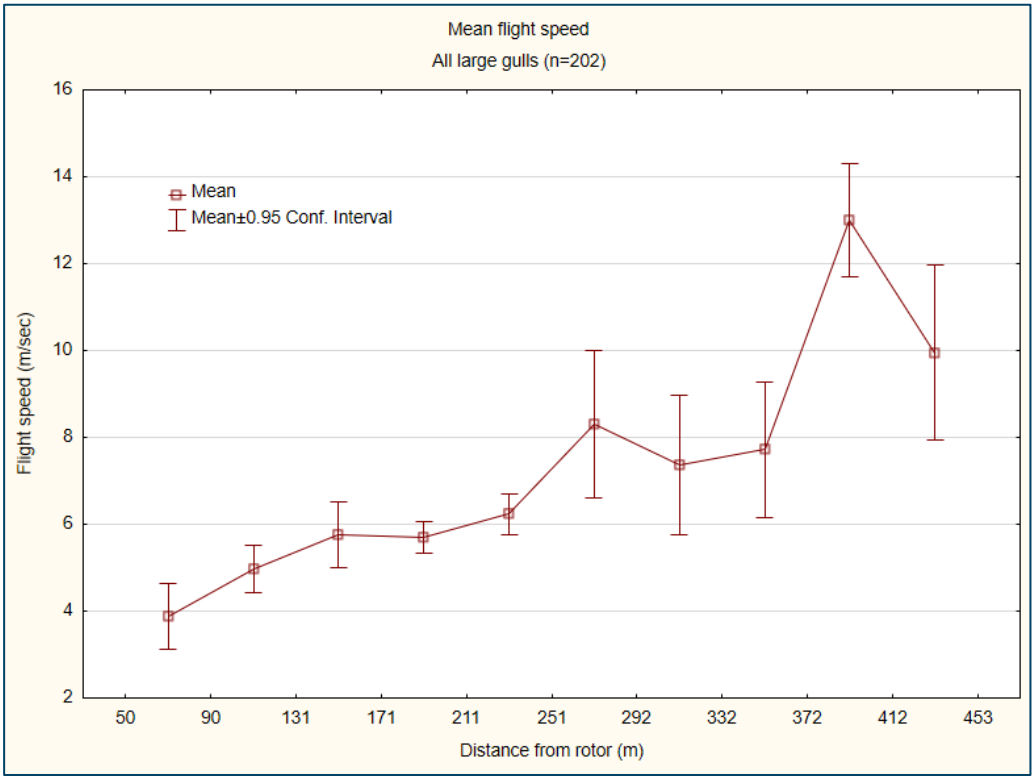

Figure 16 Mean flight speeds of all black-backed gulls and all large gulls in relation to distance (from nearest turbine during daytime hours. Sample sizes indicate number of tracks involved)

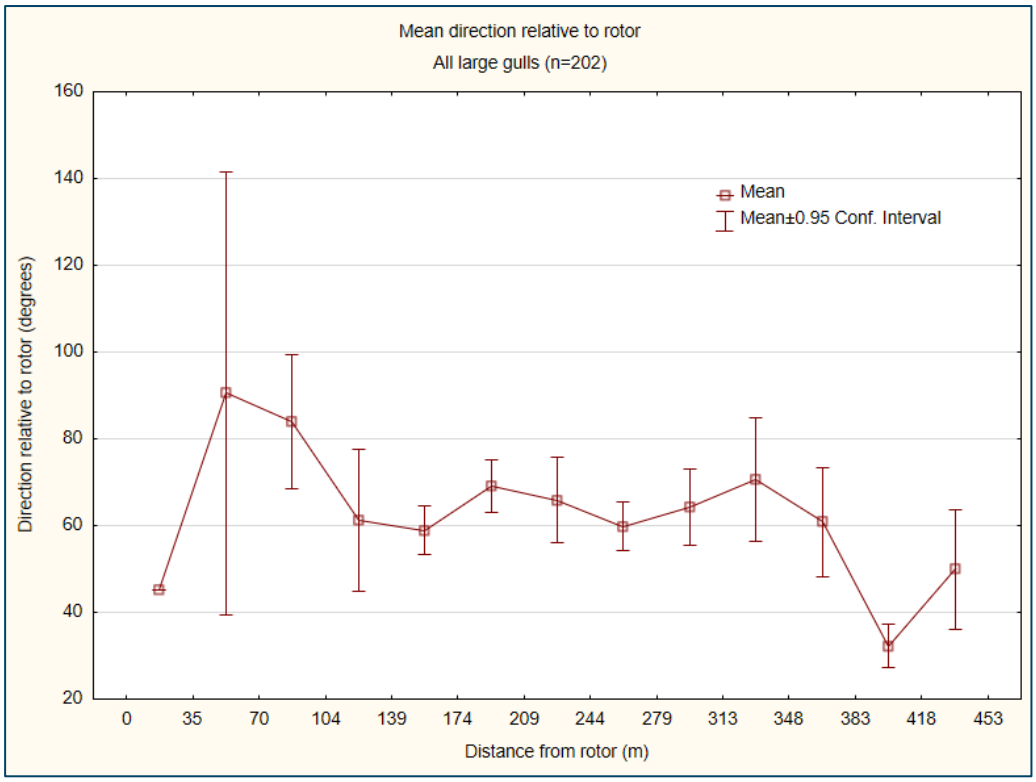

Figure 17 Mean flight direction of all large gulls in relation to orientation of rotor and distance (from nearest turbine during daytime hours. Sample sizes indicate number of tracks involved)

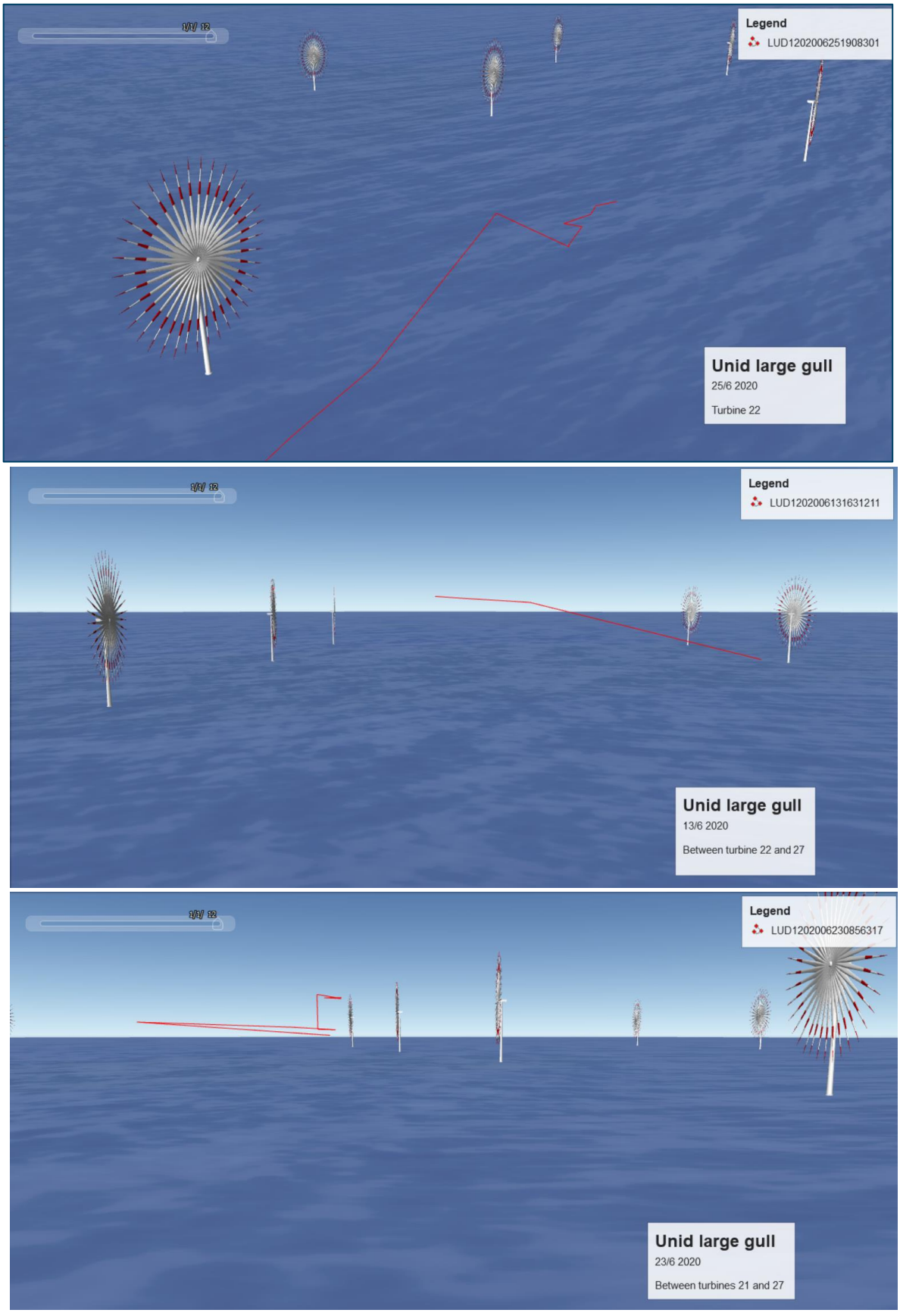

Figure 18 Examples of flight tracks of large gulls showing changes in flight height within the LUD array

6.4 Modelled flight heights, speeds, and directions of large gulls

6.4.1 Flight height

The results of the flight models revealed a high degree of variation in the effect of wind conditions on the flight altitude of large gulls (figure 19). The large gulls were predicted to fly at the same altitude at distances of more than 120m from the tip of the rotor blades, irrespectively of wind conditions. However, the general increase in flight height closer than 100m from the rotor as seen in the mean profiles was according to the model only evident in high tail and cross wind speeds.

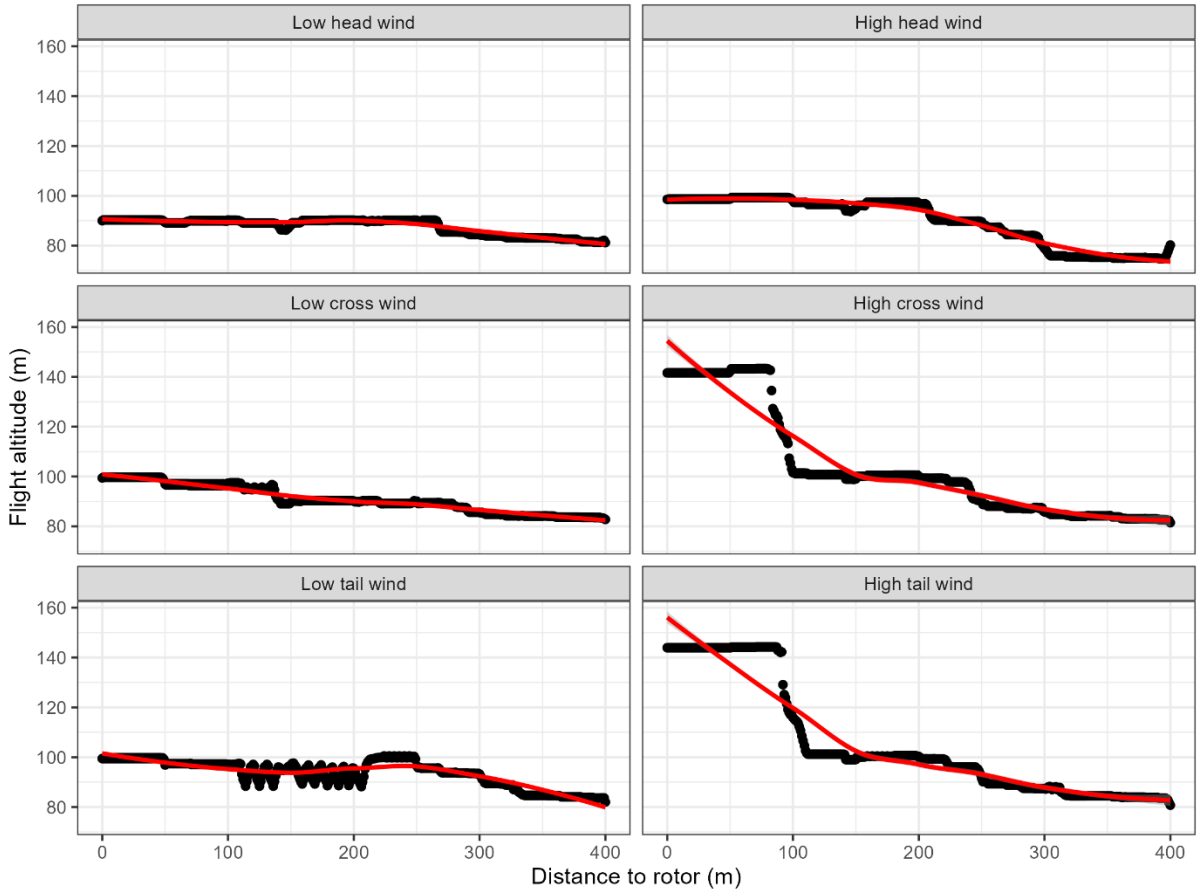

Figure 19 Predicted mean profiles of flight height of large gulls viewed from the edge of the rotor zones to the centre of the areas between turbines.

(The mean profiles are visualised in relation to relative wind direction and levels of wind speed. Left column is low wind speed scenarios and right column is high wind speed scenarios. See text for definitions of low and high levels of wind speed.)

6.4.2 Flight Speed

The results of the flight models in relation to flight speed are shown in figure 20. Large gulls were predicted to reduce flight speed when approaching the rotor during all weather scenarios, but most significantly during a strong tail wind. As seen in the mean profiles based on the recorded flight speeds, this response typically began at more than 200 m distance from the rotors, and resulted in predicted flight speeds below 8 m/sec closer than 120m from the rotor blades.

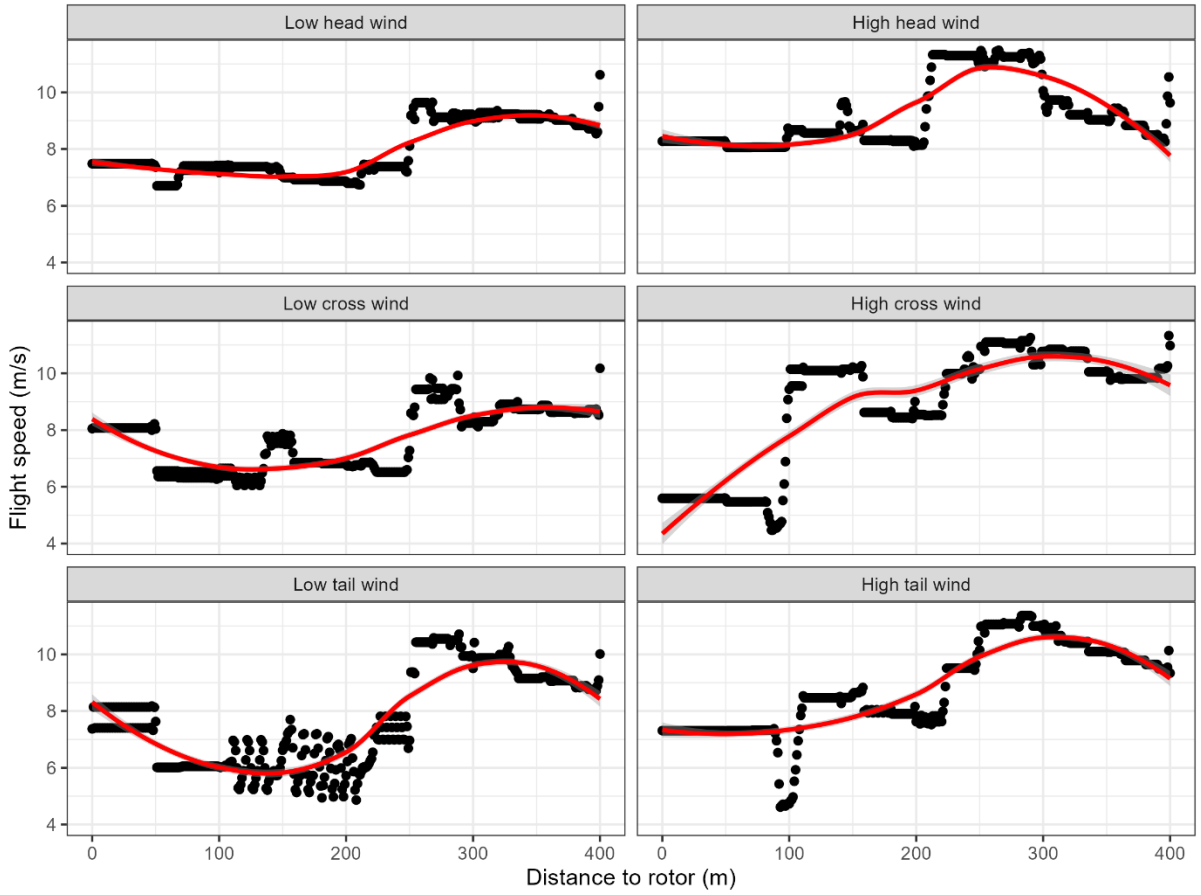

Figure 20 Predicted mean profiles of flight speed of large gulls viewed from the edge of the wind farm to the centre of the areas between turbines.

(The mean profiles are visualised in relation to relative wind direction and levels of wind speed. Left column is low wind speed scenarios and right column is high wind speed scenarios. See text for definitions of low and high levels of wind speed.)

6.4.3 Flight direction

The results of the flight models in relation to flight direction relative to the orientation of the rotor are shown in figure 21. Wind speed had a profound effect on flight direction when approaching the rotor as the tendency to deflect close to the rotor seemed to be related to situations with low wind speeds. The tendency to fly along the plane of the rotor during calm wind conditions was, however predicted to take place at longer distances from the rotor (200m).

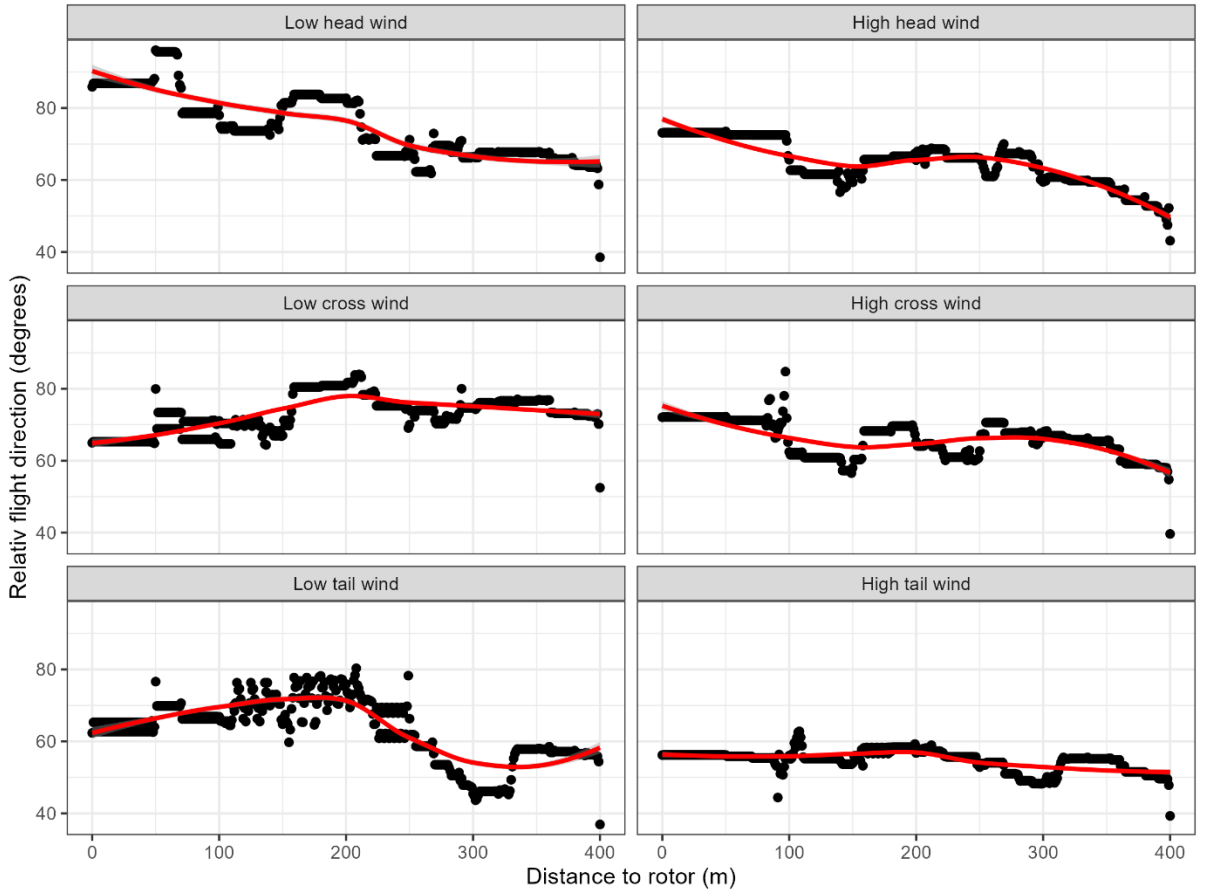

Figure 21 Predicted mean profiles of flight direction of large gulls viewed from the edge of the wind farm to the centre of the areas between turbines.

(The mean profiles are visualised in relation to relative wind direction and levels of wind speed. Left column is low wind speed scenarios and right column is high wind speed scenarios. See text for definitions of low and high levels of wind speed.)

6.5 Modelled flight heights, speeds, and directions of black-backed gulls

6.5.1 Flight height

The results of the flight models revealed a high degree of variation in the effect of wind on the flight altitude of black-based gulls. The observed tendency of black-backed gulls to increase flight height on approach to the rotor was only predicted during low wind speeds. During high wind speeds the black-backed gulls were predicted to decrease flight altitude at distances smaller than 200m from the rotor.

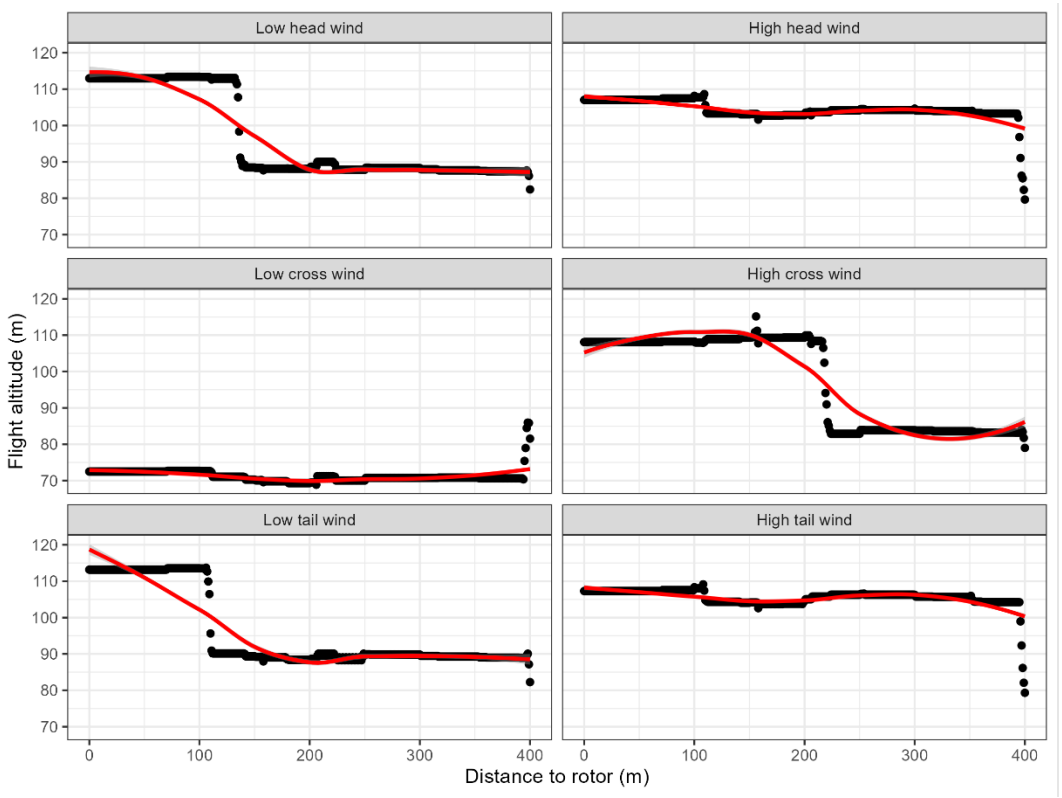

Figure 22 Predicted mean profiles of flight height of black-backed gulls viewed from the edge of the rotor zone to the centre of the areas between turbines.

(The mean profiles are visualised in relation to relative wind direction and levels of wind speed. Left column is low wind speed scenarios and right column is high wind speed scenarios. See text for definitions of low and high levels of wind speed.)

6.5.2 Flight Speed

The results of the flight models in relation to flight speed are shown in figure 23. Unlike the model predictions for all large gulls and the mean observed pattern black-backed gulls were predicted to reduce flight speed when approaching the rotor only during calm wind scenarios. During high wind speeds the black-backed gulls were predicted to increase flight speed when closer than 200m from the rotor.

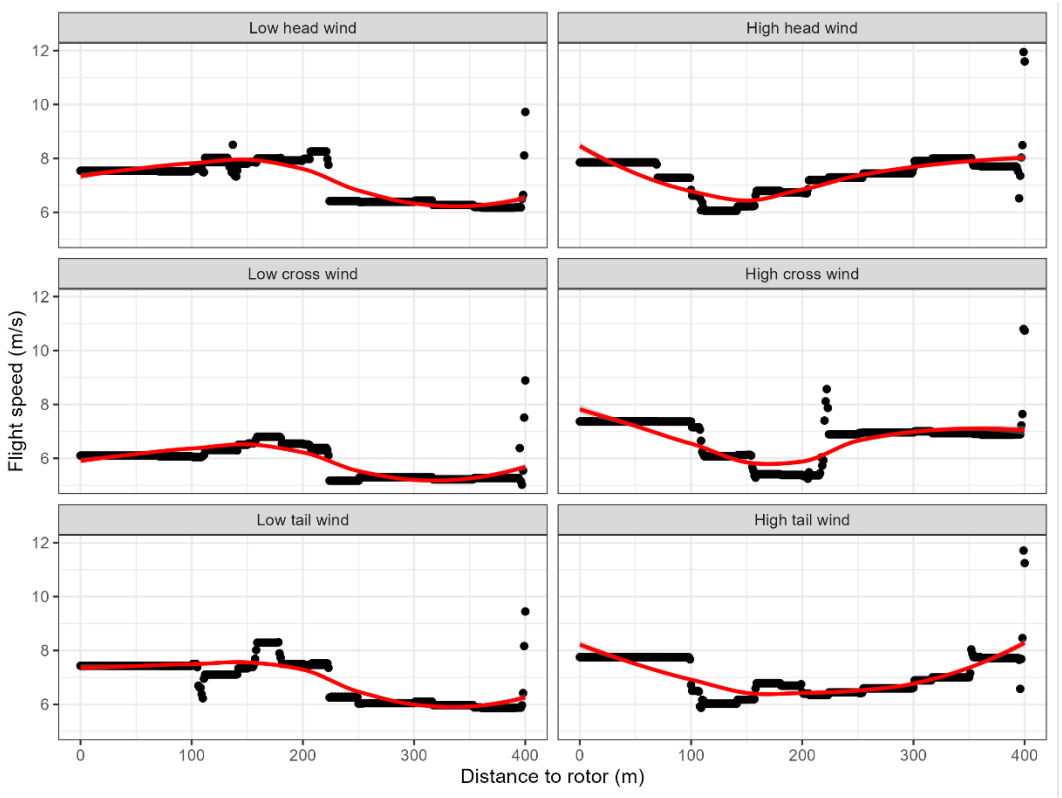

Figure 23 Predicted mean profiles of flight speed of black-backed gulls viewed from the edge of the rotor zone to the centre of the areas between turbines.

(The mean profiles are visualised in relation to relative wind direction and levels of wind speed. Left column is low wind speed scenarios and right column is high wind speed scenarios. See text for definitions of low and high levels of wind speed.)

6.5.3 Flight direction

The results of the flight models in relation to flight direction relative to the orientation of the rotor are shown in figure 24. Contrary to the other flight parameters in relation to weather conditions, the flight models showed that flight direction of black-backed gulls was affected in all scenarios. However, as seen in the model for all large gulls the effect was most pronounced during calm wind conditions when the black-backed gulls were predicted to fly parallel to the rotor blades at distances smaller than 200m from the rotor.

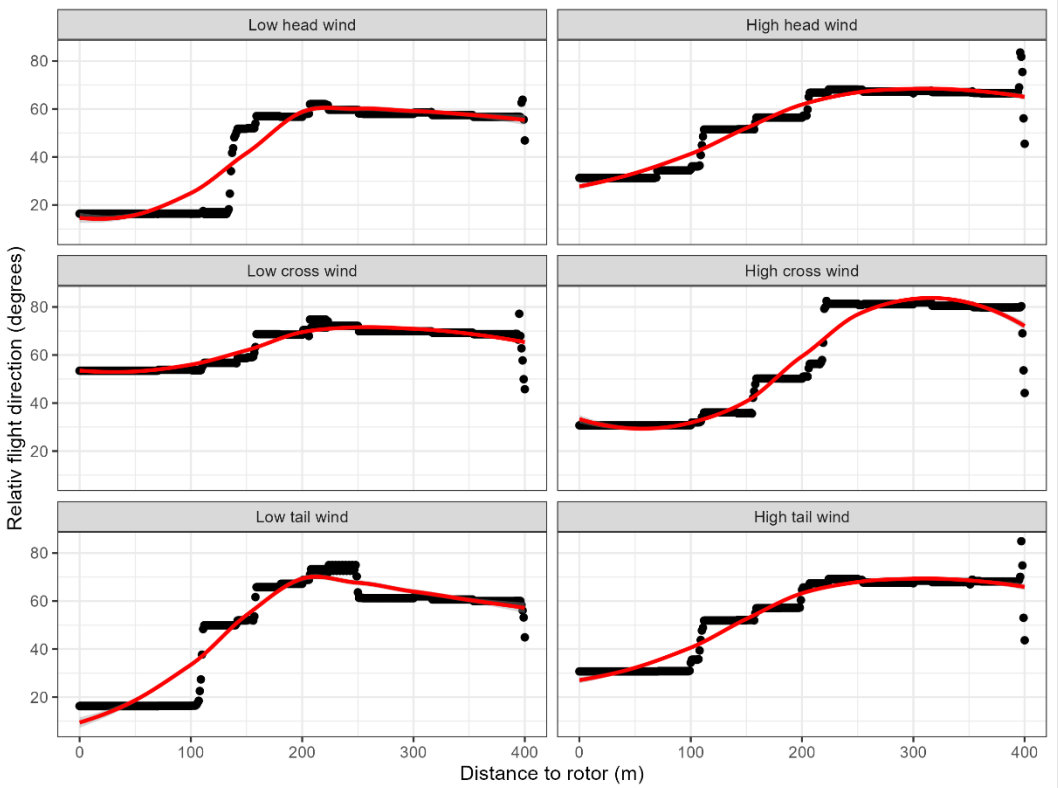

Figure 24 Predicted mean profiles of flight direction of black-backed gulls viewed from the edge of the wind farm to the centre of the areas between turbines.

(The mean profiles are visualised in relation to relative wind direction and levels of wind speed. Left column is low wind speed scenarios and right column is high wind speed scenarios. See text for definitions of low and high levels of wind speed.)

7 Discussion

7.1 Sensor equipment and design

The monitoring equipment in LUD has been operating under a requirement of 95% uptime. Uptime is here defined as time in which the system should be collecting data and does not include service and maintenance activities, power outages or other incidents outside of DHI's control. In the discussion of uptime it is also worthwhile to stress that the system has not been designed for quantifying the number of large gulls in the wind farm. Rather, the primary aim has been to measure meso and micro avoidance behaviour. This is especially important in relation to the radar which has been set to reduce false positives by applying strong dynamic clutter filters in order to remove noise from waves. The application of these filters dampens not only reflections by waves during strong weather, but it also inhibits detection of all birds. However, as seabird flight behaviour is assessed using proportional statistics the dynamic noise filters has not compromised the assessment of avoidance behaviour. Due to server breakdown in February 2020 and several minor incidents of malfunctioning the monitoring period was extended to March 2022.

The total number of radar-initiated videos (344 or 6.6 % of all bird videos) was quite limited yet following the decisions at the expert meeting in 2020 to limit the solo mode of the cameras to adverse weather conditions (wind speeds > 10 m/s) the proportion of coupled radar-videos increased. Related to the issue of coupled radar-camera data the estimation of flight heights

through triangulation has been enhanced after 1 June 2020. This change made it possible to obtain a relatively large number of flight height estimates which has allowed for detailed analyses of the three-dimensional responsive behaviour of large gulls to turbines in the wind farm.

During most of the monitoring campaign, the quality of the collected video data was judged by the video analysts as acceptable. However, the video tracker frequently got confused when multiple birds appeared in the field of view. This has been solved in version 2 of the video tracker which was introduced in 2021. The new tracker version uses AI-based algorithms to distinguish flying birds from other moving objects and has an improved capacity to keep the target bird in the centre of the field of view and allows for the use of higher zoom levels. Both characteristics increase the rate of identifying recorded birds to species levels. Unfortunately, the resolution in the RVision camera is not sufficient to apply the version 2 video tracker, and consequently the bird videos in LUD have been collected with the initial video tracker throughout the campaign.

7.2 Avoidance behaviour of large gulls

The estimates of meso avoidance in large gulls have been limited to wind speeds below 10 m/sec where the cameras were operating in dual mode and provided species id to the selected radar tracks. Although these radar tracks were selected from the pool of all radar tracks the selection was based on first detection and therefore as close to random as possible. As the calculation of the meso avoidance rates is based on proportional statistics the results for meso avoidance during wind speeds below 10 m/sec are judged as unbiased. As found in the ORJIP project meso avoidance in large gulls is relatively strong (Skov et al. 2018). The avoidance rates estimated for large gulls in LUD (0.5) are clearly lower than the rates estimated in the Thanet wind farm; 0.961 (±0.175 SD) for Herring gull, 0.894 (± 0.174 SD) for Lesser and Great black-backed gulls combined, and 0.842 (±0.177 SD) for Great black-backed gull. As the distances of birds to rotor-swept zones in the ORJIP project was determined based on the video documentation, and track lengths were estimated based on mean track speeds the meso avoidance rates from this project are likely to be more reliable. Similar differences in recorded meso avoidance rates for large gulls have been recorded using the same monitoring equipment in the Aberdeen offshore wind farm (Tjørnløv et al. 2021).

The only other empirical study which has reported on meso-avoidance is the monitoring study in the OWEZ OWF (Krijgsveld et al. 2011), who reported a meso-avoidance rate of 0.66 for all species combined. Cook et al. (2018) reviewed existing evidence from monitoring programs and suggested that meso-avoidance rates may vary between sites. The results from the LUD MEP project strongly indicates that the meso avoidance response of large gulls towards turbines mainly takes place between 75 and 100 m distance from rotors and that the response intensifies as the gulls approach the rotor blades. Overall, only 2.1 % of large gull videos showed birds inside the rotor-swept zones. In proximity to the rotors, the recorded meso-avoidance response behaviour for all three target species was manifested as a complex 3-dimensional pattern in which the gulls increased altitude and reduced flight speed while approaching the rotors and finally deflected the blades by flying along the rotor plane.

Using machine learning it was possible to investigate these flight behaviours in more detail and gain insight into the influence of wind conditions. According to the models, the increase in flight height of large gulls within 100m from the rotor as seen in the mean profiles seemed only evident in high tail and cross wind speeds, and black-backed gulls only seemed to increase flight height on approach to the rotor during low wind speeds. Whereas large gulls were predicted to reduce flight speed when approaching the rotor during all weather scenarios, black-backed gulls were predicted to do so only during calm wind scenarios. Regarding the tendency to reduce the relative difference in direction when approaching the rotor the model resolved that the flight direction of large gulls as well as black-backed gulls was most pronounced during calm wind conditions.

The change in orientation translates into flights close to but along the rotor being the dominant type of micro avoidance of large gulls, and although meso-avoidance is lower than anticipated prior to this study micro-avoidance is very strong as large gulls are rarely recorded crossing the spinning rotors. The recorded micro avoidance rates were high (0.800 for all black-backed gulls and 0.861 for all larger gulls), yet markedly lower than reported by similar methods in the ORJIP BCA study (0.957 ± 0.115 SD, Skov et al. 2018) and in the Aberdeen EOWDC study (0.96, Tjørnløv et al. 2021). Northern gannets displayed strong horizontal meso avoidance, and no birds were recorded inside the rotor-swept zones.

7.3 Conclusions

The main aim of the LUD MEP monitoring project has been to assess the meso and micro avoidance behaviour of large gulls. Compared to the ORJIP BCA study the technical improvements of the monitoring equipment employed in LUD made it possible to track large gulls inside the array and measure fluxes and meso-avoidance more confidently. Due to the full integration of radar and video tracks and the high temporal resolution of the track data (2.5 secs) the fluxes and meso-avoidance behaviour could be assessed in unprecedented spatial detail.

The target sample size for species-specific meso-avoidance of 250 was not reached for any of the three target species. This can both be explained by the relatively low density of these species in the LUD wind farm, but also by the technical standard of the optics of the RVision camera (not HD) and standard video tracking technology (not AI-based). Maximum meso-avoidance levels recorded were at least 0.5 and together with the recorded high levels of micro-avoidance it is now evident that the large gulls will be exposed to low risks of collision in this wind farm. Although the calculated micro-avoidance rates were high they were markedly lower than recorded rates in the ORJIP BCA and the Aberdeen EOWDC studies (Skov et al. 2018, Tjørnløv et al. 2021). One plausible explanation for this is that the cameras applied during these studies were high-definition, whereas the RVision cameras applied in the LUD MEP project were not. The lower resolution in the RVision cameras may to some extent have affected the recordings of micro avoidance during situations with lower visibility. The observed deterioration of the quality of the recorded videos during the later stage of the monitoring period is likely to have added to this effect.

The low risk of collision for large gulls in the LUD wind farm was also substantiated by the fact that only two collisions were recorded during the two and half years of monitoring. Scaling up from this recorded number of collisions the total annual number of collisions of seabirds in LUD can be estimated at 2.6. The results for meso avoidance and micro avoidance of large gulls in the LUD MEP project will be combined with the results of the RWS radar validation project of the Robin Radar system in LUD coordinated by Bureau Waardenburg. In order to achieve an overall avoidance rate for large gulls in LUD it is recommended to combine macro avoidance rates obtained in the RWS radar validation project with a meso avoidance rate of 0.5 and micro avoidance rates of 0.800 for Lesser and Great black-backed gulls and 0.861 for Herring gull.

As the target sample size for estimation of species-specific micro avoidance rates of 100 could not be achieved for any of the three target species it is recommended to undertake further monitoring of micro avoidance of large gulls in offshore wind farms using the best available camera technology. Increasing the sample size of large gulls recordings in the rotor-swept zone will also likely increase the micro avoidance rate to the levels recorded in the ORJIP BCA and the Aberdeen EOWDC studies.

8 References

Cook, A. S. C. P., Humphreys, E. M., Bennet, F., Masden, E. A., & Burton, N. H. K. 2018. Quantifying avian avoidance of offshore wind turbines: Current evidence and key knowledge gaps. Marine Environmental Research. https://doi.org/10.1016/j.marenvres.2018.06.017

Heinänen, S. & H. Skov. 2018. Offshore Wind Farm Eneco LUD. Ecological Monitoring of Seabirds. T3 (Final) Report. DHI Report commissioned by Eneco.

Krijgsveld, K.L., Fijn, R., Japink, M., Van Horssen, P., Heunks, C., Collier, M., Poot, M.J.M., Beuker, D., Dirksen, S. 2011. Effect studies offshore wind farm Egmond aan Zee. Final Report on fluxes, flight altitudes and behaviour of flying birds. Bureau Waardenburg bv. Nordzee Wind. 330pp.

Leemans, J.J., R.S.A. van Bemmelen, R.P. Middelveld, J. Kraal, E.L. Bravo Rebolledo, D. Beuker, K. Kuiper & A. Gyimesi. 2022. Bird fluxes, flight- and avoidance behaviour of birds in offshore wind farm LUD. Bureau Waardenburg Report 22-078. Bureau Waardenburg, Culemborg.

Skov, H., Heinänen, S., Norman, T., Ward, R.M., Méndez-Roldán, S. & Ellis, I. 2018. ORJIP Bird Collision and Avoidance Study. Final report – April 2018. The Carbon Trust. United Kingdom. 247 pp.

Tjørnløv, R.S., Skov, H., Armitage, M., Barker, M., Cuttat, F. & Thomas, K. 2021. Resolving Key Uncertainties of Seabird Flight and Avidance Behaviours at Offshore Wind Farms. Annual report for April 2020 – October 2020. Project No. DHI: 11820296; RPS: ECO00516.

Appendices

Appendix 1 Unspecified meso patterns extracted from radar data – daytime monthly mean track length density (m/m^2)

January

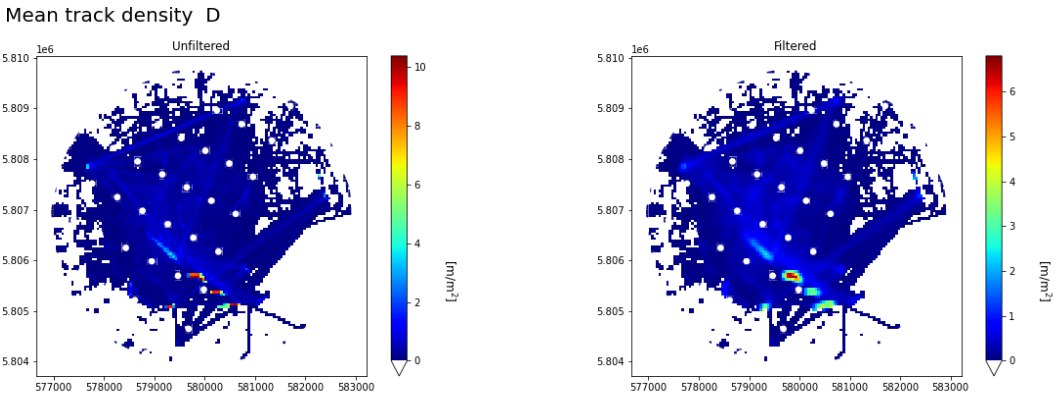

February

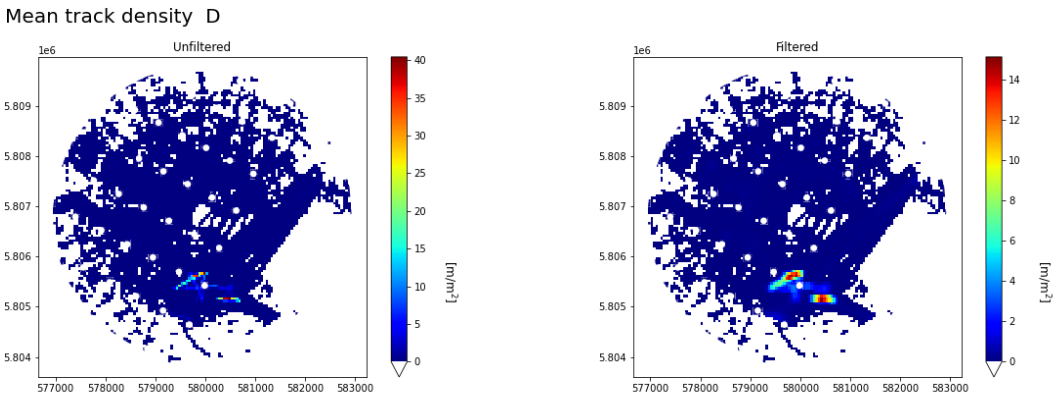

March

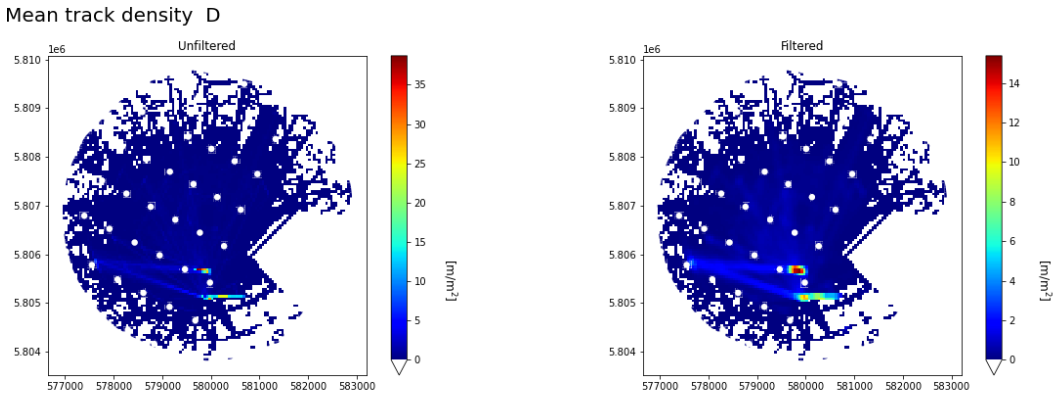

April

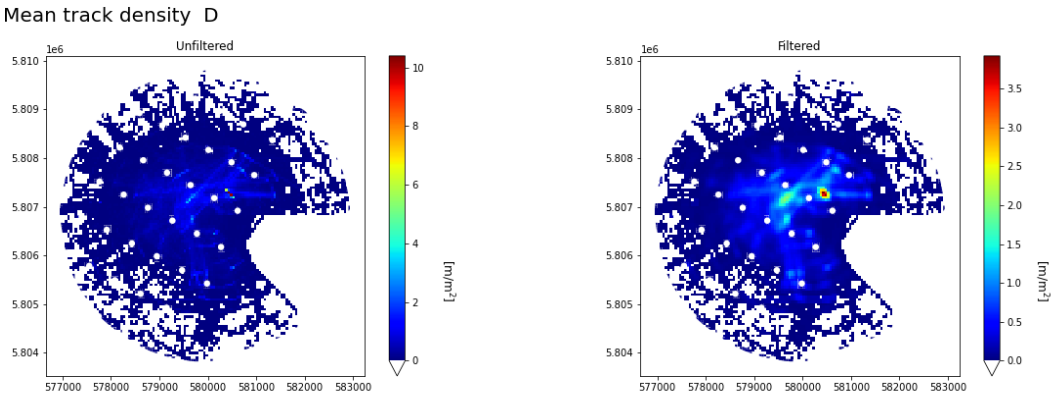

May

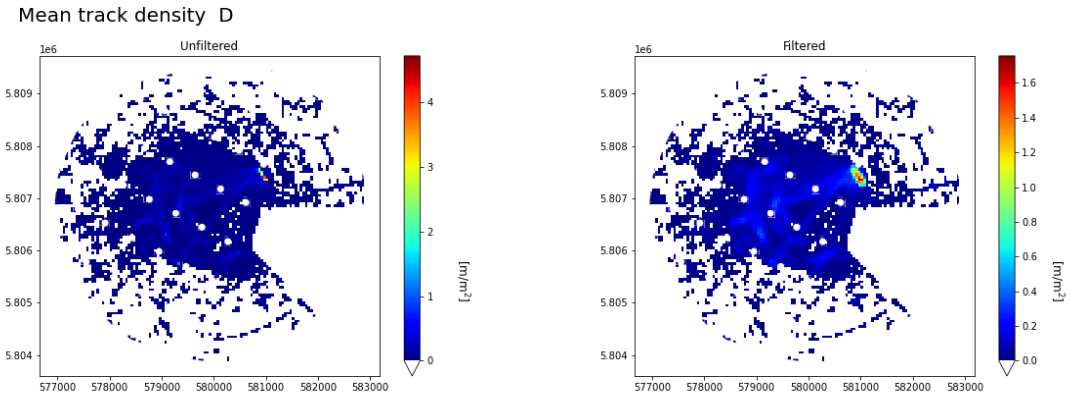

June

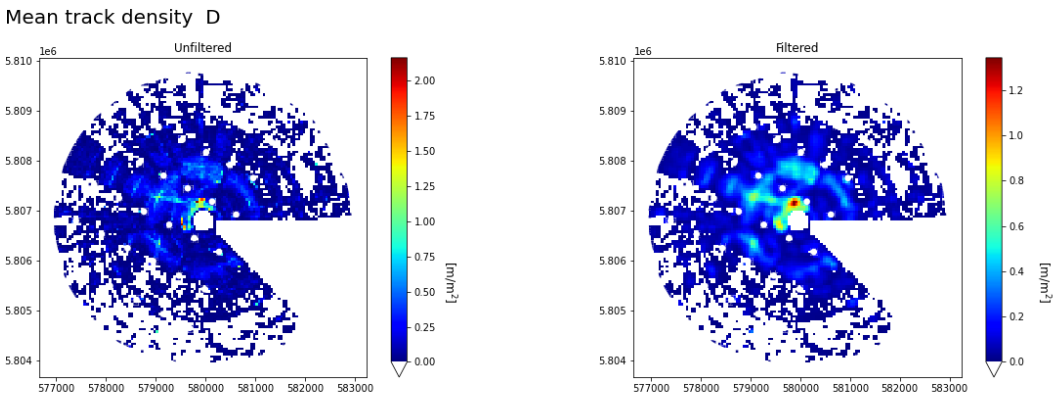

July

Mean track density D

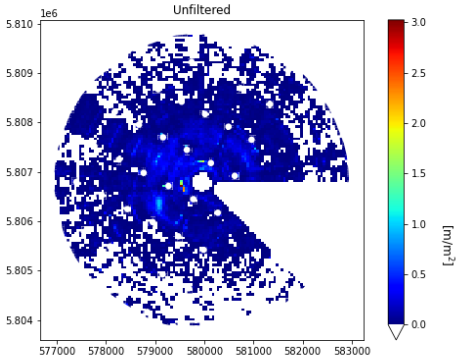

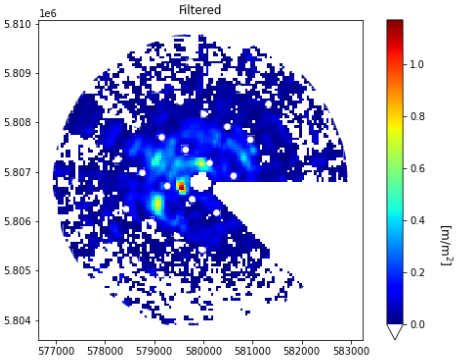

August

Mean track density D

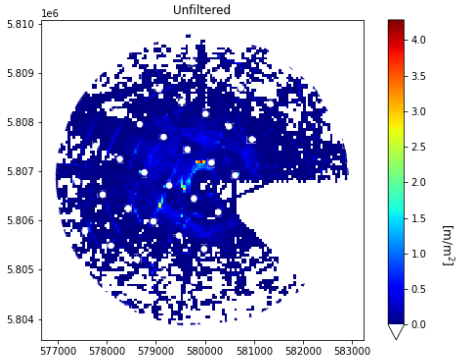

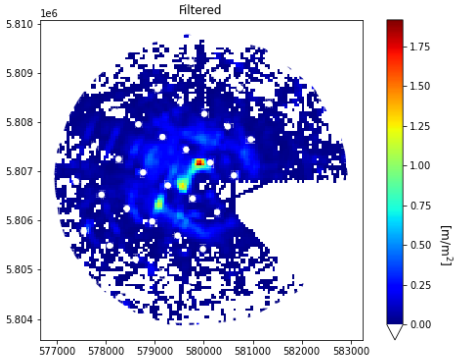

September

Mean track density D

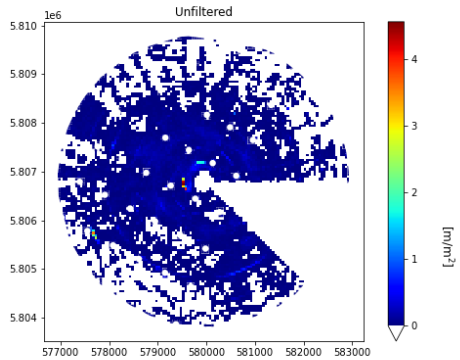

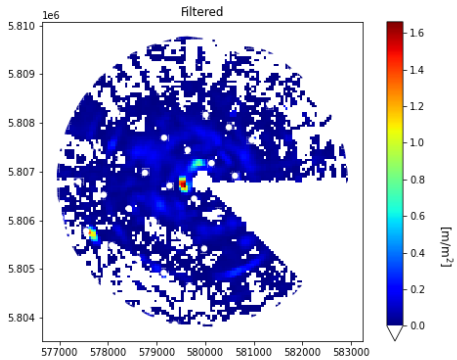

October

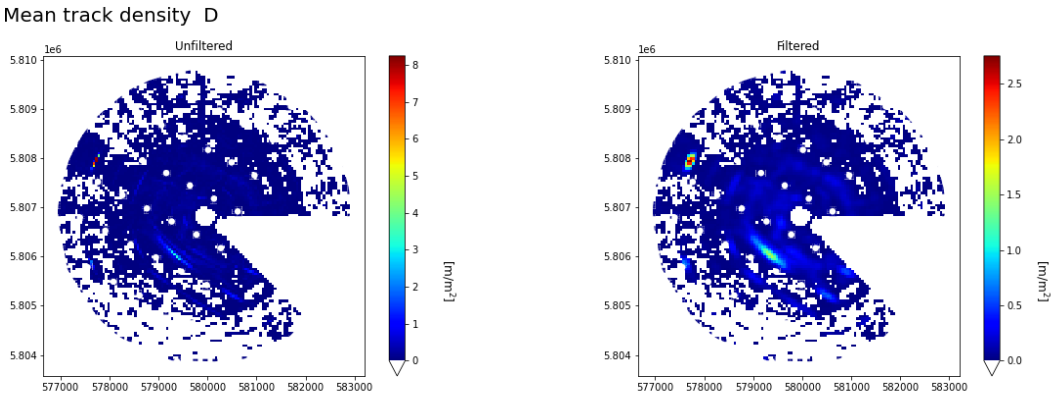

November

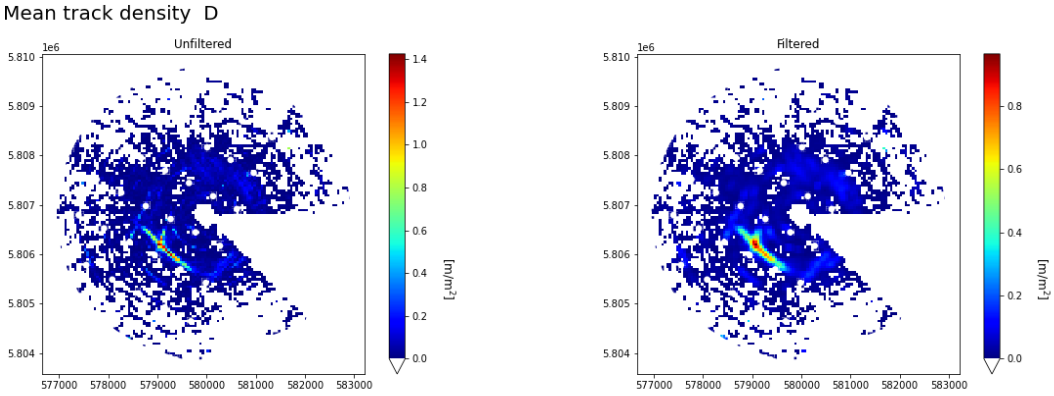

December

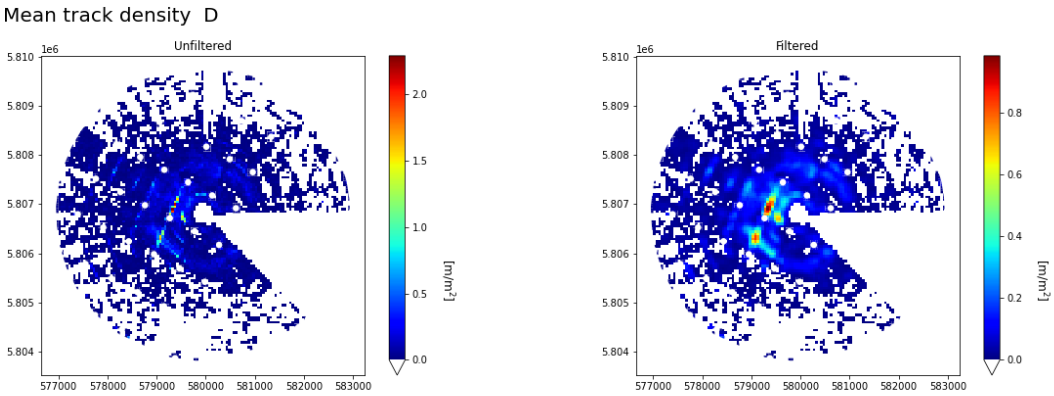

Appendix 2 Unspecified meso patterns extracted from radar data – night-time monthly mean track length density (m/m^2)

January

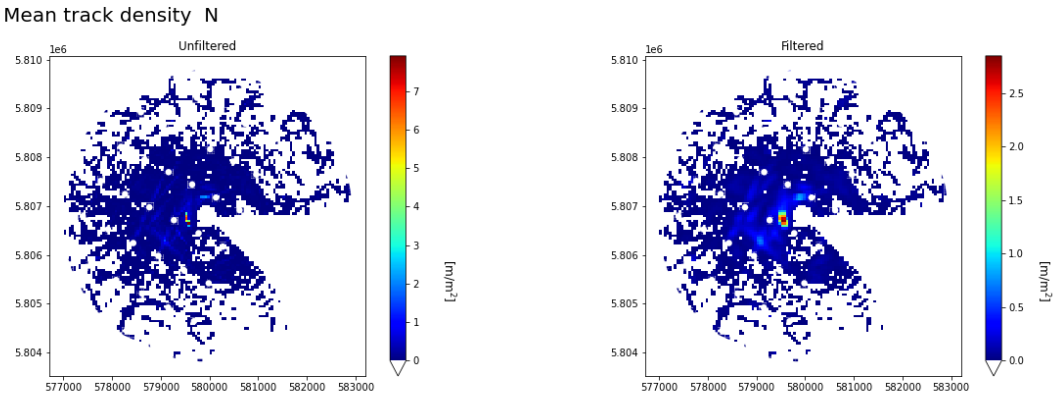

February

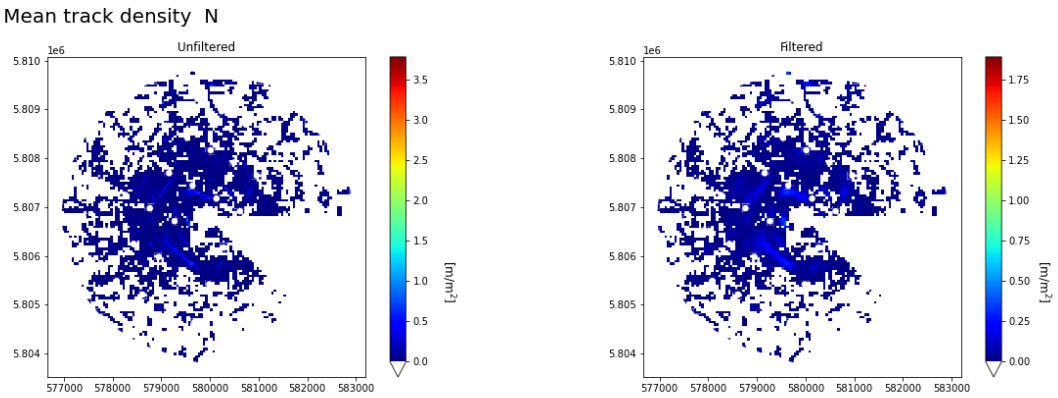

March

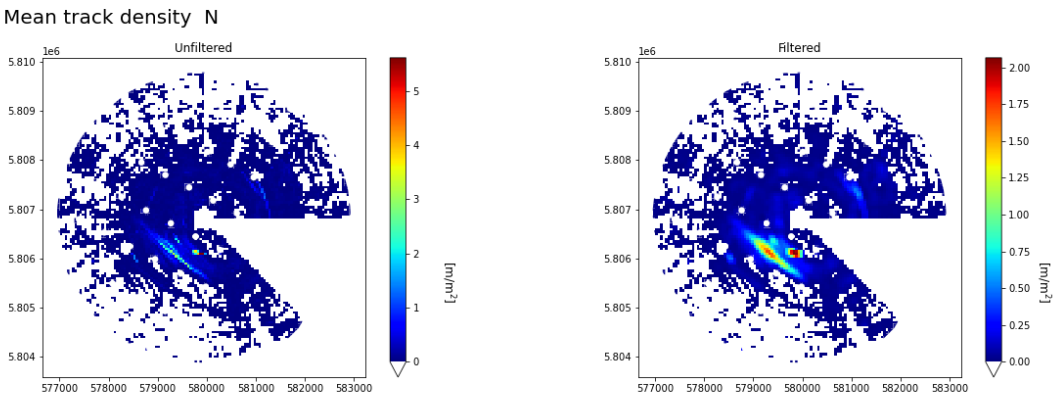

April

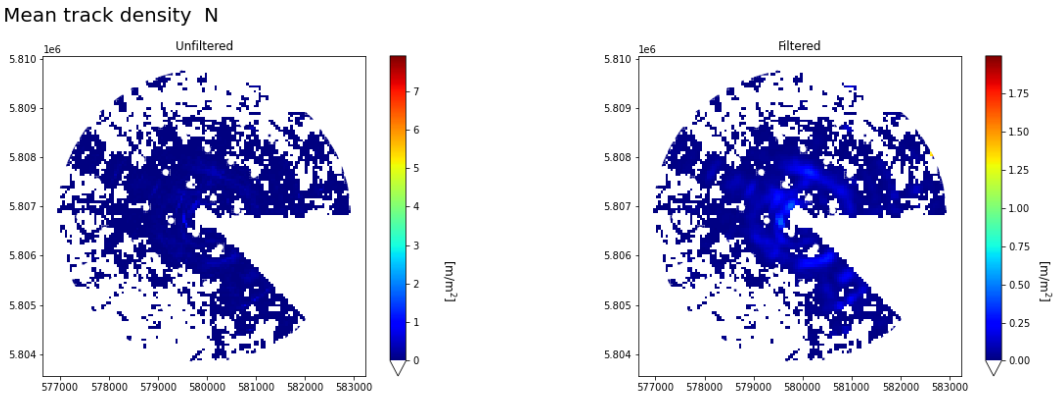

May

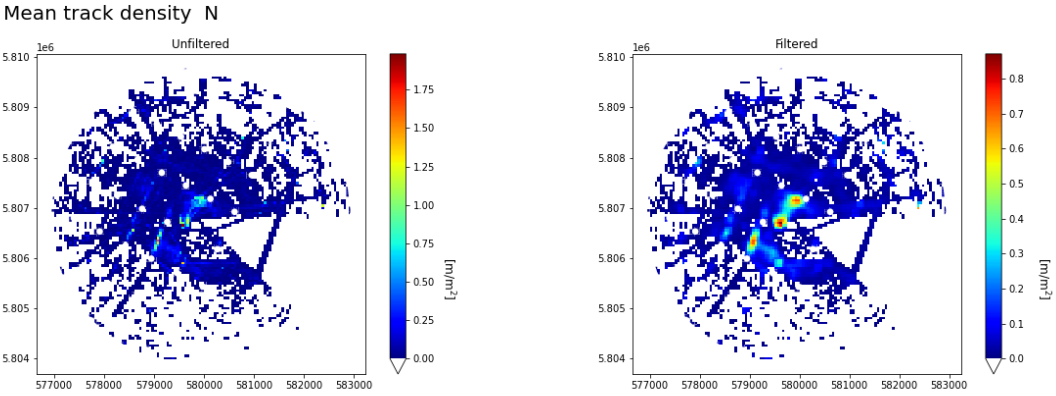

June

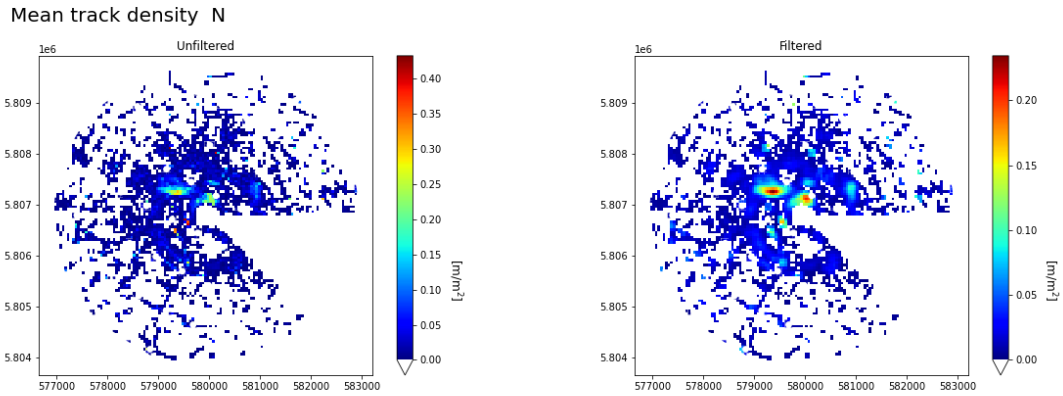

July

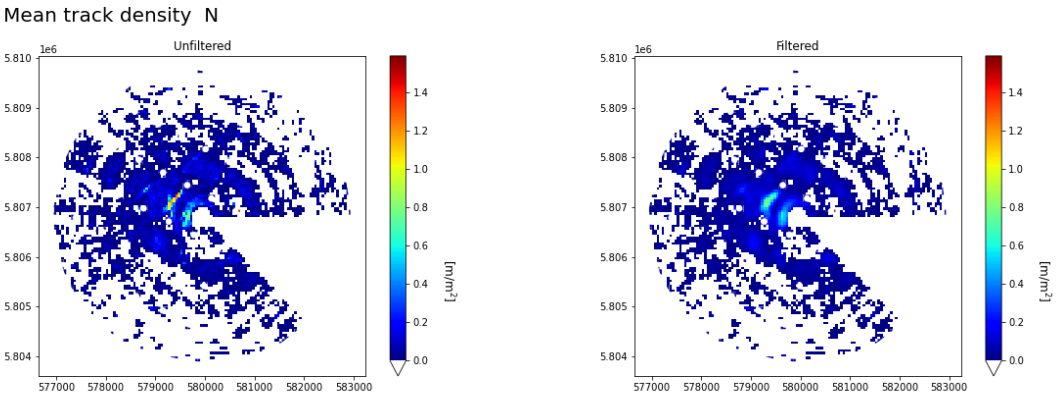

August

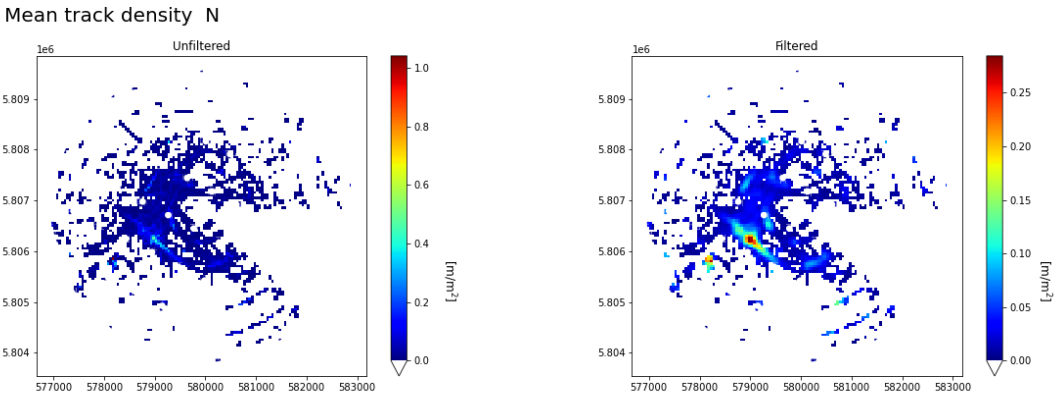

September

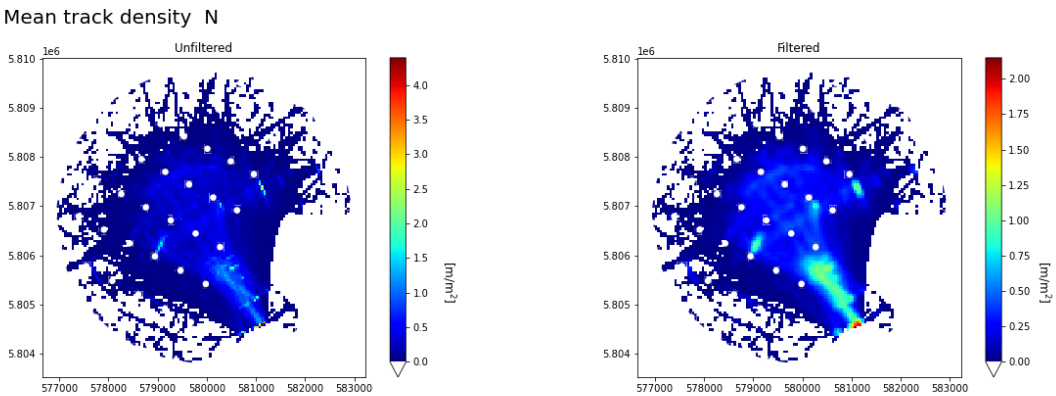

October

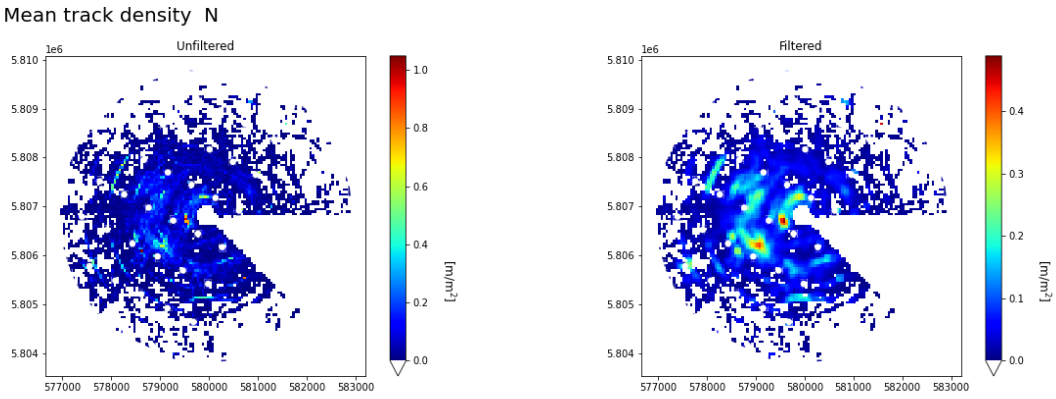

November

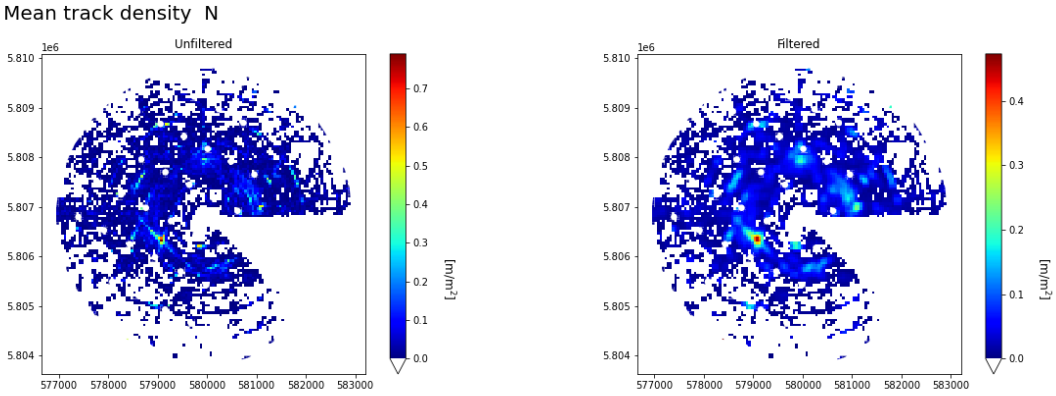

December

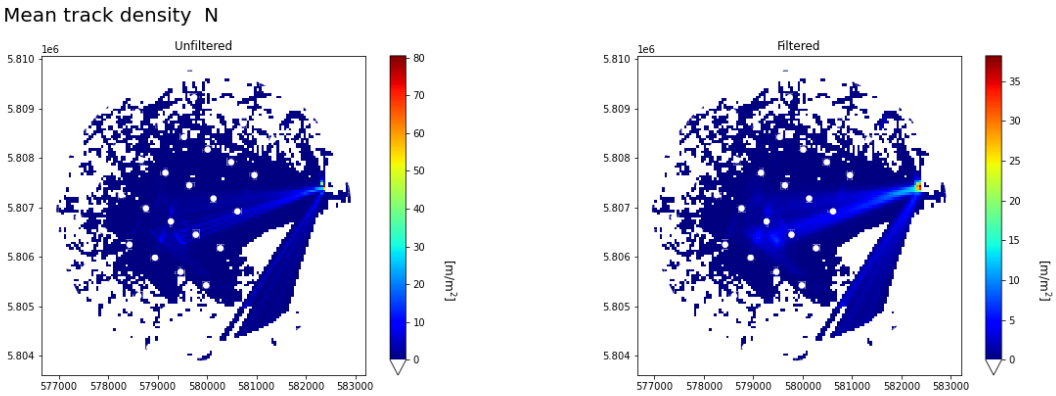

Appendix 3 Random Forest flight models – validation

Large Gulls

```
                         Sample size: 1078
                    Number of trees: 2000
          Forest terminal node size: 1
      Average no. of terminal nodes: 627.744
No. of variables tried at each split: 3
             Total no. of variables: 6
             Total no. of responses: 3
       User has requested response: Height
      Resampling used to grow trees: swor
   Resample size used to grow trees: 681
                           Analysis: mRF-R
                             Family: regr+
                    Splitting rule: mv.mse *random*
      Number of random split points: 10
                  (OOB) R squared: 0.90214837
  (OOB) Requested performance error: 73.04682816
```

```
                         Sample size: 1078
                    Number of trees: 2000
          Forest terminal node size: 1
      Average no. of terminal nodes: 627.744
No. of variables tried at each split: 3
             Total no. of variables: 6
             Total no. of responses: 3
       User has requested response: Speed
      Resampling used to grow trees: swor
   Resample size used to grow trees: 681
                           Analysis: mRF-R
                             Family: regr+
                    Splitting rule: mv.mse *random*
      Number of random split points: 10
                  (OOB) R squared: 0.18058695
  (OOB) Requested performance error: 21.18071965
```

```
                         Sample size: 1078
                    Number of trees: 2000
          Forest terminal node size: 1
      Average no. of terminal nodes: 627.744
No. of variables tried at each split: 3
             Total no. of variables: 6
             Total no. of responses: 3
       User has requested response: Relativ_direction
      Resampling used to grow trees: swor
   Resample size used to grow trees: 681
                           Analysis: mRF-R
                             Family: regr+
                    Splitting rule: mv.mse *random*
      Number of random split points: 10
                  (OOB) R squared: 0.52209278
  (OOB) Requested performance error: 1130.30820405
```

Table A3- 1 Results from multivariate random forest on Large gulls behaviour, Flight height (top), flight speed (middle), relative flight direction (bottom)

Overall there was a good correspondence when comparing predicted flight parameters with observed ones, with a correlation between observed and predicted parameters on average at 0.98 (Flight height 0.99, Flight speed 0.96, Flight direction 0.98) (Figure A3- 1).

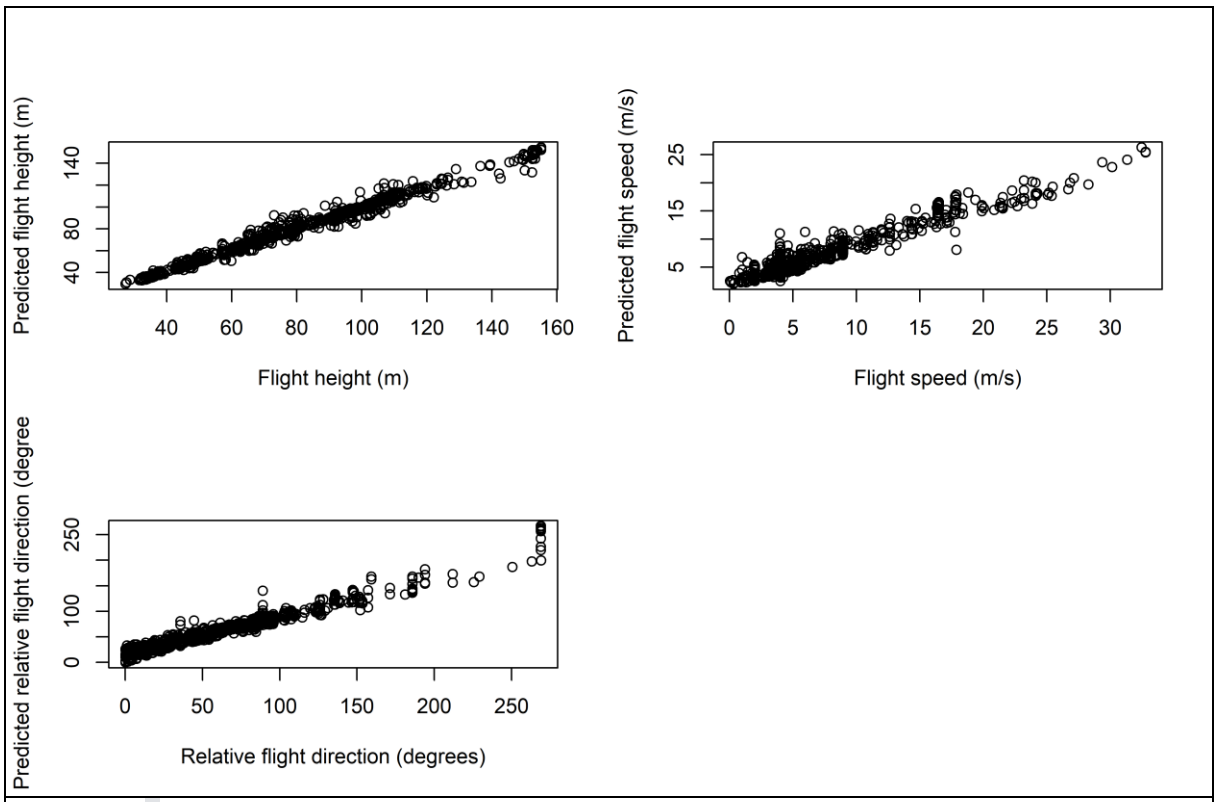

Figure A3- 1 Comparison between observed and predicted variables

Page Break

Additionally, no significant autocorrelation was evident in the residuals from the model.

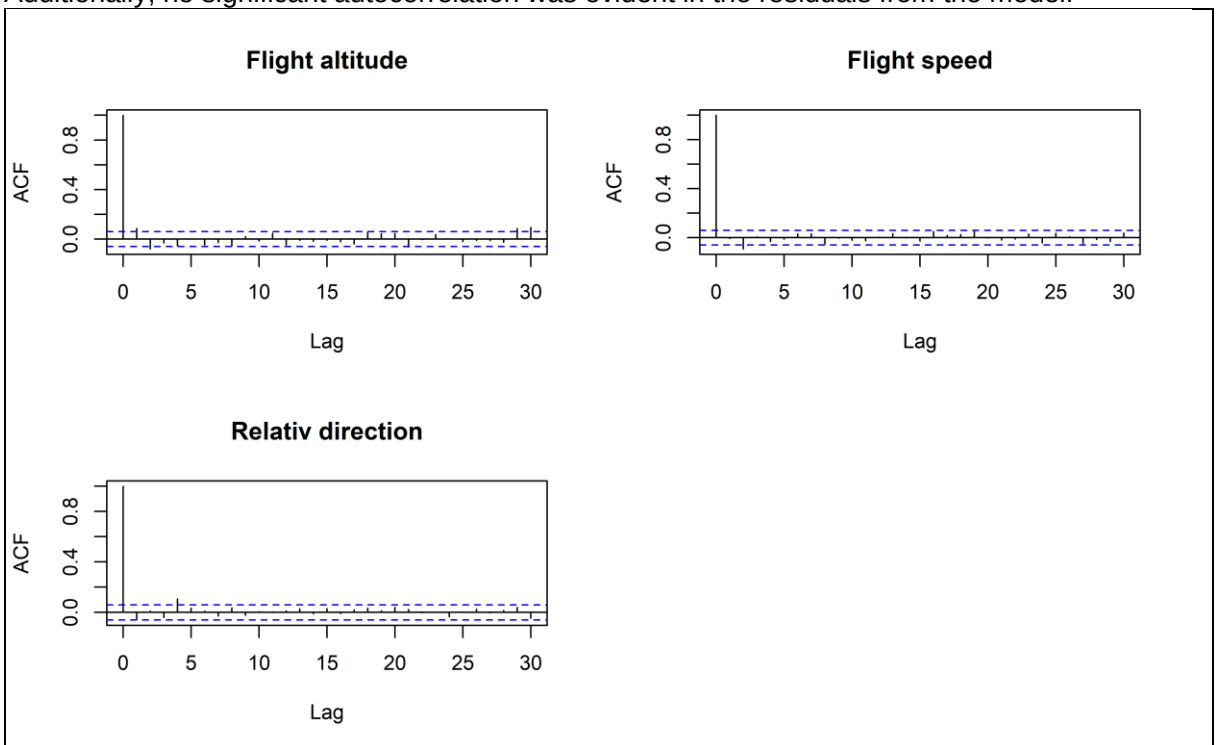

Figure A3- 2 ACF plots of residuals.

From the analysis of importance (Figure A3- 3) it was evident seen that it was not the same variables that drove each behaviour. Flight speed was primarily driven by wind speed and the distance to rotor, while flight height has determined by turbulence, wind speed and distance to rotor. Most factors determined the relative flight direction.

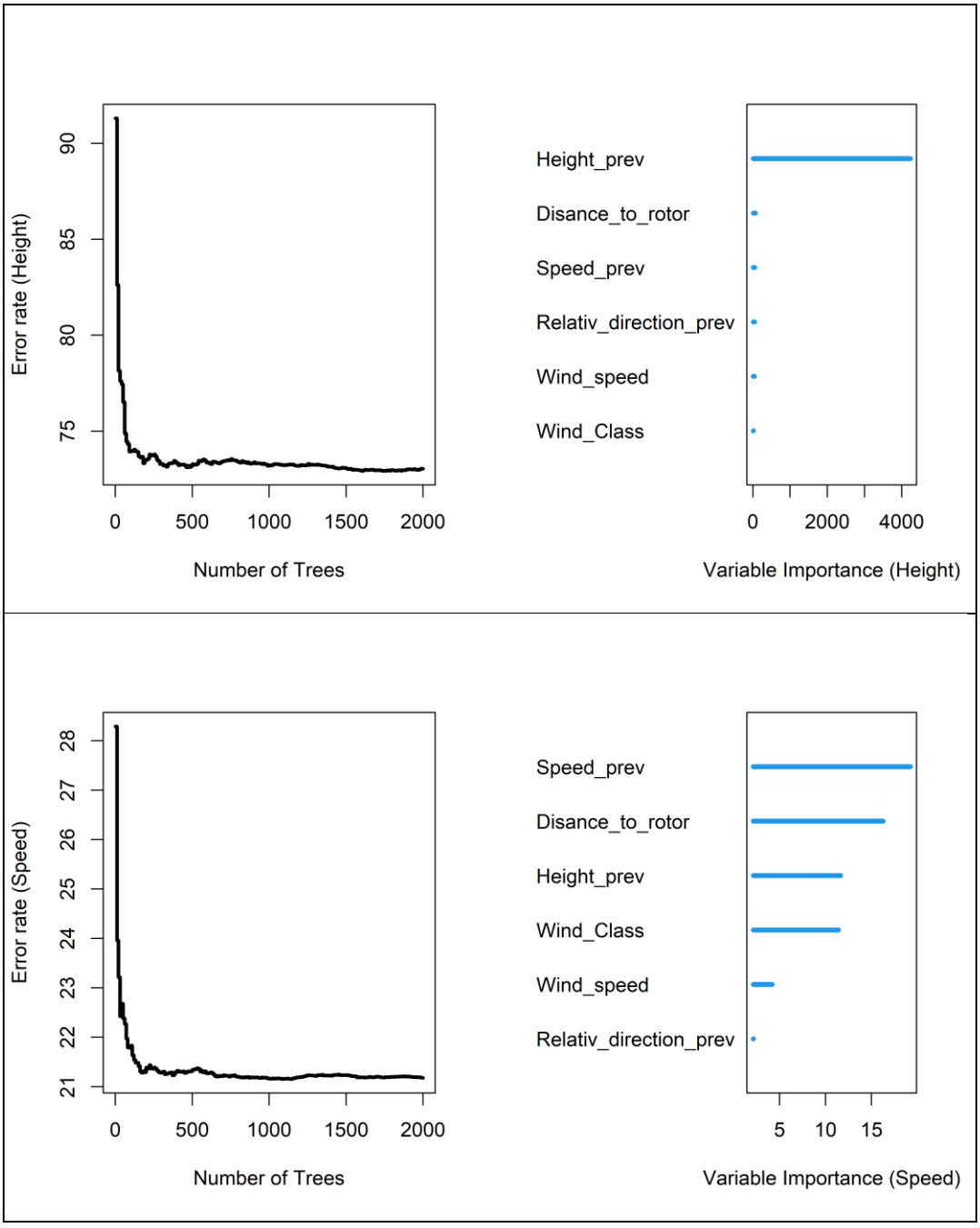

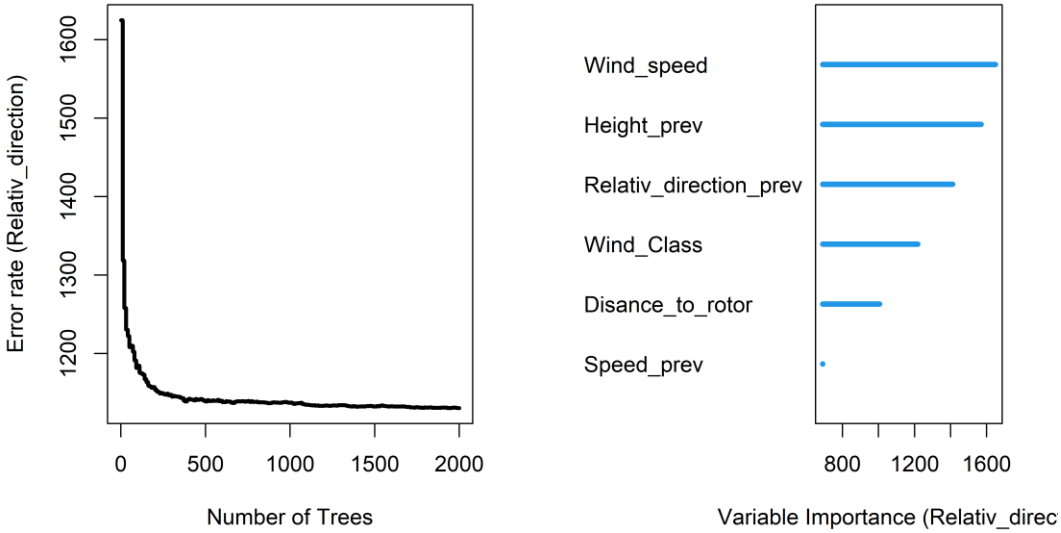

Figure A5- 3 Overview of OOB error rate and variable importance of the three behaviour models Speed (top), Height (middle) and relative direction (bottom).

Black-backed Gulls

```
                         Sample size: 97
                    Number of trees: 2000
          Forest terminal node size: 1
       Average no. of terminal nodes: 58.286
No. of variables tried at each split: 3
              Total no. of variables: 6
              Total no. of responses: 3
         User has requested response: Height
       Resampling used to grow trees: swor
    Resample size used to grow trees: 61
                            Analysis: mRF-R
                              Family: regr+
                    Splitting rule: mv.mse *random*
       Number of random split points: 10
                    (OOB) R squared: 0.88257181
   (OOB) Requested performance error: 111.56414098
```

```
                         Sample size: 97
                    Number of trees: 2000
          Forest terminal node size: 1
       Average no. of terminal nodes: 58.286
No. of variables tried at each split: 3
              Total no. of variables: 6
              Total no. of responses: 3
         User has requested response: Speed
       Resampling used to grow trees: swor
    Resample size used to grow trees: 61
                            Analysis: mRF-R
                              Family: regr+
                    Splitting rule: mv.mse *random*
       Number of random split points: 10
                    (OOB) R squared: -0.1263727
   (OOB) Requested performance error: 28.71970772
```

```
                         Sample size: 97
                    Number of trees: 2000
          Forest terminal node size: 1
       Average no. of terminal nodes: 58.286
No. of variables tried at each split: 3
              Total no. of variables: 6
              Total no. of responses: 3
         User has requested response: Relativ_direction
       Resampling used to grow trees: swor
    Resample size used to grow trees: 61
                            Analysis: mRF-R
                              Family: regr+
                    Splitting rule: mv.mse *random*
       Number of random split points: 10
                    (OOB) R squared: 0.47892429
   (OOB) Requested performance error: 514.26090111
```

Table A5- 1 Results from multivariate random forest on Black-backed gulls flight behaviour, Flight height (top), flight speed (middle), relative flight direction (bottom)

Overall there was a good correspondence when comparing predicted flight parameters with observed ones, with a correlation between observed and predicted parameters on average at 0.98 (Flight height 0.99, Flight speed 0.96, Flight direction 0.98) (Figure A5- 1).

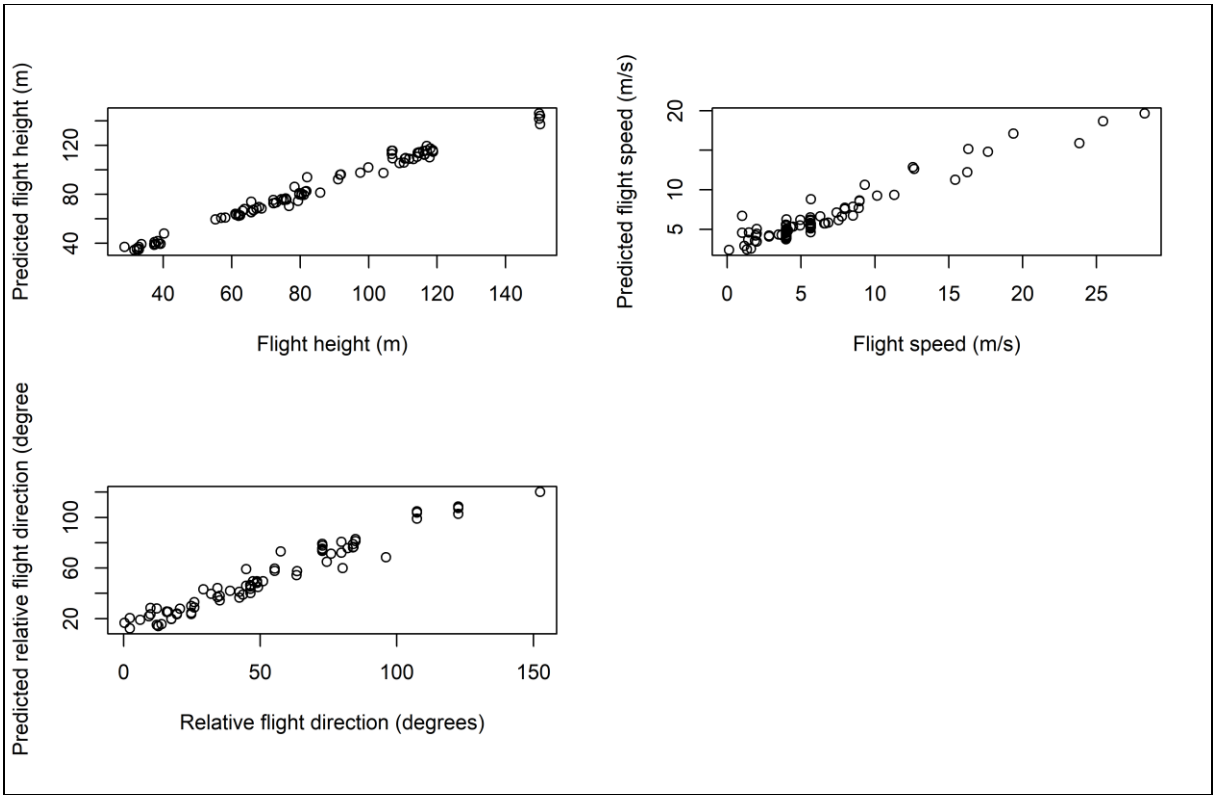

Figure A5- 1 Comparison between observed and predicted variables

Page Break

Additionally, no significant autocorrelation was evident in the residuals from the model.

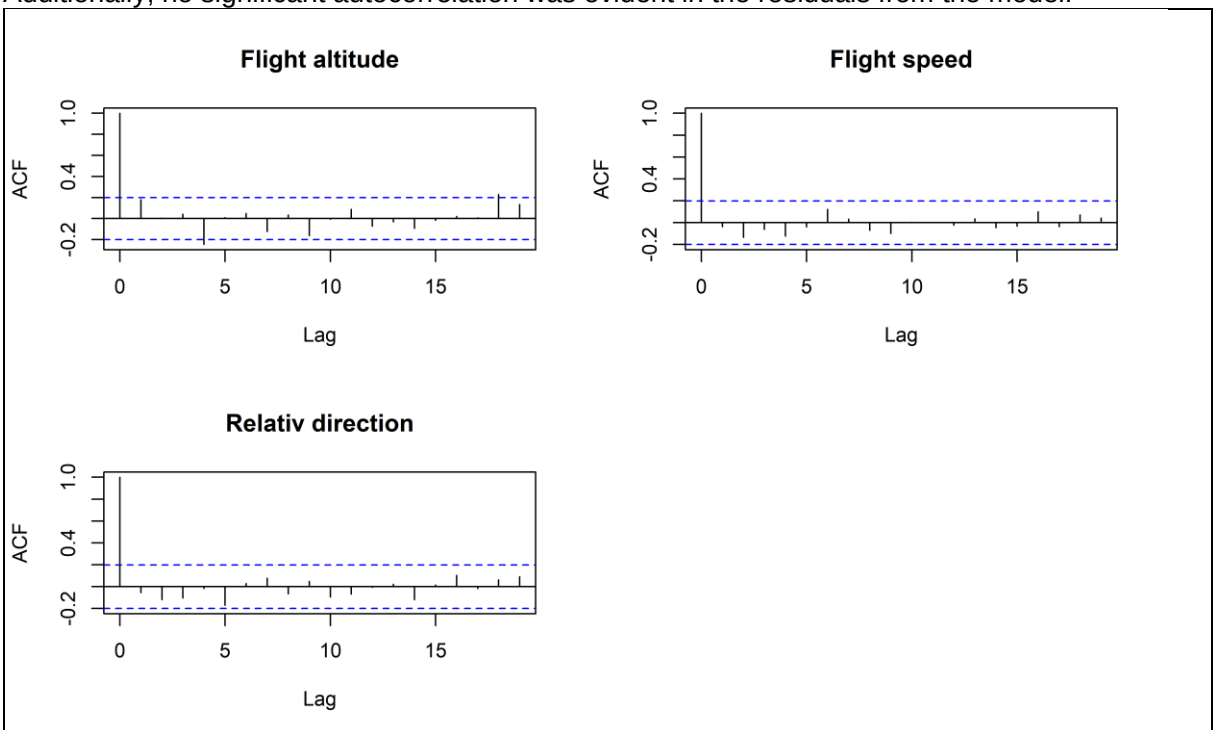

Figure A5- 2 ACF plots of residuals.

From the analysis of importance (Figure A5- 3) it was evident seen that it was not the same variables that drove each behaviour. Flight speed was primarily driven by wind speed and the distance to rotor, while flight height has determined by turbulence, wind speed and distance to rotor. Most factors determined the relative flight direction.

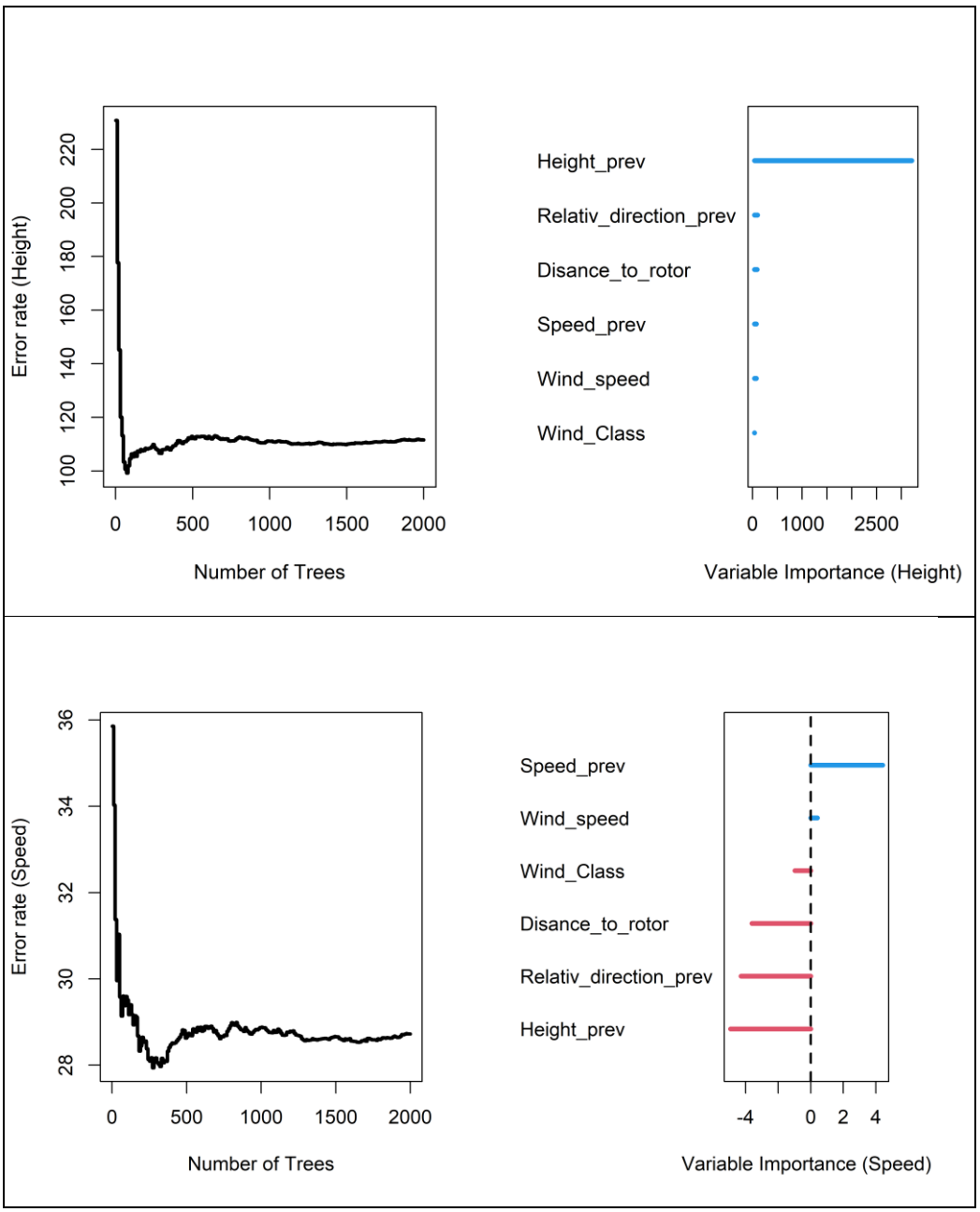

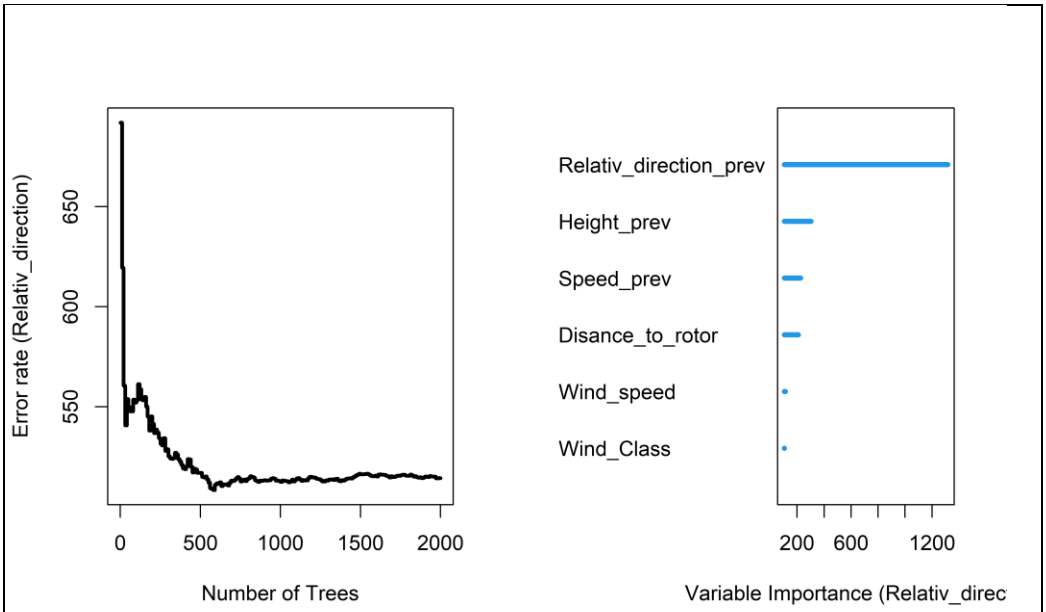

Figure A5- 3 Overview of OOB error rate and variable importance of the three behaviour models Speed (top), Height (middle) and relative direction (bottom).